Convolution Based Real-Time Control Strategy for

Vehicle Active Suspension Systems

A thesis submitted for the degree of

Doctor of Philosophy

By

Moudar Saud

Department of Mechanical Engineering

Brunel University

Abstract

A novel real-time control method that minimises linear system vibrations when it is subjected to an arbitrary external excitation is proposed in this study. The work deals with a discrete differential dynamic programming type of problem, in which an external disturbance is controlled over a time horizon by a control force strategy constituted by the well-known convolution approach. The proposed method states that if a control strategy can be established to restore an impulse external disturbance, then the convolution concept can be used to generate an overall control strategy to control the system response when it is subjected to an arbitrary external disturbance. The arbitrary disturbance is divided into impulses and by simply scaling, shifting and summation of the obtained control strategy against the impulse input for each impulse of the arbitrary disturbance, the overall control strategy will be established. Genetic Algorithm was adopted to obtain an optimal control force plan to suppress the system vibrations when it is subjected to a shock disturbance, and then the Convolution concept was used to enable the system response to be controlled in real-time using the obtained control strategy. Numerical tests were carried out on a two-degree of freedom quarter-vehicle active suspension model and the results were compared with results generated using the Linear Quadratic Regulator (LQR) method. The method was also applied to control the vibration of a seven-degree of freedom full-vehicle active suspension model. In addition, the effect of a time delay on the performance of the proposed approach was also studied. To demonstrate the applicability of the proposed method in real-time control, experimental tests were performed on a quarter-vehicle test rig equipped with a pneumatic active suspension. Numerical and experimental results showed the effectiveness of the proposed method in reducing the vehicle vibrations. One of the main contributions of this work besides using the Convolution concept to provide a real time control strategy is the reduction in the number of sensors needed to construct the proposed method as the disturbance amplitude is the only parameter needed to be measured (known). Finally, having achieved what has been proposed above, a generic robust control method is accomplished, which not only can be applied for active suspension systems but also in many other fields.

Acknowledgements

Content

List of Tables

List of Figures

Nomenclature

Acronym	Definition
CCFS	Convolution based Control Force Strategy
GA	Genetic Algorithm
PID	Proportional Integral Derivative
LQG	Linear Quadratic Gaussian
LQR	Linear Quadratic Regulator
ARC	Adaptive Robust Control
LMI	Linear Matrix Inequality
RMS	Root Mean Square
SMC	Sliding Mode Controller

Symbol	Definition
m	Mass (kg)
k	Stiffness coefficient (N/m)
c	Damping coefficient (N.s/m)
x	Vertical displacement (quarter-vehicle) (m)
u	Control force (N)
λ	The scaling factor
$h(\ )$	The impulse response function
$U(\ )$	The control force strategy
$F(\ )$	The arbitrary excitation input function
$G(\ )$	The actual external input function
$I_{5xx}, I_{5yy}.$	The inertias of the vehicle body along X,Y axis (kg.m^2)
z	Vertical displacement (full-vehicle) (m)
α	The pitch angel
β	The roll angel
B	the $n\times n$ state matrix
C	the $n\times r$ input matrix
A	the $m\times n$ output matrix

E	the $m \times r$ transfer matrix
P	population
s_i	individuals (chromosomes)
υ	Number of variables
J	the quadratic performance index
R	a real symmetric $n \times n$ positive semidefinite matrix
Q	a real symmetric $r \times r$ positive definite matrix
T	the terminal time (s)
t_0	Initial time (s)
K	The ($m \times m$) symmetric matrix
D	The optimal control gain matrix
n	population size
Obj	Objective Function

Subscripts

Symbol	Definition
s	Sprung mass
us	Unsprung mass
r, w	Road

Superscript

Symbol	Definition
'	Matrix transpose
.	First derivative (Velocity)
..	Second derivative (Acceleration)

Chapter 1

1. Introduction and Thesis Structure

1.1. Introduction

The intention of this chapter is to introduce the research carried out in this thesis to the reader starting with a brief background of the vibration isolation and control developments and its application for vehicle suspension systems. This is followed by a description of the research objectives, the main contributions and the structure of the thesis.

1.1.1. Vibration isolation and control

Mechanical systems, which comprise mass, stiffness and damping components, show vibratory activity in response to time-variant disturbances [1]. In general these disturbances can be divided into two types, vibration transmitted to bodies, machines and equipment in contact with the ground and disturbances caused by the vibratory machines passed to the ground [2]. In both cases the vibration will have a negative effect on the structure and machine parts exposed to it. Failure caused by consequential material fatigue and an increase in machine component ware rate could also result from unwanted vibration, which may also cause poor surface finishing in metal cutting and subsequent degradation in the final product quality [3]. In addition, vibrations will cause human discomfort particularly if associated with acoustics noise [4]. Therefore controlling mechanical and structural vibrations is becoming an essential part of mechanical systems and equipment design procedures. Different methods have been suggested and applied by researchers to suppress vibrations; the proposed methods can be categorized into passive, semi-active and active vibration control systems.

Passive systems are designed to isolate and protect machines, equipment and structures from unwanted vibrations [3]. Because of their simplicity, they are easy to be manufactured. In general passive control systems utilise the damping properties of various materials such as rubber or the elastic (resilient) properties of other materials for instance metal and pneumatic springs. These springs and/or dampers are usually

mounted between the vibration source and the machines or the equipments to be isolated [3]. One of the widely used vibration isolation systems employs dynamic vibration absorbers which reduce disturbance amplitudes, especially when excessive amplitudes generated during operation could cause damage to machines and/or personnel [5]. Tuned-mass dampers have also been used to passively attenuate vibrations by simply attaching the damper to the system to reduce the undesirable effects of the vibrations without a big change in the structure of the original system [4, 6 and 7]. When dealing with passive isolators one should consider the fact that a highly damped isolator is required to control the vibration at resonance, and low damping is needed for higher frequency isolation performance [8, 9]. The inability to vary fixed parameter values of passive systems imposes a limitation of using these control systems for a wide frequency range.

Semi-active control of vibration involves varying the properties of the system, such as stiffness and/or damping coefficients which vary as a function of time [9]. A very small amount of power is needed by semi-active control strategies to retain the reliability of the passive systems; however, a good performance comparable to the performance of fully active control can be achieved [9]. Optimal performance of semi-active systems can be maintained as the parameters of the system can be changed with time; in addition, due to the fast time-variation achievable a higher level of optimisation can be reached [9]. Numerous strategies for semi-active control exist in literature; some control strategies used the skyhook damper control concept [9]. Others used semi-active tuned vibration absorbers [10], and more recently Magnetorheological (MR) and Electrorheological (ER) dampers have been increasingly used in semi-active control because of their low power consumption, great reliability, guaranteed control system stability and higher capacities of control forces when compared with other damping devices [11, 12]. In addition to the low power consumption, semi-active control provides improved performance of active method without remarkably complicating the control system [13].

Great interest in the area of active control of vibration has emerged as a result of new developments in the field of digital processing, actuators and sensors technologies [4]. This enabled designers to achieve superior control over a wide range of frequencies, particularly at low frequencies where active systems could be the only

option for many situations [14]. In spite of the high cost and complexity of active systems when compared to the passive ones, they provide a superior performance and a better static stability for the equipment they support [14]. Minimising the vibration of flexible support structures at some critical points, which are far from the attachment point of the isolator, is a distinct advantage of active systems for some applications [14]. In addition active systems are able to track the changes in machine operating conditions (excitation frequencies) and can adapt to compensate. The main difference between active systems and other systems is that they can dissipate energy as well as provide it to the system [14]. There exist many works in literature that address the use, strategies and applications of active control of vibration. Many concepts have been used and studied in the area of active vibration control of structure such as structure modelling, feedback and feed forward control, robust control, optimal control, intelligent structure and controllers, adaptive control, actuator-structure interaction and optimal placement of the actuators [4].

Active control systems utilise a large number of sensors and actuators which may cause durability problems, thus extra care should be taken to make sure that all the transmission paths of vibration are accounted for when implementing an active control of vibration. Limited control to a single path with no accounting for the remaining transmission paths may result in vibration level increase at places where it should be minimised [14]. Complexity and high cost have prevented the extensive use of active control for many applications, but the control system stability and superior performance have made it viable for some applications such as suspension systems in automotive industry. A vehicle suspension system is one of the interesting applications of vibration isolation systems which will be the main subject of the current work; particularly active suspension systems which will be discussed in detail in the following sections.

1.1.2. Vehicle Suspension Systems

Vehicle suspension systems aim to improve vehicle performance which involves the following criteria [14]:
- Ride comfort: achieving improved ride comfort by reducing vibration transmitted form road disturbances through the wheels to the vehicle body.

- Handling: in terms of the vehicle body pitch and roll movements generated as results of braking and cornering motions.

- Road holding: by keeping a good contact force between the wheels and the ground all the times.

- Suspension travel (suspension deflection): this is associated with the limits of suspension working space.

- Static deflection: the suspension system should be capable of supporting the payload changes.

As the mentioned criteria conflict with each other, an effective suspension system should achieve a compromise that satisfies different design requirements. To achieve this, researchers have used many optimisation methods that accentuate some of the above criteria and set constraints on the others, the obtained results providing a compromise which presents a good solution of the suspension design problem based on the performance criteria determined by the designer.

1.1.3. Objectives

The primary objectives of this work are:

-   To develop a generic control force strategy that minimises the oscillatory system response when it is subjected to an external arbitrary excitation while retaining the other performance criteria (i.e. achieving the required compromise). The proposed method should be applicable irrespective of the nature of the external disturbance, does not require access to the system states and can provide real time control.

-   To compare the performance of the proposed method with the performance of conventional optimal control methods.

-   To investigate the time-delay effects on the proposed method.

-   To experimentally validate that the proposed method is applicable for real-time control.

Having achieved the stated objectives, a generic control strategy that minimises the system response to an arbitrary external excitation would be accomplished. The proposed method would be of great value particularly in the field of active control of

vibration; and this will be revealed throughout its application to the *active suspension system* in this study.

1.1.4. Contributions to knowledge

The main contribution of the thesis is the development of a novel Convolution based real-time control force strategy (CCFS) that minimises linear systems' vibrations when subjected to an arbitrary external excitation. The novelty of the proposed approach comes from the following points:

- Convolution integral is usually applied to find the response of the system subjected to an arbitrary excitation, however in the current work it is applied to obtain a general control force strategy, which provides a real-time control against arbitrary excitation.

- Genetic Algorithms are usually used to find the system parameters or to tune these parameters in order to find the best combination that would give improved performance, while in current study GAs are used to find the control strategy itself regardless of the system parameters.

- Most of the control methods need to access and measure most of the system states in order to construct an appropriate control strategy, while the only input needed for the proposed method is the amplitude of the disturbance. This leads to a reduction in the number of sensors needed for measurements, which in turn results in less measurement of signals which might be contaminated in a noisy environment; consequently, less construction cost.

- The simplicity of the proposed method makes the implementation straight forward, especially that the results requires the use of four variables related to the optimisation procedure, leading to less memory usage.

- The inclusion of time delay made the approach more realistic as the majority of real time applications suffer from time delay caused by many sources. This shows the robustness of the proposed method which accounts for different values of time delay and still give acceptable results.

- The applicability of the proposed method was not only shown using numerical simulations, but also through experiments using a quarter-vehicle test rig equipped with pneumatic active suspension system.

- The proposed algorithm was also implemented using a Programmable Logic Controller (PLC) to control the test rig and proved to give improved performance.
- Finally, the CCFS method is generic and can be applied in many other fields.

1.2. The structure of thesis

Chapter 1 introduces the topic of vibration isolation and control to the reader and states the suspension systems; especially the active suspension systems as the main topic of the thesis. The objectives of the work and the main contributions are also presented in chapter 1.

Chapter 2 presents a literature review of the developments accomplished in the field of vehicle suspension systems; mainly the ones achieved in the active suspension system area. Some of the drawbacks and the difficulties of achieving the required performance are also addressed.

Chapter 3 presents the proposed method "Convolution based Control Force Strategy (CCFS)" with an example to explain how the method works.

Chapter 4 presents an introduction to the optimal control theory and explains the purpose of the optimisation procedure. Also it gives details about Genetic Algorithm which is used as the global optimisation tool in the current study. Then a summary of the Linear Quadratic Regulator which involves solving the associated Riccati equation of the system is briefly given.

Chapter 5 explains how to implement the proposed method for both quarter and full vehicle model, and shows the obtained numerical results of applying the proposed method to control the vehicle model when it is subjected to random road disturbance. The time-delay effects on the proposed method performance are also introduced.

Chapter 6 describes the experimental set up of a quarter-vehicle test rig designed to apply the proposed method to control a pneumatic active suspension system in such a

way to improve the system performance regarding the displacement and acceleration responses, suspension deflection and tyre deflection.

Chapter 7 gives a comprehensive discussion about the improvements achieved by applying the proposed method based on the obtained numerical and experimental results.

Chapter 8 concludes the work completed in this thesis, and gives an idea of the planned future work to be done.

Chapter 2

2. Literature Review

Suspension system; the vehicle part responsible of vibration isolation and control, has gain more interest in the last decade because of its important roll in maintaining the ride comfort, the vehicle holding and handling during braking and cornering motions. The developments achieved in the field of vehicle suspension systems involved both the main suspension system and the control system.

The work carried out in the current study is an attempt to develop a real time control strategy for vehicle active suspension system aiming towards minimising the vehicle body vibrations caused by road excitation. Through the following chapters the novel method "Convolution based Control Strategy (CCFS)" will be explained starting with the developments achieved in the area of suspension systems which focus on what has been achieved regarding the topic of active suspension systems. The new CCFS method is then explained in details, which involves explaining the convolution theory and how it was utilised to construct the new method. Optimal control and optimization are also introduced; particularly, the use of Genetic Algorithm as a global optimisation method and the Linear Quadratic Regulator which involves solving the Riccati equation of the system are also presented. Numerical simulation and experiments are then carried out to show the improvements that can be achieved using the proposed method and the applicability of the new method for real time control. Finally, to conclude the research presented in the thesis, a comprehensive discussion with concluding remarks are given.

The research conducted in this study deals with vehicle suspension systems; particularly, the area of active suspension systems. The current chapter presents the related research in literature which gives an overview of the recent works carried out, the developments accomplished and some of the problems that need further investigations to be done to overcome these problems.

In the search for the optimum design, suspension systems have undergone many developments, different control techniques (strategies) were proposed in literature. In

general suspension systems can be divided into three main categories; passive, semi-active and active systems. Some background of the developments of suspension systems and their three categories, especially active suspension can be found in [15]. The main features of each of these systems will be discussed in the following sections.

2.1. Passive Suspension systems

Passive suspension systems used for a long time in conventional vehicles, contain springs and dampers which are the storing and dissipating parts of the passive system respectively [16]. As the characteristics of these elements are fixed, the designer should carefully choose the values of spring stiffness and damper coefficients in such a way that allows the suspension system to achieve an acceptable performance. Numerous compromises would arise at the design stage as soft suspension is needed to minimise the acceleration levels and hard suspension is required to control the altitude changes of the vehicle and to keep the contact between the wheel and the ground in a good condition [16].

x_s	sprung mass vertical displacement
x_{us}	unsprung mass vertical displacement
x_r	Road input
c_s	Damping coefficient (suspension)
c_{us}	Damping coefficient (tyre)
k_s	Stiffness coefficient (suspension)
k_{us}	Stiffness coefficient (tyre)
m_s	Sprung mass
m_{us}	Unsprung mass
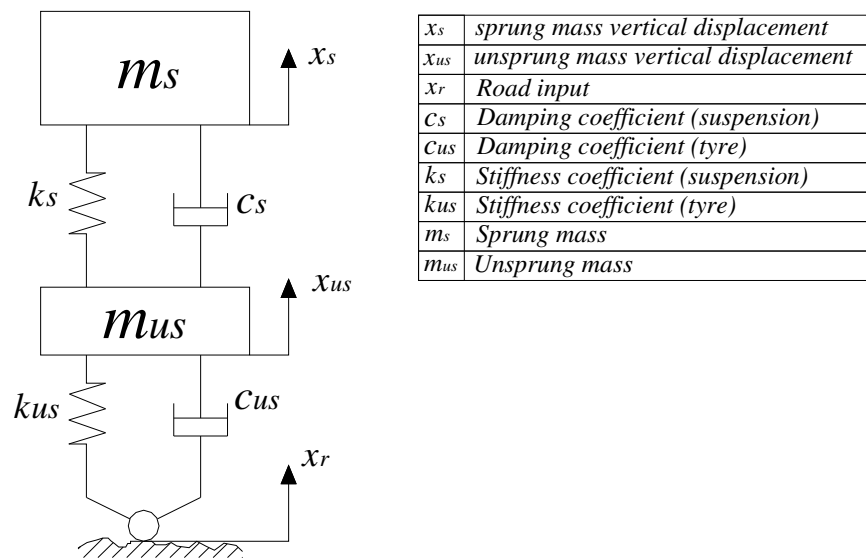
Fig 2.1 Passive suspension system

9

Fig 2.1 shows a quarter-vehicle model with passive suspension that consists of a spring and a damper with fixed stiffness and unchanging damping coefficient respectively. The equations of motion of this model are given in Eq.(2.1) and Eq.(2.2). It can be seen from these equations that the suspension is mainly storing and dissipating energy at a preset value determined at the design stage,

$$m_s \ddot{x}_s = c_s \left(\dot{x}_{us} - \dot{x}_s \right) + k_s \left(x_{us} - x_s \right), \tag{2.1}$$

$$m_{us} \ddot{x}_{us} = c_{us} \left(\dot{x}_r - \dot{x}_{us} \right) + k_{us} \left(x_r - x_{us} \right) - c_s \left(\dot{x}_{us} - \dot{x}_s \right) - k_s \left(x_{us} - x_s \right), \tag{2.2}$$

where, m_s and m_{us} are the sprung and the unsprung masses, k_s and k_{us} are the stiffness coefficients of the suspension and the tyre, c_s and c_{us} are the damping coefficients of the suspension and tyre respectively, (x_r) is the road disturbance, (x_s) is the sprung mass vertical displacement and (x_{us}) is the unsprung mass vertical displacement.

In literature, researchers used many optimisation techniques in their search for a good design of passive suspension systems. The authors of [17] used a two-degree of freedom quarter car model in order to obtain a number of analytical formulas which explain the dynamic behaviour of vehicles that use passive suspension systems subjected to random road excitation. Two different road irregularities were considered and described by different Power Spectral Densities (PSDs). The optimisation process was carried out to find the optimal values of suspension parameters that guarantee the best compromise among ride-comfort, road holding and suspension working space which would result in better performance. In their search for a tool that can help to solve problems associated with military vehicle suspension system design, the authors of [18, 19] developed a two-dimensional multi-body vehicle dynamics model to be used in computer simulation. In the first part of their study, a specific gradient based optimisation algorithm was used to obtain the vehicle suspension characteristics in respect of an objective function that guarantee the ride-comfort of the vehicle. The second part of the work described the simulation program developed using the mathematical model of the vehicle which is linked to the optimisation algorithm. The capabilities of the proposed program were presented in a case study where the optimisation system was used to perform optimisation of the developed vehicle model which appeared to give satisfactory

results. The authors of [20] obtained the Root Mean Square Acceleration Response (RMSAR) of a two-degree of freedom half-car model subjected to random road excitation. The effects of the time lag between wheels and the vehicle velocity on the RMSAR were considered in the study. In addition, an optimisation procedure was proposed to minimise the RMSAR of the vehicle suspension to obtain the values of the spring stiffness and damping coefficient of the vehicle suspension which would guarantee the passenger ride comfort.

Passive suspension systems are simple, easy to construct, implement and maintain; however, they have limitations in achieving a good compromise between the previously mentioned conflicting design criteria and this is due to the fixed suspension parameters values which once chosen cannot be changed [16]. In addition, storing and dissipating energy would happen at an invariable rate and for a limited time only [21].

2.2. Semi-active Suspension systems

To overcome the limitations caused by the fixed parameters of passive systems, a variable damper (and/or spring) was introduced to the suspension system. Introducing the semi-active elements made suspension systems capable of adapting to different driving conditions; the driving comfort and safety have been significantly enhanced by inserting a variable element when compared to passive systems with fixed parameters values [22].

x_s	*sprung mass vertical displacement*
x_{us}	*unsprung mass vertical displacement*
x_r	*Road input*
c_s	*VariableDamping coefficient (suspension)*
c_{us}	*Damping coefficient (tyre)*
k_s	*Stiffness coefficient (suspension)*
k_{us}	*Stiffness coefficient (tyre)*
m_s	*Sprung mass*
m_{us}	*Unsprung mass*
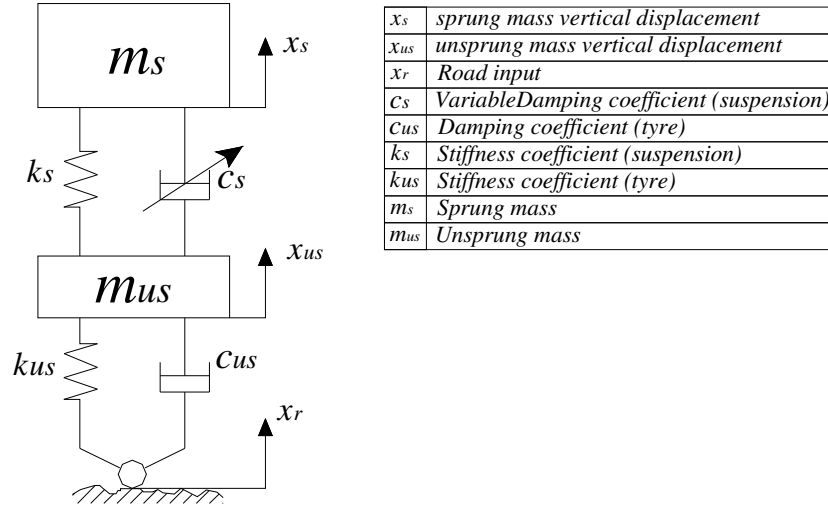
Fig 2.2 Semi-active suspension system.

Fig 2.2 shows a quarter-vehicle model with a semi-active suspension system which is similar to the passive one but with a variable damping coefficient. The equations of motion of the model are given in Eqs. (2.3), (2.4) and (2.5),

$$m_s \ddot{x}_s = k_s (x_{us} - x_s) + F_d ,$$ (2.3)

$$m_{us} \ddot{x}_{us} = c_{us}(\dot{x}_r - \dot{x}_{us}) + k_{us}(x_r - x_{us}) - k_s(x_{us} - x_s) - F_d ,$$ (2.4)

$$F_d = c_s(\dot{x}_{us} - \dot{x}_s) ,$$ (2.5)

where F_d is the variable damping force controlled by adjusting the changeable damping coefficient value.

There are two basic types of semi-active systems; the first one is the on-off type. In which damping will be invariable at the on-state but with a significantly bigger damping value than the one in the off-state. The second one is the continuously variable type. In which the damping will be varied between two values [14]. No power is provided by the semi-active system and external power is only required to operate the controller, the sensors and the valves of the damper so the characteristics values can be adjusted. Thus, semi-active systems can only dissipate the power; in

addition, they are reliable because they will keep working in passive mode when the control system fails [14, 23]. Many attempts have been made to find the best design of semi-active suspension systems. The authors of [24] proposed a new design of vehicle suspension that connects the vehicle front and rear dampers by capillary tubes. The authors analysed the effects of the preview control of the suggested system on the rear suspension. To improve the performance of the system with connected dampers, "quasi-sky-hook" systems were designed to account for the semi-active control of vehicle vertical oscillation and pitch motion. Kim and Lee [25] developed an on-off damping control law to suppress the vibration of a multi-degree of freedom suspension system which utilised semi-active actuators. The proposed technique was developed using the Lagrange's equation of motion and the concept of Lyapunov's direct method. In addition, it minimised the entire structure vibratory energy, together with the work completed by the external disturbance. The optimal ride comfort of an off-road vehicle was the main concern of the investigation completed in [26], in which the spring and damper settings were determined to ensure vehicle optimal ride comfort. The obtained results were needed in the design of a four stage semi-active hydro-pneumatic spring damper suspension system. The work showed to which degree the optimal suspension settings of vehicle ride comfort would vary with regard to roads that have different unevenness and at different velocities, as well as the ride comfort levels that can be reached.

New designs of semi-active systems have emerged as a result of exploring the benefits of smart materials such as Electrorheological (ER) and Magnetorheological (MR) fluids. ER and MR fluids have been used in semi-active dampers instead of ordinary oils; they consist of a liquid with low viscosity mixed with fine particles [23]. Applying an electric field in the case of ER dampers or a magnetic field for MR dampers will cause the particles to be formed into chain-like structures, leading to a change in the viscosity of the damper [23]. For a suspension system when the strength of the electric or the magnetic field reaches a specific value the suspension will solidify due to the high yield stress. On the other hand, removing the applied field will cause the suspension to be liquefied again; the changing procedure will happen in milliseconds [23]. The properties of the MR and ER dampers, in addition to the low energy consumption and fast response have attracted many researchers [23, 27-33] who utilised these dampers for semi-active control of vehicle suspension

systems. A new sliding mode controller is presented in [27] for the semi-active suspension system equipped with an MR damper. The proposed approach showed high robustness in accounting for the model uncertainties and the disturbances. While in [28] three different control methods were adopted by the authors and investigated to control semi-active suspension systems using commercial MR dampers. In [29] the authors presented an analytical study to explore the efficiency of using the MR dampers in a suspension system to suppress the vibration of a passenger car. A parameter optimisation and simulation study of suspension systems with controlled MR dampers was given in [30]. A novel design of ER dampers was presented by the authors of [31] to be used in a semi-active suspension system of a passenger car to suppress the encountered vibration due to road disturbances. While in [32] the performance features of the ER damper used in a semi-active suspension system were assessed throughout a field test of a full car equipped with four ER shock absorbers. The use of both ER and MR dampers was investigated in [33] in which the MR damper was used to support the car seat and the ER dampers were used for the main suspension system of the car.

2.3. Active Suspension systems

The new developments in the field of actuators, sensors and microprocessors, in addition to the improvements in performance and cost reduction have increased the number of applications in the automobile industry [34, 35]. This has resulted in a vast growth in the area of active control of vehicle suspension. A force actuator is added to the suspension system so power not only can be stored and dissipated but also can be provided it to the system [14]. The main advantage of active suspension systems is their capability of adapting to different operation conditions and satisfying the above mentioned conflicting design criteria simultaneously [14].
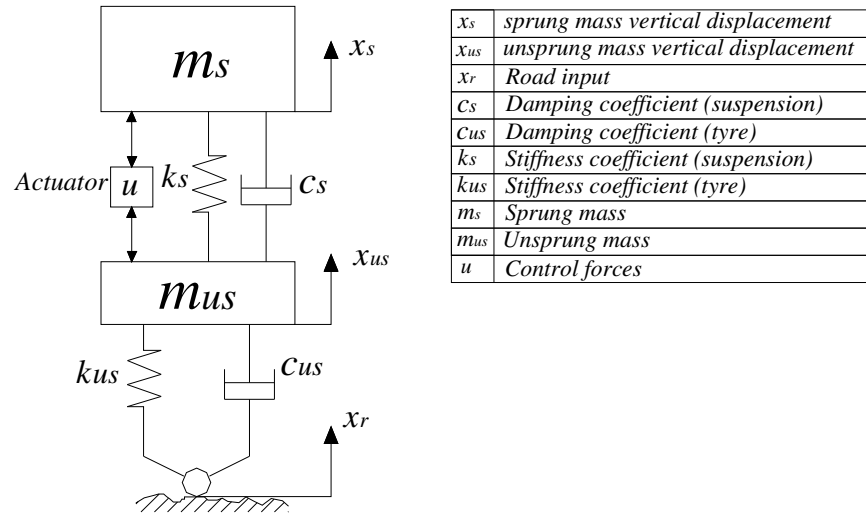
Fig 2.3 Active suspension system.

Fig 2.3 shows a quarter-vehicle model with an active suspension system, in which an actuator is added in parallel to the passive system. The equation of motion of this model is given in Eq. (2.6) and (2.7),

$$m_s \ddot{x}_s = c_s (\dot{x}_{us} - \dot{x}_s) + k_s (x_{us} - x_s) + u \,, \tag{2.6}$$

$$m_{us} \ddot{x}_{us} = c_{us} (\dot{x}_r - \dot{x}_{us}) + k_{us} (x_r - x_{us}) - c_s (\dot{x}_{us} - \dot{x}_s) - k_s (x_{us} - x_s) - u \,, \tag{2.7}$$

where, *u* is the controllable actuator force.

As the interest in active suspension systems has increased in the last decade, researchers have contributed to this field by introducing many different methods and techniques to improve the quality and performance of the suspension system taking into account the cost, power consumption, and achieving a good compromise of the suspension criteria. The models suggested by researchers varied from one degree of freedom (ODOF) quarter-vehicle to multi-degree of freedom (MDOF) full-vehicle models. Many approaches have been proposed to control these suspension models. Numerical simulations supported by experimental tests were used by researchers to show the effectiveness and improvements achieved as a result of applying their control strategies. However, several of these methods which were argued to achieve

good performance have some drawbacks especially when it comes to real life applications.

In literature, different approaches have been employed for designing active vehicle suspension systems. In his survey [35], Hrovat addressed the main control methods used to design an active suspension system such as modal analysis, classical control techniques, neural networks, fuzzy logic and many other methods. He focused on the developments achieved using the optimal control theory; particularly, the application of Linear Quadratic (LQ) and Linear Quadratic Gaussian (LQG) optimal control techniques, and summarised the materials needed to design an optimally controlled suspension system. Williams in [36, 37] mainly attempted in [36] to review the compromises that can be achieved to satisfy the suspension conflicting criteria, which are essential to the design of a conventional passive suspension system. The author then demonstrated the changes that could occur to these compromises when active components were introduced to the system. In the second part [37] Williams presented a brief description of the hardware used in suspension systems including the simple switched damper as an example of adaptive suspension, the two state and the variable dampers for the semi-active suspension, and high and low bandwidth active suspensions. In addition, practical considerations which should be taken into account when designing suspension systems have been given, with emphasis on operating power consumption.

The objective of the work done by Türkaya and Akçay [38] was to investigate the limits of vehicle performance which was actively controlled and subjected to the road excitation. The response constraints of the quarter-car active suspension system were derived for different suspension parameters using measurements of vertical acceleration and/or the suspension travel for feedback control. The authors investigated tyre damping effects on the active suspension system design by using the feedback stability factorization approach, and argued that by coupling the sprung and unsprung masses motions a constraint of the wheel-hop mode was removed. The author also used a combination of LQG and interpolation techniques to demonstrate the effect of tyre damping on the design of a lightly damped quarter-car model with active suspension.

The superior performance of active and semi-active suspension systems was shown in a comparative study completed by Mantaras and Luque [39], in which seven different active and semi-active suspension systems, LQR-LQG, Robust design, Kalman filter, Pole-assignment, Neural network, Fuzzy logic and skyhook damper were analyzed. The ride comfort and handling stability were the criteria of interest for which the performance of the mentioned suspension systems was compared with equivalent passive suspension systems. Numerical results of the simulations, which used a 2-DOF quarter-car model subjected to the road inputs, showed the improvement in ride comfort achieved using active suspension systems employing fuzzy logic, neural network and pole assignment methods. The authors argued that the weights and control parameters choice affect the performance of the other method which can be further improved with different values. The ride comfort improvements came at the cost of poor stability performance as these two criteria conflict with each other.

Peng et al. [40] proposed a new method to design an active suspension system of a quarter-car model. The new approach used Virtual Input Based (VIB) signals by which the dynamics of a quarter car suspension was transformed to make it independent of the vehicle parameters. The VIB signals were first designed using the LQ optimisation method and then used to build the desired trajectory of the sub-loop control system which was one of the design drawbacks of the traditional approaches. The sub-loop feedback control was based on a simple proportional control algorithm which employed the preview control. Simulation results showed that the use of preview control led to substantial tyre deflection and ride quality improvements while a slight increase in the control force magnitude and advanced in phase was achieved. Nevertheless, these improvements were attained at the cost of an obvious suspension stroke increase.

A comparative study of active and semi-active suspension properties was completed in [41]. The authors used the result of previous work, which involved semi-active suspension using controlled hydraulic damper done by [42], to be compared with the results of an active suspension system using a controllable air-spring. The RMS vertical acceleration of the sprung mass, the RMS value of the dynamic force of the tyre and the energy consumption of the suspension system were the comparison

criteria. It was concluded that the active system was more effective than semi-active systems but at the price of more power consumption.

Ikenaga et al. in [43] proposed an active suspension control approach consisting of inner and outer control loops with an input decoupling transformation to combine these two loops in a formal mathematical style for a full-vehicle model. The disturbances caused by uneven terrain are rejected by the ride control loops (inner loops) that isolate the car body while the heave, pitch and roll responses are stabilized by the outer control loops. The authors used active filtering of spring and damping coefficients through the inner control loops and skyhook damping of heave, pitch and roll velocities through the outer loops to minimize the motion of the sprung mass above and below the wheel frequency. Simulation results revealed that the heave, pitch and roll acceleration was improved by the active damping at both high and low frequencies. The inclusion of skyhook damping led to performance improvements although there were no considerable improvements at the wheel frequency.

Kumar and Vijayarangan in [44] developed a Proportional Integral Derivative (PID) controller for an active suspension quarter-car model subjected to bumpy road input. A specific tuning method was used to determine the characteristics of the PID controller. The performance of the proposed system that used a hydraulic actuator was compared to the performance of the passive suspension system. Results were verified by experimental tests where it was shown that the active suspension system improved the ride comfort, road holding and suspension travel. However, at higher frequencies active suspension performance deteriorated due to the difficulty of force tracking.

Alleyne et al. in [45] also investigated the use of a PID controller algorithm for hydraulic active suspension systems. It was shown to be an inappropriate option for some systems, particularly when a specific force profile that contains considerable frequency components required tracking. The authors argued that the reason was the feedback was unable to change the lightly damped zeros (LDZ) of the open loop of the given model reduction, resulting in a limited bandwidth of the PID algorithm. An identical observation was made by the authors of [57] when they tried to use the PID

controller for force tracking but they claimed that the inadequate robustness of the PID controller was responsible for the poor performance of the controller. Similarly, the lightly damped zeros (LDZ) for the servo-loop system generated by the lightly damped modes due to the interaction between the hydraulic actuator and the suspension system, were claimed by the authors [46] to be the cause for the closed loop performance of the suspension system to lock up within the low frequency range. The authors introduced four different solutions; alternative actuator, suspension parameters modification, using vibration absorber as an example of add-on mode and using advanced control strategies to decrease the effects of the LDZ on the performance of the suspension. The effects of applying any of the mentioned remedies (treatments) were also analysed.

An intelligent feedback linearization (IFL) for an active suspension system controller was proposed by Buckner et al. [47, 48]. The proposed approach utilised artificial neural networks and adaptive control techniques to cancel the nonlinearities of the vehicle suspension to enable the use of linear control laws. The authors argued that the new control approach is capable of improving the active suspension performance with regards to both ride comfort and handling. In [48] the authors used the proposed method to control a "HMMWV" [48] vehicle in real-time. The field results showed that the IFL improved the sprung mass acceleration and reduced the absorbed power significantly in comparison to the passive suspension performance. Comparisons of the suspension deflection and tyre deflection were not included in the study, which would otherwise provide insight into whether the improvements achieved resulted in the degradation of these performance criteria.

To overcome the drawback of the realistic skyhook damping method, Parthasarathy and Srinivasa [49] proposed a Model Reference Control (MRC) method. This method was based on making a specified system operate as a desired system by simply applying appropriate control forces. The difference error signal between the model output and the actual system response output was used to construct the requested input of the controller. The proposed method was applied on a quarter-car suspension system; simulation results showed that applying the MRC method improved the sprung mass response, degraded the unsprung mass response and maintained the suspension travel and wheel position responses almost equivalent to

responses in the case of ideal and practical skyhook. The authors argued that this happened as a result of the unsprung mass being affected by an inevitable controller force input reaction.

A fuzzy logic controller for vehicle active suspension system was designed by Barr and Ray [50] to improve ride comfort taking into account the constraints of suspension deflection and handling. The proposed method was applied to two degrees of freedom quarter car model and compared with LQG optimal method and with the passive system using Simulink. Using the RMS values of the evaluation criteria (i.e. body acceleration, suspension deflection and tyre deflection), the simulation results showed that the proposed fuzzy suspension improved the sprung mass acceleration response for both the random linear PSD and Gaussian input, while the LQG suspension led to an improvement of the suspension deflection over the fuzzy suspension. Both methods failed to improve the handling properties; moreover, handling performance deteriorated when compared to passive suspension response. Another fuzzy controller based on genetic algorithm was designed by Moon and Kwon [51] for an active suspension system. A half-car model was used for simulation with three different models of road disturbance. The body acceleration and front and rear suspension deflections were the only measurements to be used by the controller. The membership functions of the proposed fuzzy rules were tuned using a Genetic algorithm based tuning method. Simulation results showed that the ride quality and vehicle maneuverability were improved by the proposed controller. Moreover the proposed design was able to overcome some uncertainties of the model parameters without the need for the complete system state. The authors of [52] also proposed an active suspension system for passenger cars using a combination of two kinds; linear and fuzzy-logic controls. Linear control was obtained using the car body vertical acceleration whilst fuzzy-logic control was used for the nonlinear complementary control. The model used in the work was a half-car subjected to the uneven road surface. The mean squares of the vehicle body response was to be minimised in order to determine fuzzy control rules, taking into account some specific constraint such as the suspension working space and tyre deflection. The objective was to minimise vertical and rotary acceleration of the vehicle body in order to ensure the ride comfort criteria. Simulation results showed that the proposed active suspension system was effective in improving the ride comfort and gave

satisfactory performance for the mentioned constraints. One issue with the proposed method was the assumption that the vehicle body vertical acceleration, velocities, and displacements at the front and rear suspensions were measured at each time sampling instance, making the implementation of the proposed method in practical application difficult.

In [53] Sun and Sun set up an active suspension model based on an adjustable fuzzy controller to improve the ride comfort and road holding. The authors argued that the proposed method would not only illustrate the benefit of fuzzy logic concept but would also overcome the drawback of general fuzzy control methods that rely on experience. The Least Mean Square (LMS) adaptive method was applied for fuzzy control, simulation results of a tow degree of freedom quarter vehicle suspension model subjected to road input (simulated as PSD signal) showed that the proposed method improved the sprung mass acceleration, in addition to the vehicle handling safety.

An optimal adaptive control law to design an active-passive suspension system was presented in the works of Giua et al. [54] and [55]. The proposed method switched between different constants of state feedback gains which ascertain a compromise between performance and power needs. The optimisation process was carried out to minimise a performance index which penalises the suspension and tyre deflections whilst ensuring that the magnitude of the forces generated by the actuator and the general forces that applied between the car body and the wheels remained within the set limits. It was pointed out in this work that as a strict bound on the magnitude of the control forces was imposed, reduced performance in terms of sprung mass displacement would be obtained. Also the designed law required the knowledge of the system state that was usually not directly measurable.

Chantranuwathana and Peng [56-59] have dedicated their work to Adaptive Robust Control (ARC) for designing active suspension controllers that achieved desirable performance by compensating for the dynamics of the hydraulic actuator. ARC developed from combining the benefits of Deterministic Robust control and Adaptive control methods. The main advantage of the ARC is its ability to guarantee both the transient and steady-state tracking accuracy. In [56] the authors proposed an

active suspension system controller where the desired force was calculated by the main-loop while the Adaptive Robust Control technique was used by the sub-loop to track the control forces and to keep it close to the desired forces. Due to the cost of the force cell, it was replaced by a force observer to estimate the force values which required adaptation of the used sup-loop. Simulation results of a quarter-car model showed that the suggested ARC controller performed well in comparison to the PID controller. Then in [57] the authors tried to show the experimental verifications of the proposed method which appeared to achieve a reliable force tracking up to 5 Hz. In [58] they modified their work and tried to identify the cause of unreliable force tracking performance above 5 Hz, particularly when high frequency disturbance was present. They argued that the unmodeled dynamics such as the delay in implementing the control signal was the main cause of the problem, and introduced three controller modifications to reduce the effect of the unmodeled dynamics. In [59] a modified technique called Modular Adaptive Robust Control (MARC) was introduced to design the force-loop controller of an electro-hydraulic active suspension system. The major advantage of the modular design method was the ability of designing the adaptation algorithm for clear estimation convergence, guaranteeing a certain control performance since the effect of parameter adaptation on force tracking can be compensated. The experimental results showed that MARC controller achieved the task of force tracking up to 10 Hz for ride comfort and up to 2 Hz for tyre deflections, which could be an adequate improvement.

A novel approach was proposed by Fialho and Balas [60] in which linear parameter-varying control (LPV) was used with the nonlinear backsteping method to design a road adaptive active suspension system. The authors aimed to minimise the car body acceleration taking into account the suspension deflection restrictions. As these two criteria conflict each other, the proposed suspension controller focused on minimising the car body acceleration when the suspension deflection was small, while it minimised the suspension deflection when the deflection approached the limits. The switching procedure was based on the suspension deflection which was used as a measure of the road condition. Nonlinear simulations using a quarter car suspension model that made use of a nonlinear dynamic model of the hydraulic actuator showed that the proposed technique managed to provide a good ride comfort for different road conditions. A similar approach was done by Liu and Luo [61] in

which the gain scheduling technique was used to develop an adaptive control strategy of a vehicle active suspension system. A combination of LQR control with nonlinear backsteping methods was used to design the active suspension controller. Similar to the above work the proposed method aimed to provide an optimal performance of the suspension system so it can adapt to changes in road conditions. Simulation results showed the feasibility and effectiveness of the proposed method.

Setting up an accurate dynamical model to design a model-based controller for an active suspension system with a hydraulic actuator is very difficult due to the nonlinearity and time-changeable characteristic of the system. Therefore, Chen and Huang in [62] and Huang and Chen in [63] proposed a functional approximation based adaptive sliding controller which uses a fuzzy compensator to control the sprung mass response of quarter-car suspension system subjected to different road surface inputs. Numerical results in [62] and experimental results in [63] showed that the proposed technique successfully decreased the sprung mass oscillations for better ride comfort and improved handling ability.

Aiming toward simpler and achievable implementation of output feedback control of automotive active suspension systems, Hayakawa et al. [64] showed that using similarity transformation could provide a "block-coupled" [64] of a linearized 7-degree of freedom full-car model, considerably reducing the controller complexity. The robustness of the proposed method was guaranteed by implementing the robust H∞ controller of the block-coupled system that took into consideration uncertainties that resulted from the unmodeled dynamics, the variations of the parameters and nonlinear behaviour of the real system. Three different experimental tests were conducted using a commercial car, a shaker test in which the proposed method improves the car body acceleration at 2 Hz but slightly increased in the 3-7 Hz range, bad road test in which the vertical acceleration of the vehicle improved at the 2 Hz range but not below the 1 Hz, and the lane change test in which the lateral body levelling was substantially improved but the authors neglected to mention the acceleration response in the final test.

A constrained H_{∞} active suspension system design was proposed by Chen et al. in [65]. The authors argued that the formulation of the active suspension control

problem as a disturbance reduction problem with hard constraints of the time-domain would be more natural. The Linear Matrix Inequality (LMI) approach was used to optimise an active suspension system of a half-car model in such a way to achieve the best viable ride comfort while maintaining the control inputs and the suspension strokes to be in the permissible bounds as well as keeping a good wheel-road contact. The simulation results showed the ride comfort improvements achieved using the proposed method while keeping the other conflicting criteria within the predetermined bounds. In addition, they demonstrated that the proposed design can overcome the degradation of the system performance due to the actuator dynamics.

A delay-dependent H_∞ controller was designed by Du and Zhang [66]; the proposed method involved designing a memoryless state feedback control law that required solving certain delay-dependent matrix inequalities using standard numerical algorithms. The proposed controller was used to control a quarter-car active suspension system subjected to different road disturbances. The main contribution of this work was including the time-delay in the control loop at the H_∞ controller design stage. Previous works assumed that the control input could be directly realised without any time delay, method proved to be not viable to implement practically. Simulation results showed that to some extent the proposed controller including the actuator time delay could effectively improve the vehicle performance.

The concept of sliding mode control was used by Yoshimura et al. in [67] to build a quarter car active suspension system. The switching function and equivalent control were utilised to construct the proposed active control system. LQ control was used to find the sliding surface where a linear system was transformed from its exact nonlinear system. A pneumatic actuator was used to provide the control forces generated by the non-negligible time delay controller. Sinusoidal and random roads were used as inputs in the experimental tests, where a minimum order observer was used to estimate the road profile. Results showed the improvements in oscillation reduction achieved by applying the proposed design in comparison to the LQ based control and passive control design.

A new approach that used Proportional Integral Sliding Mode Control (PISMC) for the design of an active suspension system controller was proposed by Sam et al. in

[68, 69]. The authors argued that the proposed controller was capable of overcoming the mismatched condition problem caused by the road profile in the system as a result of the phase difference between the disturbance input and the actuator input. The effectiveness and robustness of the proposed design were evaluated by comparing its performance to both the LQR and the passive suspension system. Simulation results on a quarter-car model showed that the proposed PISMC design system was able to improve the ride comfort while maintaining the road holding criterion. These results were insufficient to persuade Ji et al. in [70] in which they argued that there was incorrect evidence in the mentioned work, and the theory proposed is not enough to claim that the PISMC is more robust than the LQ regulator method.

To avoid the risk of damage due to car vibration and guarantee safe driving, Chamseddine et al. in [71] proposed a Sliding Mode Controller (SMC) for a full vehicle active suspension system. The authors highlighted the issue of sensors availability from prototypes and at industrial level (availability, cost and procedures to obtain necessary data). They mentioned that in many works the designed control strategy required all state of the system to be known. The problem with the proposed technique six out of fourteenth states should be known. The simulation results showed that the proposed controller of the active suspension system improved the ride comfort for the values below the frequency of the wheel, but showed no sign of improved performance at the wheel frequency. Moreover, the author argued that if the road input is rough there would be slight improvements.

The preview control concept was used by Thompson and Pearce [72] to design a linear active preview-type suspension system for a half-car model excited by step units. The computation process for optimal control involved solving the Lyapunov and Riccati equations. The effect of increasing the preview sensor distances on the performance index was studied and the results showed that the half-car performance with inclusion of the preview concept was significantly better than the performance using only the state feedback.

Roh and Park [73] investigated the preview control with an estimation scheme designed for an active suspension system that utilised look-ahead sensors. They

presumed imperfect and noisy measurements of the states and the road input before deriving the solution for the stochastic optimal, output feedback, preview regulator problem which was reduced to a LQG problem. The previewed road input dynamics and the original system dynamics were augmented to solve the LQG problem. Numerical examples of a quarter car model were given to validate the improvements of the performance achieved by the proposed preview control. To a certain extent, the further the preview distance, the better the controller performance. Nevertheless, it was found that the imprecise velocity information of the vehicle could result in deterioration of the preview control performance. While Kim et al. in [74] designed a road profile measuring system based on road sensing technique, where an algorithm was developed while the measured data was intermixed with the vehicle dynamic response. To improve the frequency response of the system, a two sensor system constituted a composite sensor which was designed to enable an optimally shaped transfer function to be obtained. The Preview control with the proposed sensing system was used to improve the performance of a 7-degree of freedom full car active suspension system. The results showed that improvement could be achieved while maintaining the suspension working space in comparison to the passive and non-preview active suspension systems.

Preview control was also used by Marzbanrad et al. in [75] to overcome the limitation of active suspension systems related to the servo control system which should react rapidly to reduce the effects of the disturbances encountered by the vehicle. Two non-contact sensors were fastened to the front bumper of the vehicle to supply information pertaining to road elevation a short distance from the left and right sides of the vehicle. A full-vehicle model subjected to different white noise models as road input was used for analysis. Simulation results showed that the designed optimal active suspension system with preview control was effective in improving the performance index and vehicle response to rough road disturbances. However, the preference of the designer would directly affect the vehicle response to the generated disturbance. For example, the acceleration response of the optimal preview control in case of ride comfort preference was much lower than the acceleration response regarding the road holding preference, while tyre deflection and suspension working space were higher. Similar work was completed by Marzbanrad et al. in [76] using a four-degree of freedom half-car model. The relative

velocities between vehicle body and the unsprung mass in the front and rear suspension spaces were the only accessible parameters for measurement. The full state of the car needed to be estimated using the concept of Kalman filter and LQG controller.

A new scheme which uses the spectral decomposition method to calculate the RMS values of the control forces, suspension and tyre deflection, was proposed by Thompson and Davis [77]. A half-car model supported by an optimally controlled active suspension system with preview was used in this study. The authors argued that the proposed technique was able to overcome the limitations of the previously suggested method to directly compute RMS values at low vehicle speeds. The proposed method was however impractical as it was based on the assumption that the actuator forces were directly applied without considering the additional dynamics that should be compensated.

Recently, Jonasson and Roos [78] proposed an electromechanical wheel suspension system, in which electric levelling and damper actuators were attached to the upper arm of the wheel suspension. The electric levelling actuator would actively alter the car body corner level throughout roll and pitch motions at low bandwidth 1-5Hz, while the fully active damper actuator would act at higher frequencies > 5Hz. A skyhook control technique was used for the active suspension control law, and the controller parameters and spring rates were optimised using Genetic Algorithm. Simulation results of a quarter-car model subjected to different road inputs showed that the proposed design improved the car body isolation while at the wheel-hop frequencies there was less improvement when compared to the passive suspension performance. The authors argued that this occurred due to the adopted control law.

Yoshimura and Takagi [79] built a pneumatic active suspension system for a quarter-car model using fuzzy reasoning and disturbance observer techniques. The pneumatic actuator provided the system with the desired control force and to overcome the performance degradation of the model caused by the actuator time delay, a phase lead-lag device that worked as a compensator was inserted after the sensors to measure the displacement, velocity and acceleration time responses of the car body. The proposed disturbance observer effectively estimated the road excitation based on

the road profile. It was revealed by the experimental results that vibration suppression performance was enhanced by the proposed active suspension system with the disturbance observer along with the robustness of the active control.

A full car dynamic model with passengers was proposed by Kruczek and Stribrsky [80]. The model was build up by connecting four quarter-car suspension models using solid rods and taking into account the moment of inertia of the pitch and roll motions. The authors attempted to provide directions on simulating the car behaviour and to make it easy for simulation software implementation, particularly for the design of active suspension system. They also tried to include the steering wheel and tires influence on the motion into their model. Many issues had to be neglected to overcome the complexity and nonlinearity of some processes such as cornering in order to simplify the implementation of the software model.

Backstepping control was used by Yagiz and Hacioglu in [81] to design an active suspension system for a 7-degree of freedom non-linear full vehicle model. The authors argued that the stability of the system was guaranteed as the backstepping control offered a systematic process of the Lyapunov functions construction and related feedback control rules. The work aimed to improve the ride comfort of the passengers taking into account the pitch, roll, and heave motions of the vehicle body and the bounce motion of the wheels. Simulation results showed the robustness of the proposed method and ride comfort improvements achieved when the model was subjected to different road inputs even with parameter variations.

Trying to solve the multi-objective control problem of a vehicle active suspension system that contains uncertain parameters, Gao et al. [82] proposed a new design of a load-dependent controller. The main difference between the proposed approach and previous methods was the control gain matrix, which was not a constant gain matrix that would be used for all values of the vehicle body mass. Instead the proposed controller gain matrix depended on the body mass information which was not difficult to be obtained online. The proposed method could therefore account for any change in the sprung mass of a quarter car model considering other requirements such as ride comfort, road holding, suspension working space and maximum control forces. Simulation results showed that the load-dependent controller method was able

to provide the desired control where the constant controller approach failed to find possible solutions for certain changes in the car body.

A stochastic multi-objective optimisation technique to design a vehicle suspension system was proposed by Gobbi et al. in [83]. The relative displacement between the vehicle body and the wheel, the vehicle body acceleration and the force acting between wheel and road were considered as the performance indices for the optimisation process, the technique aimed to optimise the stiffness and damping for vehicle passive suspension system and the gains of the controller of the vehicle active suspension system. The authors tried to develop a mathematical expression to describe the relation between the vehicle design parameters and performance indices. The compromise solutions were derived in a deterministic and in a stochastic framework. The obtained result formed analytical rules which could be used in the initial design stage of vehicle suspension systems.

Elbeheiry and Karnopp [84] designed a stochastic LQG controller to be applied in five different types of suspension system designs and to solve the problem of the limited-state regulator they developed a new generalized algorithm. The suggested policy for adapting the suspension system was based on suspension deflection. The performance index of a quarter-car model, containing a weighted sum of variances of the acceleration of the sprung mass, suspension deflection, tyre deflection and the control forces, was used in the optimisation process to find the best possible isolation. Simulation results showed the superiority of the fully active suspension performance, especially for large road disturbances and the ability to control the sprung mass response for majority of the exciting frequencies. This performance decreased at low road disturbance levels where the other control method displayed better road holding capability.

Choi et al. [85] proposed an algorithm for a new control system design which utilised the properties of both LQR and the Eigenstructure assignment method. The new algorithm eliminated drawbacks imposed by each method, with the LQR method providing the full state feedback stability robustness and the Eigenstructure assignment with the flexibility of shaping the closed-loop system response. The proposed method was applied to an active suspension control system for a half-car

model, where simulation results showed that the proposed method reduced the peak values of the vertical and angular acceleration of the car body assuring good ride comfort.

Singular value inequalities and optimal control theory were used by ElMadany and Abduljabbar [86] to design a linear multivariable controller in the frequency domain for a quarter-car active suspension system. To assess how the order being followed and the robustness of the proposed controller to the errors of the low-frequency modelling and noise disturbances the Singular value analysis was used. The author addressed the major problems of applying LQR and briefly presented techniques used in literature to overcome these problems. The optimisation process was carried out to minimise a performance index that comprised the ride comfort, suspension working space, tyre deflection, the overall system stiffness and control forces. The proposed method offered a systematic procedure that guaranteed the compromise between performance and robustness in the design of linear quadratic Gaussian based multivariable control. An estimator was designed based on Kalman filter to realise the controller full state feedback, as state variables were not completely accessible from direct measurements; moreover, it was contaminated with noise. The simulation results showed the efficiency of the proposed method in providing outstanding attitude control without degradation in the ride comfort provided by the controllers with state variable feedback.

The traditional linear quadratic regulator (LQR) method was also used by Sam et al. [87] to design a quarter-car active suspension system controller. The method involved obtaining the control forces that would improve the ride comfort quality. Simulation results were generated using a quarter-car suspension model subjected to a step and random input signals. They showed that the LQR controller could be regarded as a good quality solution for road holding and outstanding ride comfort.

Taking into account the performance requirements and the model uncertainties, Gaspar et al. [88] constructed the linear parameter-varying (LPV) technique to be applied to a vehicle active suspension system, using the parameters dependent gains they guaranteed the compromise between the performance demands of ride comfort, suspension deflection, tyre deflection and control forces. The LPV approach allowed

the designer to consider the prevalent non-linear effects in the description of the state space to enable the structure of the model to be nonlinear in the parameters but linear in the states.

Genetic Algorithms were used by many researchers as an optimisation tool to achieve a good compromise of the suspension systems conflicting criteria of ride comfort, road holding, suspension deflection and maximum control forces; for example, Tsao and Chen [89] used a Genetic Algorithm (GA) in the design of a half-car active suspension system, where the GA was applied to search for the parameters of damping ratios and springs stiffness to achieve an optimum compromise. Simulation results showed that the proposed technique was capable of improving the ride comfort while maintaining the suspension deflection. They also showed the effectiveness of employing a GA, as a few solutions were used in the search space to find acceptable results and the objective function swiftly decreased. Sun et al. [90] also proposed a useful method for solving the design problem of an active suspension system, in which the compensator worked to reject the disturbances and to endure the body mass variations. A new stability condition to deal with the system uncertainties was derived, and a simple Genetic Algorithm was used to obtain the elements of a robust controller in such a way to minimise the H_2 norm based on an objective function that involved stability conditions. A Genetic Algorithm was also used by Du et al. in [91] to solve the problem of the static output feedback H∞ controller design and non-fragile controller using a quarter-car active suspension system model. The designed non-fragile static output feedback proved to have better a non-fragility features in comparison to the static one under the same performance level. He and McPhee [92] used Genetic Algorithms to optimise the combined mechanical and control model in a multidisciplinary design optimisation for a quarter-car active suspension system. In the proposed method a multibody dynamic software package was utilised to design the linear mechanical model of the vehicle. The linear quadratic Gaussian (LQG) method and Kalman filter were used to construct the controller and the estimators. Simulation results when applying the proposed method for the system subjected to both deterministic and random road inputs, showed that the multidisciplinary optimisation based active suspension system improved the vehicle performance in comparison to the conventional LQG method.

Genetic Algorithms (GAs) and Neural Networks (NN) were used by Chuanyin and Tiaoxia [93] to design an active suspension controller. The GA was used to optimise the acceleration of the vehicle body which would be used as the NN control system objective output. A four-degree of freedom half-car model subjected to road disturbances was used in this study to compare the performance of the proposed controller with the performance of LQG (Linear Quadratic Gaussian) controller. Simulation results showed the effectiveness of the proposed controller in determining the suspension performance, especially rotary acceleration. The authors also stated that this controller was not suitable for real-time control due to the excessive time duration for the computational procedures.

Kumar in [94] proposed a new approach to design an active suspension system for a quarter-car model using proportional derivative controller in a closed loop circuit with suspension travel feedback to improve the vehicle performance. The parameters of the proportional and derivative controller were optimised by Genetic Algorithm. The objective function aimed to minimise the sprung mass acceleration peak overshoot and settling time with the constraints of suspension travel limits and tyre deflection. Simulation results of applying the proposed technique to control a quarter-car model subjected to random road disturbances showed the performance improvements achieved in terms of acceleration overshoot peak and suspension and tyre deflection. To demonstrate the effectiveness of using evolutionary methods as an optimisation technique to solve the active suspension system design problem, Shirahatt et al. [95] used Genetic Algorithms (GAs) to optimise the parameters for a full-vehicle active suspension system at the design stage. The Linear Quadratic Regulator (LQR) was used for the active suspension control. The work illustrated that similar performance measures were obtained when comparing the GA obtained results to the ones obtained using the simulated annealing optimisation method. Superior improvements achieved in ride comfort and road holding had a detrimental effect on the performance of active suspension travel when compared to the passive system performance. Du and Zhang in [96] proposed a H_∞ and generalized H_2 (GH_2) static-output feedback controller design method, in which the control gain matrix was obtained using the stochastic search capability of a GA and solving the associated Linear Matrix Inequalities (LMIs) of the system. The method aimed at

improving the ride-comfort performance considering the road- holding, suspension deflection and maximum control force limitations. Simulations carried out on a four-degree of freedom half-car model subjected to both bump and random road inputs showed that the proposed method was able to improve the vehicle suspension performance when compared to the state or the dynamic-output feedback control.

The main aim of the literature stated above was to give the reader an idea regarding different categories of suspension systems (i.e. passive, semi-active and active) and different methods used to control these systems, particularly the works that have been done in the area of active suspension system. it is clearly seen that the research in the area of active suspension systems has vastly increased, aiming at better performance, lower power consumption and less complexity. As better performance involves attaining a good compromise or at least improving the criteria of interest without any degradation of the other suspension criteria, the improvement achieved in many of the mentioned works came at the cost of other criteria being degraded particularly [36, 37, 39, 41, 42, 43, 44, 47, 48, 49, 50, 64, 71, 75, 76 and 78] in which the other suspension criteria being badly affected or even not mentioned.

Moreover, methods such as the ones presented in [38, 40, 44, 45, 46, 47, 54, 55, 57, 60, 61, 67, 68, 69, 82, 84, 85, 86, 87 and 88] that used conventional methods such as proportional integral derivative (PID), linear quadratic, linear quadratic Gaussian, linear parameter-varying control and classical optimal theory needed information regarding the full system states or some of them that might be inaccessible or very difficult to be measured and require the use of a large number of sensors. Additional problems related to the sensors/actuator placement in practical applications may arise together with the possibility of contaminated signals in a noisy environment which usually need conditioning using filters, increasing the total cost of the system.

In addition, methods that used the modern intelligent control theory (H_∞, fuzzy logic control and artificial intelligent techniques) such as the works presented in [50, 51, 52, 53, 62, 63, 65, 66, 79, 90, 91, 93, and 96] achieved good results but they are complex raising the difficulty of the implementation issue. Another important concern that arises for some of the proposed methods is the application in real-time

control. Many of the method that achieved well through simulation will fail to achieve a similarly good performance in reality such as the work in [93].

The methods that used Genetic Algorithm (GA) as an optimisation tool such as in [89, 90, 91, 92, 93, 94, 95 and 96] clearly stated that GA was used to obtain the best values of the system parameters or to tune the parameters of the control methods which could results in good performance of the system subjected to a certain inputs.

Motivated by the desire to find an alternative method that can overcome some of the above mentioned problems, the work carried out in this study is an attempt to develop a real-time control strategy that minimises the system vibration when it is subjected to an external arbitrary excitation, regardless of the disturbance nature and without the need to access the system state, utilizing the properties of Genetic algorithm as a powerful optimization tool. The new method is called "Convolution based Control Force Strategy" (CCFS), which provides a real-time control strategy based on the concept of Convolution Integral. The new method will be explained and verified through simulations and experiments in the following chapters.

Chapter 3

3. The Novel Method "Convolution based Control Force Strategy"

3.1. Introduction

The novel method proposed in the current work "Convolution based Control Force Strategy (CCFS)" may provide a useful insight in the area of automotive suspension system design. The method is simply based on the well known concept of Convolution integral. Convolution Integral has been used in literature to find the response of linear systems under an arbitrary external excitation by knowing the system response to an impulse input. To explain how Convolution works the following concepts should be introduced.

3.1.1. The Linearity Concept

Usually if the system output is proportional to its input it is said to be linear [97]; however, linearity also involves the following properties:

- **Additivity property**

Additivity implies that if a system is subjected to a number of inputs, then the entire effect of these inputs on the system can be established by taking into account a single input at a time and assuming that the other inputs are zeros [97]. As a result, the total effect can be found by summing the effects of all components. In other words, if y_1 is the effect of applying the input x_1 to a linear system (LS) and y_2 is the effect of applying another input x_2 alone, then, if the systems is subjected to both inputs ($x_1 + x_2$) the overall outcome will be ($y_1 + y_2$) as shown in Fig 3.1 [97].
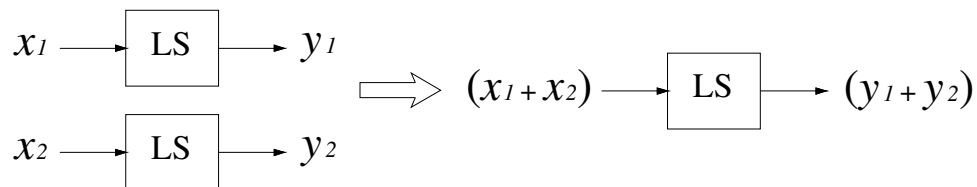
Fig 3.1 The Additivity property.

- **The Homogeneity (scaling) property**

Homogeneity declares that amplifying the input *x* by *k*-fold, will lead to increase the effect *y* by *k*-fold as shown in Fig 3.2 [97], where *k* is a real or imaginary number.

$$x \longrightarrow \boxed{LS} \longrightarrow y$$

$$k\,x \longrightarrow \boxed{LS} \longrightarrow k\,y$$
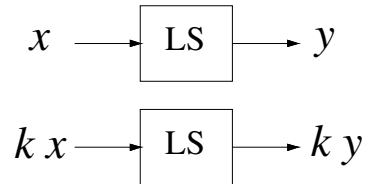
Fig 3.2 The Homogeneity property.

The above mentioned properties are combined into the *superposition* property which can be explained as follows:

For all values of k_1 and k_2, Fig 3.3 is true for all x_1 and x_2 [97].

$$x_1 \longrightarrow \boxed{LS} \longrightarrow y_1$$
$$x_2 \longrightarrow \boxed{LS} \longrightarrow y_2 \quad \Longrightarrow \quad (k_1\,x_1 + k_2\,x_2) \longrightarrow \boxed{LS} \longrightarrow (k_1\,y_1 + k_2\,y_2)$$
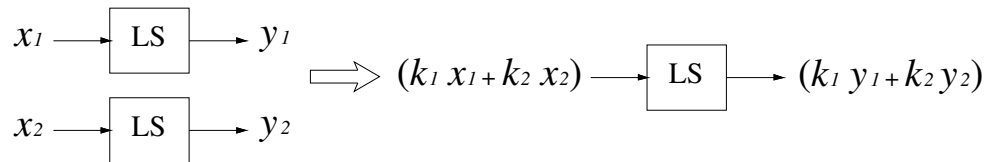
Fig 3.3 Superposition property.

3.1.2. Time invariant systems

Time-Invariant systems are the systems that have unchangeable parameters with time. This means, the output of a time-delayed input $x(t)$ by T seconds (i.e. $x(t - T)$) would be the same output $y(t)$ of the original input $x(t)$ but delayed by T seconds (i.e. $y(t - T)$). Fig 3.4 shows this property graphically [97].
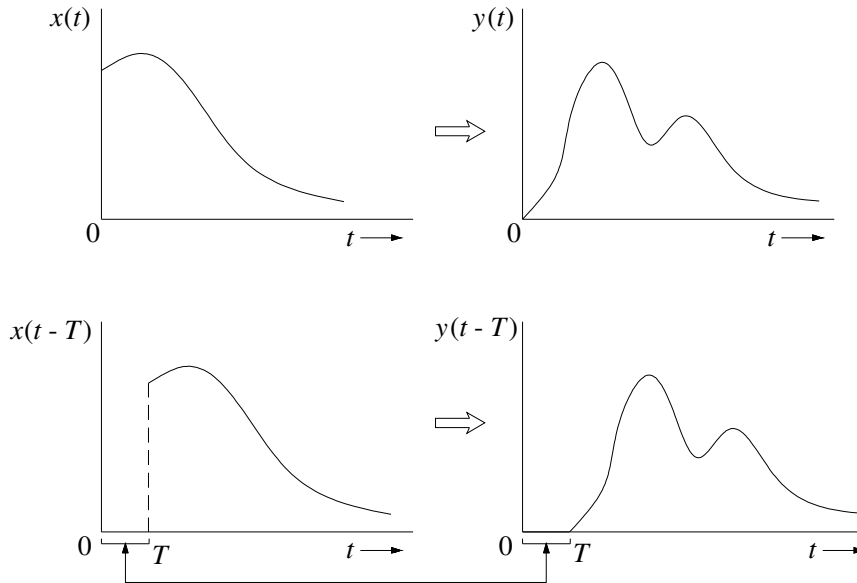
Fig 3.4 Time-invariance property [97].

To further explain this property, the output $y(t)$ of applying the input $x(t)$ to the system can be delayed by T seconds to obtain the delayed output $y(t - T)$ as shown in Fig 3.5-(a). For time-invariant system, delaying the input $x(t)$ by T seconds (i.e. $x(t - T)$) would result in the same delayed output $y(t - T)$ as shown in Fig 3.5-(b) [97].

(a)

(b)
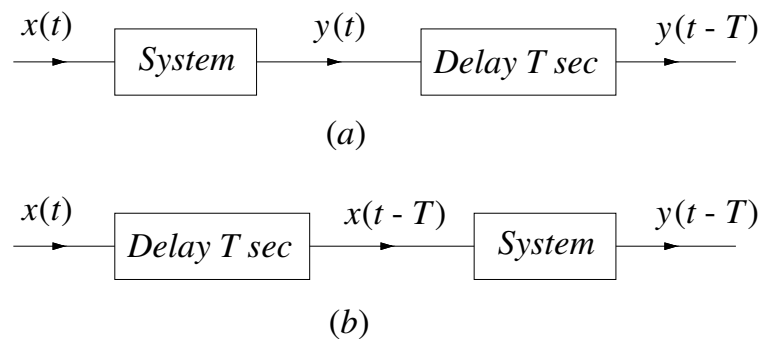
Fig 3.5 time invariant property [97].

Having introduced the important linearity and time invariant concepts, the Convolution Integral can be clearly explained as follows.

3.2. Convolution Integral

To explain the convolution concept, first the impulse response of the system should be clarified. The impulsive force can be represented by a force with large amplitude *P* acting for a very small time interval Δt [3].

In general, the impulse magnitude $\tilde{p}$ can be written as follow [3]:

$$\tilde{p} = \int_{t}^{t+\Delta t} p \, dt \tag{3.1}$$

If a pulse *p(t)* that has a unit height and $\Delta \tau$ width is considered as shown in Fig 3.6-(*a*), then any arbitrary input such as *x(t)* can be represented as a set of these rectangular pulses as shown in Fig 3.6-(*b*). For the pulse that starts at $t = n\Delta\tau$, the height would be $x(n\Delta\tau)$, this pulse can be represented as $[\, x(n\Delta\tau)\, p(t-n\Delta\tau)\,]$, where $p(t-n\Delta\tau)$ is the same pulse $p(t)$, but shifted by the time $n\Delta\tau$ [97]. As the arbitrary input $x(t)$ is a set of similar pulses, it can be expressed as follows [97],

$$x(t) = \lim_{\Delta\tau \to 0} \sum_{\tau} x(n\Delta\tau)\, p(t - n\Delta\tau) = \lim_{\Delta\tau \to 0} \sum_{\tau} \left[\frac{x(n\Delta\tau)}{\Delta\tau} \right] p(t - n\Delta\tau)\Delta\tau , \tag{3.2}$$

where, $p(t - n\Delta\tau)$ and $\left[\dfrac{x(n\Delta\tau)}{\Delta\tau} \right]$ is the pulse and the height of this pulse respectively.

Letting $\Delta\tau \to 0$ will make the height reaches infinity but the area will stay $x(n\Delta\tau)$ and the narrow piece can be approximated an impulse $[\, x(n\Delta\tau)\delta(t - n\Delta\tau)\,]$ [97]. Then the arbitrary input *x(t)* can be represented as follows [97],

$$x(t) = \lim_{\Delta\tau \to 0} \sum_{\tau} x(n\Delta\tau)\delta(t - n\Delta\tau)\Delta\tau , \tag{3.3}$$

where $\delta(t)$ is the unit impulse function.

To find the system response to the arbitrary input *x(t)*, the pairs of input and associated output are considered as illustrated in Fig 3.6-(c to f) which can be further explained as follows [97]:

$$
\begin{array}{rcl}
\textbf{Input} & \Rightarrow & \textbf{Output} \\[4pt]
\delta(t) & \Rightarrow & h(t) \\[4pt]
\delta(t - n\Delta\tau) & \Rightarrow & h(t - n\Delta\tau) \\[4pt]
[x(n\Delta\tau)\Delta\tau]\delta(t - n\Delta\tau) & \Rightarrow & [x(n\Delta\tau)\Delta\tau]h(t - n\Delta\tau) \\[4pt]
\displaystyle\lim_{\Delta\tau\to0}\sum_{\tau} x(n\Delta\tau)\delta(t - n\Delta\tau)\Delta\tau & \Rightarrow & \displaystyle\lim_{\Delta\tau\to0}\sum_{\tau} x(n\Delta\tau)h(t - n\Delta\tau)\Delta\tau
\end{array}
$$

$$\underbrace{\qquad\qquad\qquad}_{x(t)} \qquad\qquad \underbrace{\qquad\qquad\qquad}_{y(t)}$$

Consequently,

$$y(t) = \lim_{\Delta\tau\to0}\sum_{\tau} x(n\Delta\tau)h(t - n\Delta\tau)\Delta\tau \qquad\qquad (3.4)$$

$$y(t) = \int_{-\infty}^{\infty} x(\tau)h(t - \tau)d\tau \qquad\qquad (3.5)$$

The integral in Eq. (3.5) is called the *Convolution Integral* and it states that if the impulse response of the system is known, the system response to any arbitrary input can be determined using Eq. (3.5) (i.e. summation (or integration) of the scaled, time-shifted response of each impulse of the arbitrary input as shown in Fig 3.6-(*f*)) [97].

(a)

(b)

(c)

$\delta(t - n\Delta\tau)$

$0 \quad n\Delta\tau \qquad t$

$h(t - n\Delta\tau)$

$0 \quad n\Delta\tau \qquad t$

(*d*)

$[x(n\Delta\tau)\Delta\tau] \, \delta(t - n\Delta\tau)$

$0 \quad n\Delta\tau \qquad t$

$[x(n\Delta\tau)\Delta\tau] \, h(t - n\Delta\tau)$

$0 \quad n\Delta\tau \qquad t$

(*e*)

$y(t)$

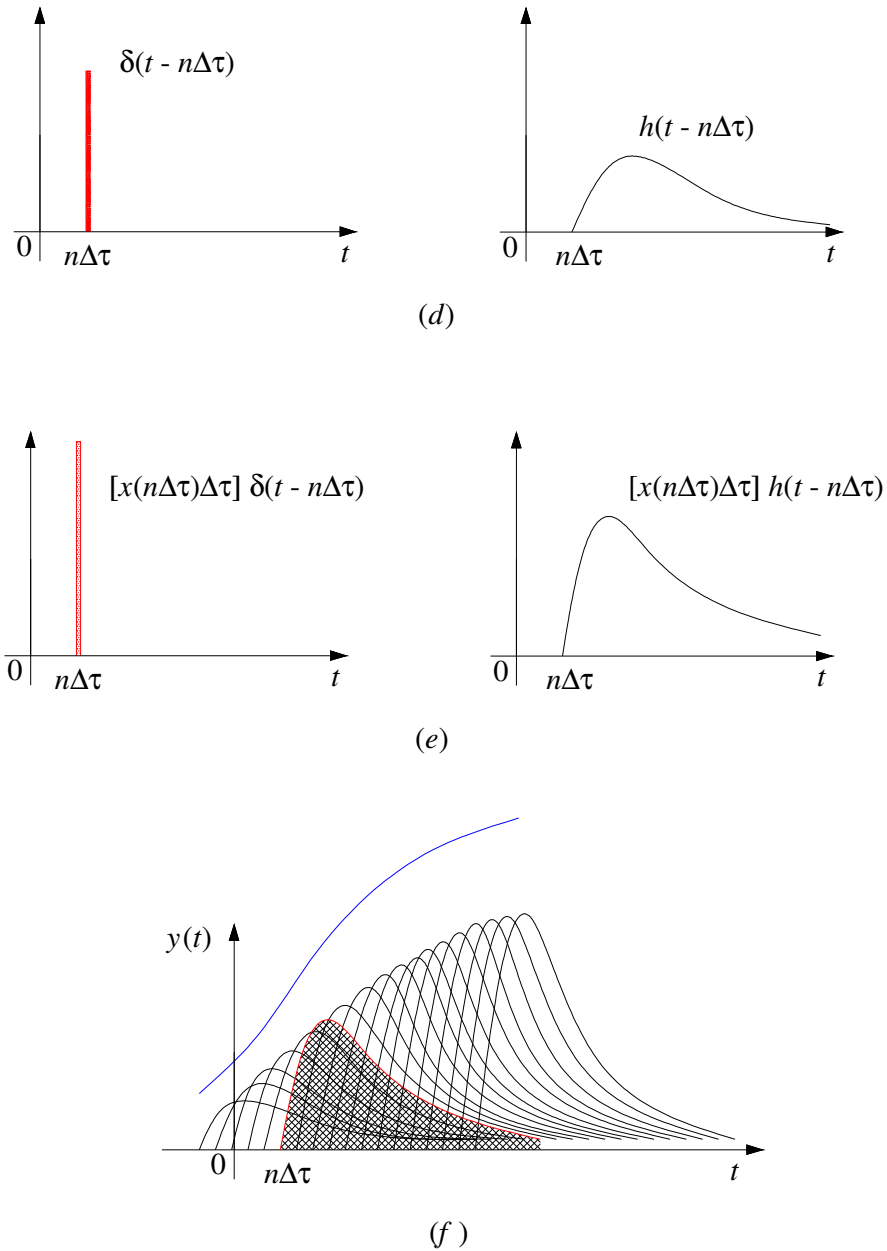$0 \quad n\Delta\tau \qquad t$

(*f*)
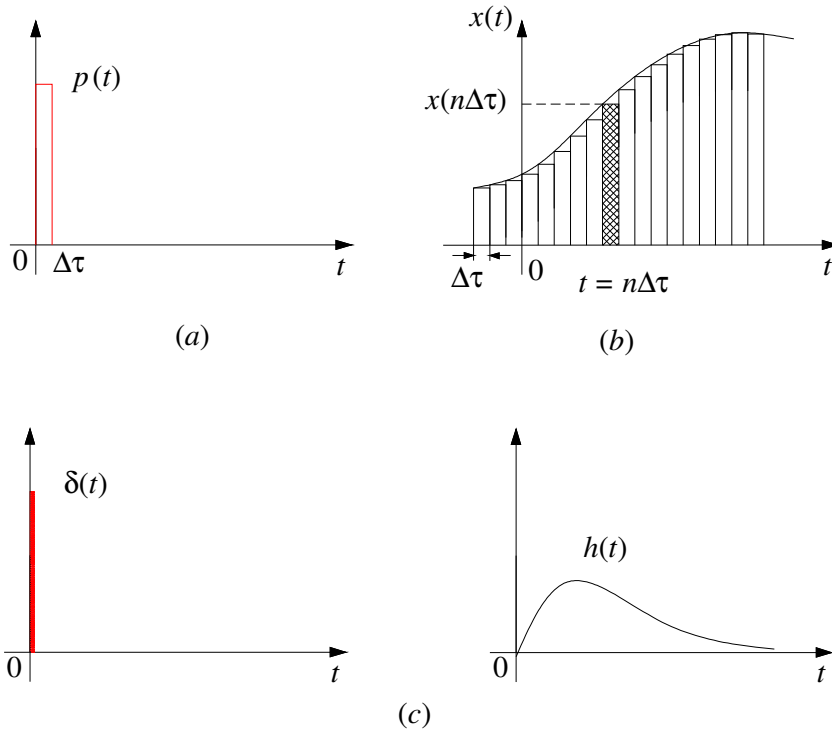
Fig 3.6 Obtaining the system response to an arbitrary excitation [97].

Where,

- ▨ : The response of the hatched strip in (*b*).

- (———): The response to each impulse of the arbitrary input in (*b*).

- (———): Summation of the scaled, time-shifted responses of the arbitrary input impulses.
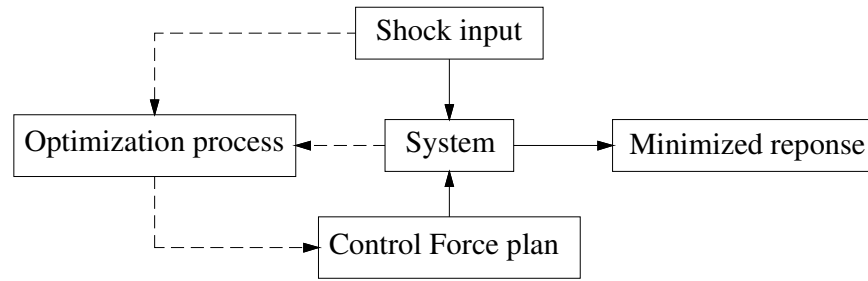
3.3. The Novel Method "Convolution based Control Force Strategy (CCFS)"

The proposed CCFS method is based on the concept of Convolution Integral presented in section 3.2. As stated before Convolution Integral has been used in literature to find the response of linear systems subjected to an arbitrary external excitation by knowing the system response to an impulse input.

The new CCFS method follows a similar approach and it is modified as follows: if the response of a system to an impulse excitation was controlled by a control strategy (optimal or otherwise) then it would be possible to obtain the control of the system when it is subjected to an arbitrary external excitation by simply scaling, shifting and summing the control strategy to the impulse input. The scaling would be according to the ratio between the unit impulse and the arbitrary excitation amplitude at each interval of integration step [98-100].

The CCFS method is illustrated in Fig 3.7, in which the method is divided into two parts:
1- The optimization method is applied to find the best *control force plan* that results in the best response (i.e. minimised response) of the system when it is subjected to a shock input as shown in Fig 3.7-(*a*).
2- Having obtained and saved the control force plan against the shock input, the *control force strategy* against an arbitrary input can be obtained using the Convolution Integral concept (i.e. scaling, shifting the optimised control force plan for each impulse of the arbitrary input) as shown in Fig 3.7-(*b*).

(*a*)
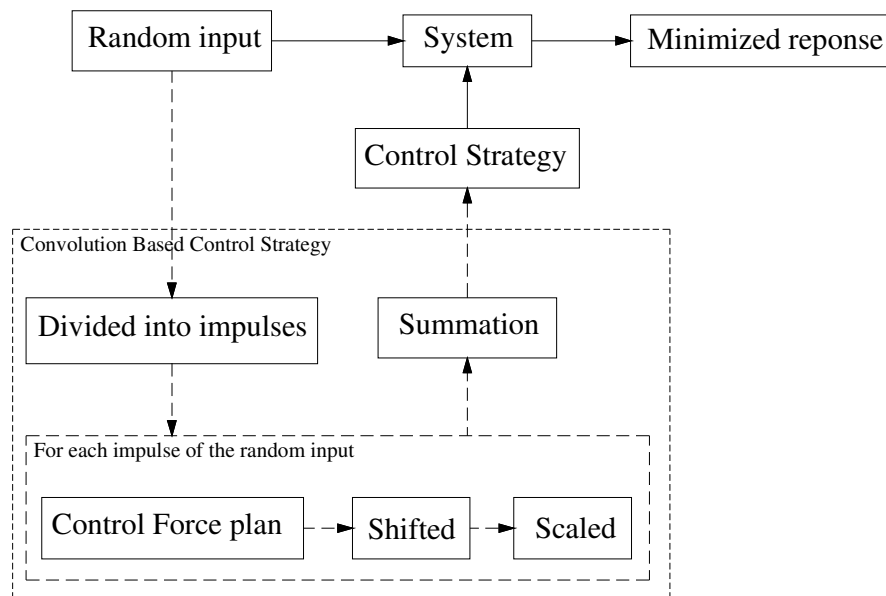
(*b*)

Fig 3.7 Schematic of the Convolution Based Control Force Strategy

To explain how the method works, a viscously under damped single degree of freedom (SDOF) spring-mass system subjected to external arbitrary excitation is considered. The equation of motion is given in Eq. (3.6).

$$m\ddot{x} + c\dot{x} + kx = F(t) \tag{3.6}$$

Where, m: is the mass of the system, c: the damping coefficient, k: the stiffness coefficient, $F(t)$: the external disturbance.

The SDOF system response to the shock input shown in Fig 3.8 is illustrated in Fig 3.9. Taking into account the *control force plan* (Fig 3.10) obtained by the

optimisation process, which would result in the best response of the system against shock input, the controlled response of the SDOF system is shown in Fig 3.11 which is much better than the non-controlled response as shown in Fig 3.12.
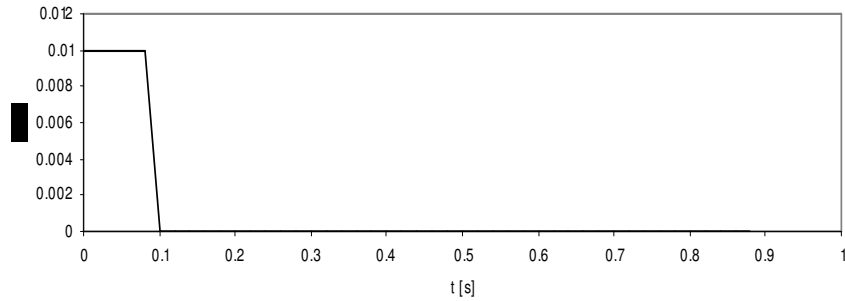
Fig 3.8 The Shock input.
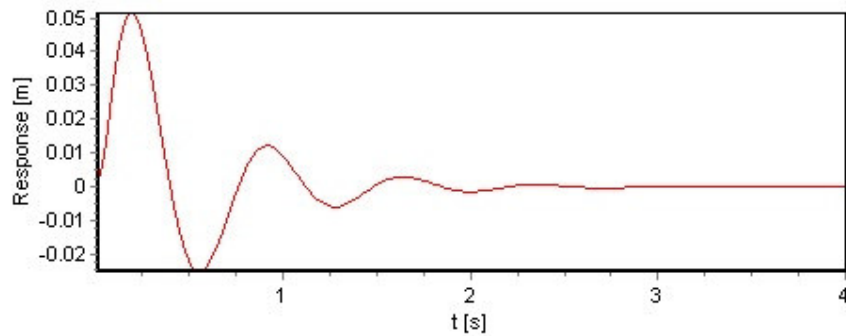
Fig 3.9 The system response to the shock input.
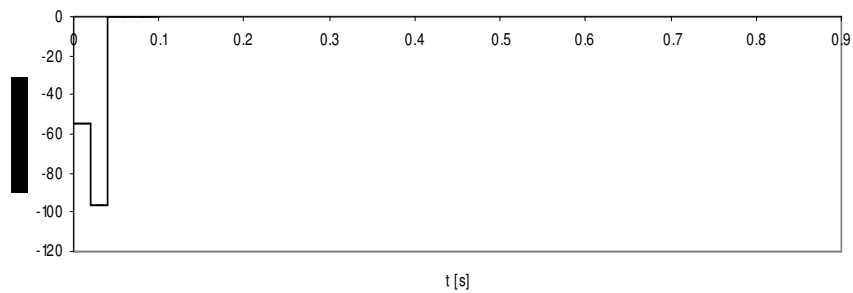
Fig 3.10 The control force plan against shock input.
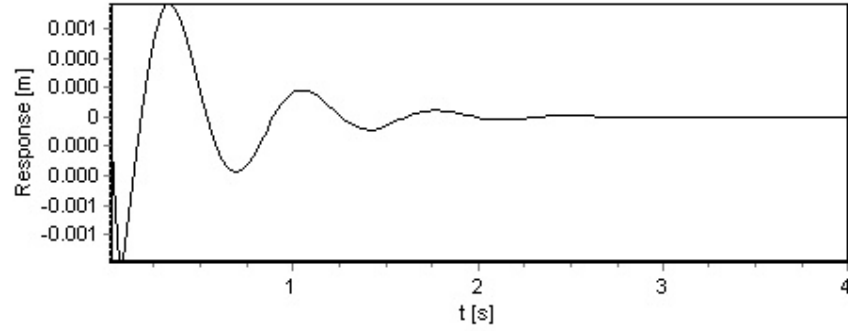
Fig 3.11 The controlled system response to the shock input.
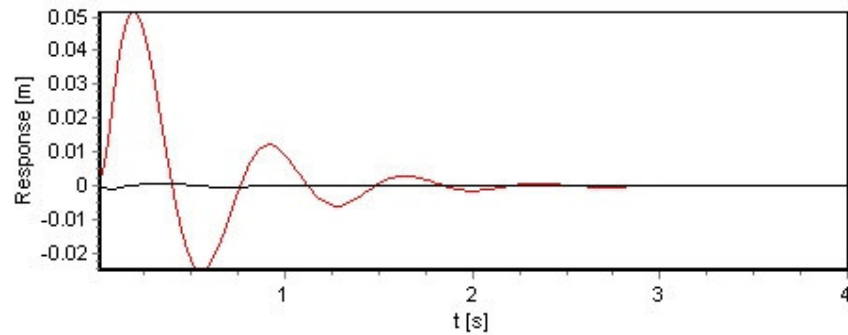
Fig 3.12 the system controlled response (——) Vs non-controlled response (——).

To control the SDOF system response using the proposed CCFS method when the system is subjected to the arbitrary excitation shown in Fig 3.13, the arbitrary excitation is divided into impulses as shown in Fig 3.14. For each impulse, the obtained *control force plan* (Fig 3.10) is scaled by the ratio (λ) given in Eq. (3.7). Then it is shifted by the same time (Δt) at which the associated impulse is applied as shown in Fig 3.14 and Fig 3.15. By summation of all the scaled, time-shifted control force plans, the overall control force strategy is obtained, which results in the best response of the SDOF system against the arbitrary excitation as shown in Fig 3.16. This response is much better than the non-controlled response as shown in Fig 3.17.

$$\lambda = \frac{the\ amplitude\ of\ the\ current\ impulse}{the\ amplitude\ of\ the\ initial\ impluse} \qquad (3.7)$$

44
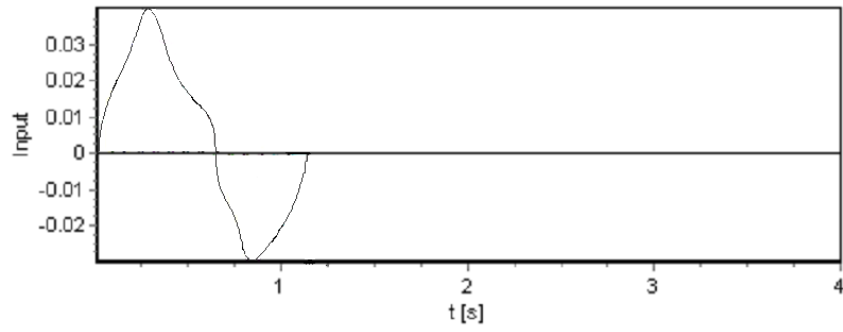
Fig 3.13 An arbitrary excitation.
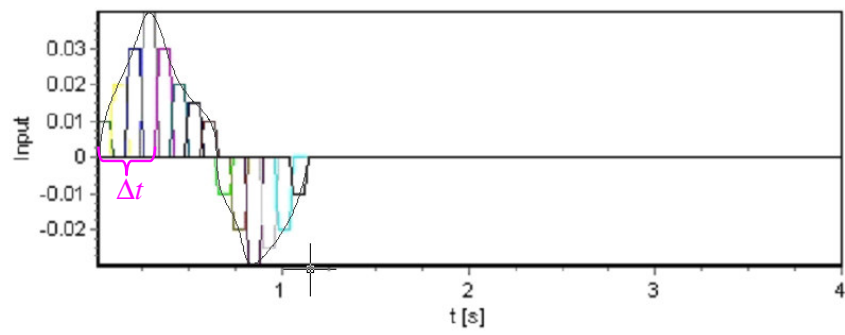
Fig 3.14 The arbitrary excitation divided into impulses.
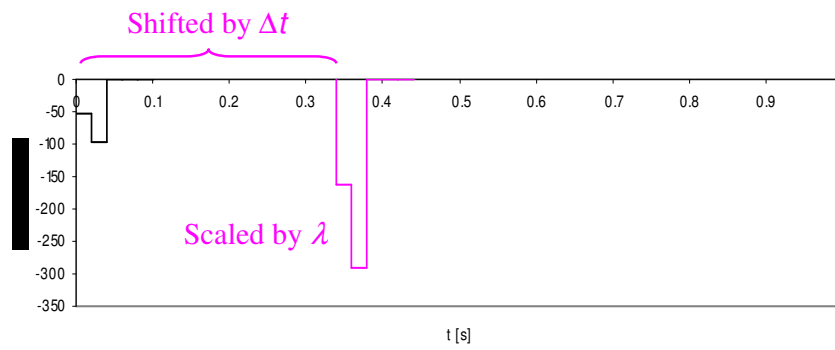
Fig 3.15 Scaled, time-shifted control force plan.

45
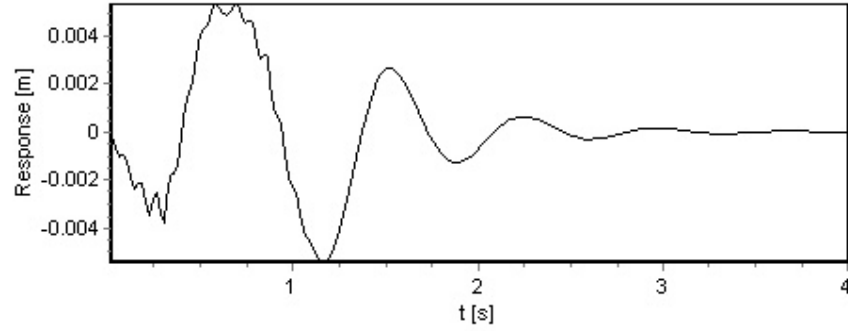
Fig 3.16 The SDOF controlled response using the CCFS method.
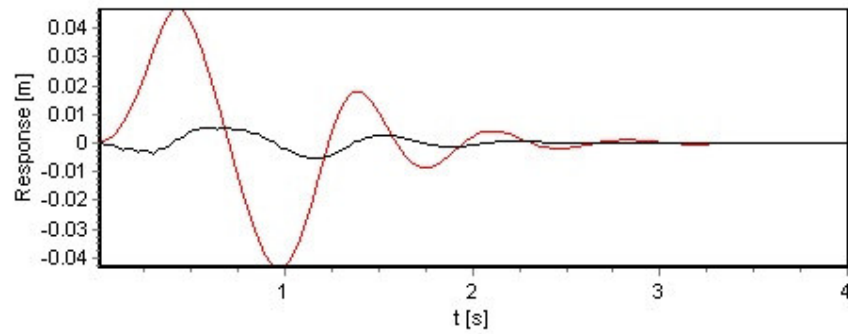
Fig 3.17 the SDOF system controlled response (——) using CCFS method Vs non-

controlled response (——).

For the proposed method Eq. (3.5) is modified to accommodate the arbitrary excitation and the control forces as follows:

$$G(\tau) = [F(\tau) + \lambda \cdot U(t - \tau)] \tag{3.8}$$

where,

$F(\ )$:   is the arbitrary excitation input function.

$U(\ )$:   is the control force plan

$h(\ )$:   is the impulse response function.

λ: is the scaling factor given in Eq. (3.7).

$G(\ )$:   is the new input function.

Consequently,

$$x(t) = \int\limits_0^t G(\tau)\, h(t - \tau) d\tau \tag{3.9}$$

46

It is possible to treat $U(\ )$ as a part of the external excitation without conflicting with the idea of the convolution integral. Therefore, the definition of the convolution integral can be applied to constitute a control strategy in order to provide an overall controlled motion.

To achieve the proposed method one should obtain the optimal control strategy to suppress the vibration of the system when it is subjected to an impulse input. To accomplish this, there are many methods from the classic optimal theory; however, Genetic Algorithm (GA) can be adopted as an alternative way to optimise the control strategy which will be explained in details in the following chapter. Having obtained the control strategy, the results can be used to obtain the general control strategy against any arbitrary excitation as described above.

What is interesting and makes the proposed method powerful is that it can be used for real-time control situations. With the control strategy for the impulse disturbance being determined, this strategy can be applied at each time step when online control is needed, so the system can be controlled in real-time irrespective of the nature of the external excitation. The method involves only multiplication and saving of four numbers (the control force plan) which means a very small memory usage is needed for real-time control. This simplicity makes its implementation rather straight forward [98, 99]. Moreover, as explained in the literature part, most of the control methods need to access and measure the system states or at least some of them in order to construct the appropriate control strategy, while in the proposed method the only input needed is the amplitude of the disturbance. Consequently, this will results in less number of sensors to be used in the system thus less measurements of signals which could be contaminated by noisy environment. Finally, the CCFS method is a generic method that can be applied in many other fields.

Chapter 4

4. Optimal Control and Optimisation

4.1. Optimal Control

Systems in general can be represented by models described by mathematical relations, which could be deterministic and/or stochastic differential equations [101]. To change the condition of the system from one state to another, external inputs/ controls should be applied. Sometimes, assuming that this change is possible, there are many ways to carry it out, so one should search for the best manner of doing the task taking into account the constraints that limit the systems performance. The input to the system which causes the best situation to happen is called optimal control. The measure that involves finding the optimal way is called the performance index (PI) or objective function [101]. Usually the system is represented by state variables, which provide a complete description of the system. Finding the control signals, which will make sure a plant satisfies some physical requirements and does not exceed some constraints whilst minimising or maximizing a preferred performance index, is the main goal of optimal control [101]. To formulate an optimal control problem one needs a mathematical model of the system which is usually described using state space equations, an appropriate performance index, and knowledge of the constraints and the boundary conditions of the system states and the control elements [101].

4.1.1. The plant

The physical plant is expressed by a group of linear or non-linear differential equations. Eq. (4.1) and Eq. (4.2) describe the state and output equations of linear time-invariant systems [101].

$$\dot{x}(t) = \mathbf{B}x(t) + \mathbf{C}u(t) \tag{4.1}$$

$$y(t) = \mathbf{A}x(t) + \mathbf{E}u(t) \tag{4.2}$$

Where, $\mathbf{B}$ is the $n \times n$ state matrix, $\mathbf{C}$ is the $n \times r$ input matrix, $\mathbf{A}$ is the $m \times n$ output matrix, $\mathbf{E}$ is the $m \times r$ transfer matrix, $x(t)$ is the n state vector, $u(t)$ is the r control vector, $y(t)$ is the m output vector.

In a similar way, Eq. (4.3) and Eq. (4.4) describe the non-linear systems [101].

$$\dot{x}(t) = f\big(x(t), u(t), t\big) \tag{4.3}$$

$$y(t) = g\big(x(t), u(t), t\big) \tag{4.4}$$

Usually to construct the controls most of the state variables should be available, so designers assume that the system states are measurable or they build an estimator to estimate these values.

4.1.2. Performance Index

A mathematical expression formed by the designer taking into account the limitations applied to the system. This expression can be maximized or minimised while searching for the optimum solution that makes the dynamical system attain a specific goal or follow a particular trajectory [101]. Therefore the performance index can take many forms according to the problem that should be solved.

4.1.3. Constraints

The physical situation of the system to be controlled will impose some limitations that cause the state and/or the controls to be constrained. The motor speed, the suspension working space and the pressure in pneumatic system, are physical constraints which have minimum and maximum values which the designer should take them into account so they are not exceeded [101].

4.1.4. Independent Variables

The selection of the independent variables which are sufficient enough to characterize the feasible candidate designs or the system working circumstances is also a key issue in the optimisation problem formulation [102].

The optimisation process and efficiency of the chosen optimisation technique, which affect the results of finding the optimal control that fits properly the designed model, will be discussed in the following section.

4.2. Optimisation

Optimisation refers to the mathematical procedure used to obtain the best solution of the optimisation problem among many other alternatives without having to identify and assess all the possible solutions. Also it takes into account the constraints that limit the system from reaching certain performance and tries to improve that performance towards some optimal levels. Optimisation theory has been used in most engineering fields such as system component designs, analysing and planning operations and dynamic system control [102].

To solve an engineering problem by applying the mathematical methods and numerical techniques, various considerations need to be taken into account including a clear definition of the engineering system boundaries to be optimised, identifying a specific criterion based on which candidates will be ranked to find out the "best" solution, choosing the system variables through which the candidates will be identified and describing the model that will state the way in which the variables are related. All of these categories are the key issues in order for the optimisation process to be successful [102].

Many optimisation methods have been used in literature, but in this study one of the most effective stochastic optimisation methods "Genetic Algorithm" (GA) will be used. What are Genetic Algorithms? What kind of applications are they applicable for? In what ways they differ form other methods? The answers for these questions will be discussed in the following sections.

4.2.1. Genetic Algorithm (GA)

The Genetic Algorithm (GA) is a global stochastic search procedure based on the process of natural selection and genetic modifications related to the evolution in nature. It was first developed by John Holland and his colleagues at the University of Michigan in 1960s and 1970s [104]. "Survival of the fittest", Darwin's principle of natural selection, ignites the idea of mimicking natural selection and applying it to artificial life. The GA is an optimisation method that operates with a population of possible solutions of the optimisation problem; these solutions are evaluated based on their fitness values that indicate how well the optimised solution will fit or will

solve the optimisation problem [103-105]. The Genetic Algorithm terms can be described as follows:

- The population (P): The GA population consists of individuals (chromosomes) (s_i), $i =1,2,\ldots,\zeta$ [103].

$$P = \{s_1, s_2, \ldots, s_\zeta\} \tag{4.5}$$

- Individual s_i represents a possible solution of the optimisation problem. (s_i) is a υ-dimensional vector consists of υ variables (s_j) where $j =1,2,\ldots, \upsilon$. These variables are called genes [103].

$$s_i = [s_{i1}, s_{i2}, \ldots, s_{ij}, \ldots, s_{i\upsilon}] \tag{4.6}$$

- The fitness of the individual which will be used to measure how suitable an individual is as a solution to the problem; this fitness will be decided by a user defined fitness function. Individuals are usually coded either in binary or real numbers. Choosing the coding type is influenced by the nature of the problem that the Genetic Algorithm is going to solve. The simple form of Genetic Algorithm uses three types of operators: selection, crossover and mutation [103].

4.2.1.1. Selection

The selection operator chooses individuals (also called chromosomes) from the current generation's population to continue to the next generation. Picking the fitter individuals is the main strategy of the selection process, which hopefully will lead to the production of offspring with higher fitness to be selected in the next generation, a process which is repeated until termination. The higher the fitness of the chromosome, the greater the probability of this chromosome to be selected [103-104].

4.2.1.2. Crossover

The crossover operator chooses two individuals (parents) to create two new offspring [104]; consequently, the crossover operator produces new assemblage of material by swapping the genetic material between the selected individuals of the population [103]. The new offspring will provide a better solution than their parents when they take the best features from the parents [106], but the crossover strategy may lead to the loss of the good genetic pattern [103]. Although the crossover process recognises patterns, it doesn't introduce new information to the population, except that some patterns are more effective than others. After two individuals have been chosen randomly, the crossover cut points decide how the genetic material of the offspring will be made up from the material of the chosen individuals [103].

4.2.1.3. Mutation

Mutation is the occasional random change of the gene value in the randomly selected individual. If binary coding is used, the mutation operator will flip one or more randomly selected bits in the chromosome. This process occurs with mutation probability, which is usually very small with a fixed value assigned before the optimisation process. This operator gives the GA more power to explore the search space and will guarantee provided a good use of selection and crossover operators, that there will be no early loss of the important individuals [103, 105].

4.2.1.4. Termination

The Genetic Algorithm will use the termination condition to decide whether or not to continue the searching process. After each generation the termination condition will be checked by the GA to confirm if it is a good time to discontinue or not [106]. The termination criterion varies based on the purpose of the optimisation process.

As mentioned before the Genetic Algorithm is a global search tool. Indirect optimisation methods usually look for a local extremum by solving the equations that result from setting the gradient of the objective function equal to zero. Direct methods search for the local optima by climbing on the function and moving in the permissible direction associated with the local gradient. These two methods lack

robustness as they are local in scope and like other calculus optimisation methods they rely on the existence of objective function derivatives [105]. Also, the idea behind enumerative methods is straightforward, using a search algorithm to look at the values of the objective function at each point of the finite search space, one at a time. This will cause inefficiency of the method as practical search spaces are too big to be explored one at a time whilst consecutively providing useable information for practical use. This means some of these procedures may collapse for some moderate size and complexity problems [105].

The main differences between Genetic Algorithms and other optimisation techniques can be summarized as follows [105]:

- Genetic algorithms do not work with the parameters themselves; but operate with a code of the parameter group.
- Genetic algorithms do not search depending on one point; they search from a population of points.
- Genetic algorithms do not depend on the auxiliary information or the derivatives; they need just the objective function information.
- Genetic algorithms are not deterministic search techniques, because they use operators with probabilistic transition rules [105].

For the aforementioned reasons Genetic Algorithms were used in this work as the optimisation tool to find the control force strategy that minimises the system response to an impulse input as it will be explained in the following sections.

4.2.2. Obtaining the control force plane using Genetic Algorithm

As explained a Genetic Algorithm (GA) will be used to optimise the control force plan that minimises the response of the sprung mass (vehicle body) to a shock input. The optimised control strategy will be saved, and then the general control force strategy which will minimise the response of the system when it is subjected to an arbitrary excitation can be obtained using the idea of Convolution Integral.

The first step of the GA is to form an initial population. A random generation of forces values in each control force plan vector is required. The initial population is a collection of control force plans, with each plan representing a chromosome as shown in Fig 4.1.
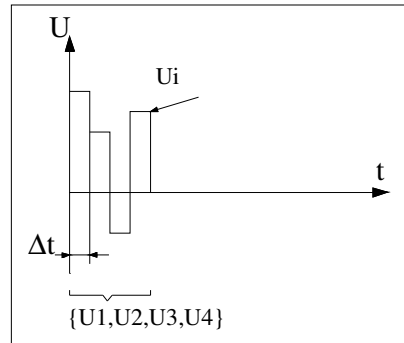

Fig 4.1 The chromosome (control force plan)

Each member of the chromosome is a control force value (U_{ij}) that corresponds to a time step, in other words, the time horizon (t) is divided into a number of steps and at each step a control force value is selected, forming a control force vector (chromosome). In this work a real coded GA is used where each variable is represented by a real number.

To generate the initial population, the following parameters values should be defined for the GA to run:

- The number of variables (NO OF Variables), which represents the number of forces. This is a user definable value.

- The Population Size that refers to how many chromosomes will be generated during each generation. For example, if the NO OF Variables is four, the Population Size will decide how many sets of four variables will be used to evaluate the Objective function.

- The search space is defined by inserting the upper and the lower bounds of each variable.

The chromosomes (individuals) of the initial population will undergo the evaluation process as shown in Fig 4.2, in which the GA uses an Objective Function (*Obj*) (i.e. performance index) to evaluate and try to select the best individuals. The Objective Function in this study is given in Eq. (4.7) and can be defined as minimisation of the sum of absolute values of all of the selected variables over a given time horizon [98-99]:

$$Obj = \sum_{i=1}^{n}\sum_{j=1}^{v}\left|x_s(t)\right| \tag{4.7}$$

Where, $t \in [0,T]$, n: is the total number of time steps, v: number of variables.
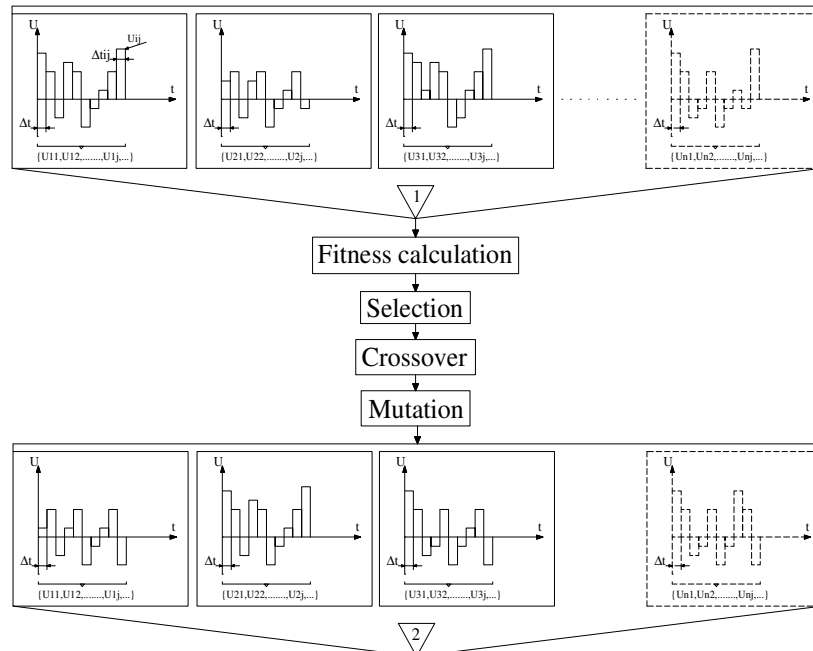
Fig 4.2 A population goes through GA operators

One can notice that there are no explicit control force terms in the objective function; however, (x_s) is the result of the external disturbance and the applied control force. To achieve the objective, i.e. minimisation of the overall response of the system, the selection of the correct control force values at each time step is required. This involves the selection of control forces on a time horizon to form the control force strategy. The evaluated individuals are assigned a fitness value dependent on how well they solve the problem.

The individuals will go through the selection process, in which each population will be "stacked" based on the ratio *R(j)* defined in Eq. (4.8):

$$R(j) = \frac{\sum\limits_{i=1}^{j} Obj(i)}{\sum\limits_{i=1}^{n} Obj(i)} \tag{4.8}$$

Where, *j* is the index of the current population, *n* is the population size, $R(n)=1$.

The ratio *R(j)* will generate a roulette-wheel which is divided into regions; the area of these regions will be in proportion with the fitness of the associated variables. The GA will generate a random number between 0 and 1 and try to find in which region this number is placed; this selection process is expected to find the large regions that represent the fitter individuals. After that the crossover operator starts, which involves the exchange of a variable between two selected individuals. The variable to be selected is randomly determined by generating a random integer between one and the maximum number of variables in each chromosome. This integer represents the variable number to be exchanged.

However, with the basic GA there is a problem, depending on the fitness distribution among the population the best individual may not get selected to the next generation. To ensure that the best individuals will not be lost in the processes, the elitism technique is utilised in the selection process. Elitism ensures that the Genetic Algorithm retains some of the best individuals at each generation. In this work it is ensured that the best individual of the previous generation will populate 10% of the next generation. The GA will iterate until an acceptable convergence is reached and a good solution (control force plan) is obtained.

To further explain how GA works with regards to the optimisation problem of finding the control force plan, a pseudo code was written to give details on how GA operates to solve the problem and gives the optimal solution as follows:

Get the following variables:

NoOfGeneration: the total number of generations

PopulationSize: the total number of populations

NoOfVariables: the total number of variables

LowerBound: the minimum value can be assigned to a variable

UpperBound: the maximum value can be assigned to a variable

FOR each generation of NoOfGeneration

      FOR each population of PopulationSize

            FOR each variable of NoOfVariavles

                  IF it is the initial generation THEN

                        Randomly generate the variables values of the first generation

                        (Each variable takes a random value between the upper and the lower bounds)

                  ELSE

                        FOR each population of PopulationSize

                              FOR each variable of NoOfVariavles

                                    Use the new variables generated and stored from previous generation

                              END FOR

                        END FOR

                END IF

            END FOR

      Compute the Objective Function (ObjFun) for each population[1]

      END FOR

      Set the value of the AccumObj to zero

      (AccumObj represents the accumulation of the Objective Function values)

      FOR each population of PopulationSize

Find the value of the AccumObj by adding the objective function value (ObjFun) of the current population to the value of AccumObj

END FOR

Set the value of MaxObj to the value of the AccumObj at PopulationSize

Store MaxObj

FOR each population of PopulationSize

Find the Ratio between AccumObj of the current population and the MaxObj

END FOR

FOR each population of PopulationSize

Randomly generate a number (RNAD) between 0 and 1 (greater or equal to 0 and less than 1)

FOR each population of PopulationSize

Find where this random number is located

IF RAND is greater than the AccumObj of the current population AND RAND is less than the AccumObj of the next population THEN

Choose the INDEX of the current population

EXIT FOR

END IF

Add 1 to the INDEX

Store the New INDEX

Select the population that has the New INDEX

END FOR

Set the value of the elitism index E-INDEX to 1

Set the Maximum value of the Objective Function (MaxObj) to 0

FOR each population of PopulationSize

'Find the Maximum value of the Objective Function

      IF the value of the Objective Function of the current population (Obj) is bigger than MaxObj THEN

            Set the value of the MaxObj to this value (Obj)

            Store the INDEX at which the Maximum value of the Objective Function is found

            Set the value of E-INDEX to the value of the stored INDEX

      END IF

END FOR

Make the population that has the E-INDEX to be selected to form 10% of the PopulationSize.

For each population of PopulationSize

      Randomly generate a variable (VAR) which has a value between 1 and the NoOfVariables

            For each variable of NoOfVariables

                  IF the variable index V-INDEX equal to VAR THEN

                        Exchange the variables between two selected populations starting from that variable onwards to generate the new populations

                        Store the new generated populations to be used in the next generation

                  ELSE

                        Keep the selected populations

                        Store those populations to be used in the next generation

                  END IF

            END FOR

      END FOR

END FOR (next generation)

Display Results

(1) The Objective Function

Set the value Objective Function (Obj) to 0

Add the absolute value of sprung mass displacement to the Obj

The value of the Objective Function (ObjFun) equals to 1 over the value of Obj

The described optimisation process that employed the GA was used to find the best control force plan to control the system when it was subjected to an impulse input. Once completed the next step of the proposed method involves using the Convolution integral as described in Chapter 3 to find the general control force strategy against any arbitrary excitation. To do so one should find the control force plan against each impulse of the arbitrary excitation. However this does not require repetition of the whole optimisation process to obtain the control force strategy against each of the arbitrary excitation impulses. Instead one needs first to calculate the ratio (λ_i) between the impulse amplitude used for GA optimisation and amplitudes of the arbitrary excitation impulses; this ratio is given in Eq. (4.9). The control force plan for each of these impulses equals to the optimised control force plan multiplied by the ratio (λ_i),

$$\lambda_i = \frac{x_{ri}}{x_r},$$
(4.9)

where, x_r: is the amplitude of the impulse used for GA optimisation.

x_{ri}: is the amplitude at the ith impulse (treated as impulse in the short time interval) of the arbitrary excitation.

The scaled control force plans will be shifted by time, then by summation the general control force strategy can be obtained resulting in the minimum response of the system against an arbitrary excitation.

4.2.3. Linear Quadratic Regulator (LQR)

The optimal control theory has been widely applied in literature to the design of vehicle suspension systems. For comparison reasons the application of Linear Quadratic Regulator (LQR) to control a quarter-vehicle model will be introduced in this section.

If a linear dynamical system characterized by Eq. (4.1) is considered, with $x(t_0) = x_0$, the optimal linear regulator problem of the mentioned system is to determine the optimal control $\mathbf{u}(t)$, $t \in [t_0, T]$ which will minimise the quadratic form of the cost function J (performance index) given in Eq. (4.10):

$$J = \int_0^T \left(\mathbf{x}'\mathbf{R}\mathbf{x} + \mathbf{u}'\mathbf{Q}\mathbf{u} \right) dt \tag{4.10}$$

Where, J is the quadratic performance index to be minimised. The superscript ($'$) denotes the matrix transposition. $\mathbf{R}$ is a real symmetric $n \times n$ positive semidefinite matrix, $\mathbf{Q}$ is a real symmetric $r \times r$ positive definite matrix, the terminal time $T > t_0$, $t_0 = 0$ [107]. The trajectory weighting matrix $\mathbf{R}$ and the control weighting matrix $\mathbf{Q}$ selection is not based on a rigorous scientific method. It is somehow based on the control-system designers experience and will usually be determined by experimentation. These weighting matrices will play the main rule of deciding the relative importance of suppressing the response of a specific system state or bounding the control attempt [14, 107].

One of the most common techniques in literature to find the control gain matrix that minimises the cost function J given in Eq. (4.10) is dynamic programming which is based on the "principle of optimality" [14]. Based on this method the sequence of the optimal control is computed using the relationships of backward recursion, which starts with the best possible final point [14]. It was realised by [108] that the control $\mathbf{u}$ that would minimise the mentioned performance index is:

$$\mathbf{u} = -\mathbf{Q}^{-1}\mathbf{C}'\mathbf{K}\,\mathbf{x} = -\mathbf{D}\,\mathbf{x} \qquad\qquad (4.11)$$

$$\mathbf{D} = \mathbf{Q}^{-1}\mathbf{C}'\mathbf{K} \qquad\qquad (4.12)$$

Where $\mathbf{K}$ is a $(m \times m)$ symmetric matrix, and can be calculated from the following equation:

$$\dot{\mathbf{K}} = \mathbf{KCQ}^{-1}\mathbf{C}'\mathbf{K} - \mathbf{R} - \mathbf{B}'\mathbf{K} - \mathbf{KB} \qquad\qquad (4.13)$$

Where Eq. (4.13) is the generalized form of Riccati differential equation. The matrix $\mathbf{D}$ is called the optimal control gain matrix.

Chapter 5

5. Proposed method implementation and Numerical Results

This chapter will be divided into two parts; the first part will focus on controlling the quarter-vehicle model using the CCFS method and compare the results with the ones obtained using the LQR regulator and with the results of passive (non-controlled) suspension system. The second part will show the application of the CCFS method to control the vibration of a full-vehicle model and will demonstrate the effects of time delay on the proposed method performance.

5.1. Part I: Quarter-vehicle

5.1.1. Mathematical Model

A two-degree of freedom quarter-vehicle model subjected to road disturbances is shown in Fig 5.1, where, m_s and m_{us} are the sprung and the unsprung masses, k_s and k_{us} are the stiffness coefficients of the suspension and the tyre, c_s and c_{us} are the damping coefficients of the suspension and tyre, and u is the control force. (x_r) is the road disturbance, (x_s) is the sprung mass vertical displacement and (x_{us}) is the unsprung mass vertical displacement.

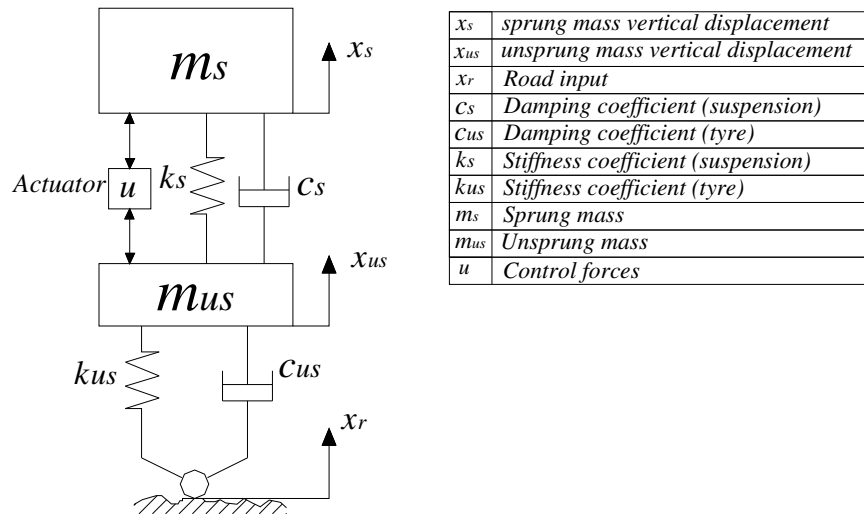| x_s	sprung mass vertical displacement
x_{us}	unsprung mass vertical displacement
x_r	Road input
c_s	Damping coefficient (suspension)
c_{us}	Damping coefficient (tyre)
k_s	Stiffness coefficient (suspension)
k_{us}	Stiffness coefficient (tyre)
m_s	Sprung mass
m_{us}	Unsprung mass
u	Control forces

Fig 5.1 Quarter-vehicle active suspension model.

The values of the model variables are given in Table 5.1 [109].

The equations of motion of the 2-DOF quarter-vehicle model are:

$$
\begin{bmatrix} m_s & 0 \\ 0 & m_{us} \end{bmatrix} \begin{bmatrix} \ddot{x}_s \\ \ddot{x}_{us} \end{bmatrix} =
$$

$$
\begin{bmatrix} -c_s & +c_s \\ +c_s & -(c_s + c_{us}) \end{bmatrix} \begin{bmatrix} \dot{x}_s \\ \dot{x}_{us} \end{bmatrix} + \begin{bmatrix} -k_s & +k_s \\ +k_s & -(k_s + k_{us}) \end{bmatrix} \begin{bmatrix} x_s \\ x_{us} \end{bmatrix} + \begin{bmatrix} 0 \\ k_{us} \end{bmatrix} x_r + \begin{bmatrix} 0 \\ c_{us} \end{bmatrix} \dot{x}_r + \begin{bmatrix} +1 \\ -1 \end{bmatrix} u \quad (5.1)
$$

Representing the system in state space form:

$$
\dot{\mathbf{x}}(t) = \mathbf{B}\mathbf{x}(t) + \mathbf{C}u(t) + \mathbf{F}\dot{x}_r(t) \tag{5.2}
$$

Or in matrix form:

$$
\begin{bmatrix} \dot{x}_{us} - \dot{x}_r \\ \ddot{x}_{us} \\ \dot{x}_s - \dot{x}_{us} \\ \ddot{x}_s \end{bmatrix} = \begin{bmatrix} 0 & +1 & 0 & 0 \\ -\dfrac{k_{us}}{m_{us}} & -\dfrac{c_s + c_{us}}{m_{us}} & \dfrac{k_s}{m_{us}} & \dfrac{c_s}{m_{us}} \\ 0 & -1 & 0 & 1 \\ 0 & -\dfrac{c_s}{m_s} & -\dfrac{k_s}{m_s} & -\dfrac{c_s}{m_s} \end{bmatrix} \begin{bmatrix} x_{us} - x_r \\ \dot{x}_{us} \\ x_s - x_{us} \\ \dot{x}_s \end{bmatrix} + \begin{bmatrix} 0 \\ -\dfrac{1}{m_{us}} \\ 0 \\ \dfrac{1}{m_s} \end{bmatrix} u + \begin{bmatrix} -1 \\ \dfrac{c_{us}}{m_{us}} \\ 0 \\ 0 \end{bmatrix} \dot{x}_r \quad (5.3)
$$

If we assume that:

$$
x_1 = x_{us} - x_r \tag{5.4}
$$

$$
x_2 = \dot{x}_{us} \tag{5.5}
$$

$$
x_3 = x_s - x_{us} \tag{5.6}
$$

$$
x_4 = \dot{x}_s \tag{5.7}
$$

Then the state space representation of Eq. (5.3) will be:

$$\begin{bmatrix} \dot{x}_1 \\ \dot{x}_2 \\ \dot{x}_3 \\ \dot{x}_4 \end{bmatrix} = \begin{bmatrix} 0 & +1 & 0 & 0 \\ -\dfrac{k_{us}}{m_{us}} & -\dfrac{c_s+c_{us}}{m_{us}} & \dfrac{k_s}{m_{us}} & \dfrac{c_s}{m_{us}} \\ 0 & -1 & 0 & 1 \\ 0 & -\dfrac{c_s}{m_s} & -\dfrac{k_s}{m_s} & -\dfrac{c_s}{m_s} \end{bmatrix} \begin{bmatrix} x_1 \\ x_2 \\ x_3 \\ x_4 \end{bmatrix} + \begin{bmatrix} 0 \\ -\dfrac{1}{m_{us}} \\ 0 \\ \dfrac{1}{m_s} \end{bmatrix} u + \begin{bmatrix} -1 \\ \dfrac{c_{us}}{m_{us}} \\ 0 \\ 0 \end{bmatrix} \dot{x}_r \qquad (5.8)$$

After converting the equation of motion to the state space form, it can be solved in time domain using the Runge Kutta numerical integration algorithm.

Table 5.1 The values of the model variables [109].

Model Variables	Values	Unit
m_s	2500	kg
m_{us}	320	kg
k_s	80000	N m^{-1}
k_{us}	500000	N m^{-1}
c_s	500	N s m^{-1}
c_{us}	20	N s m^{-1}

5.1.2. Quarter-vehicle response to a shock input

The optimisation process was carried out to find the optimal control force plan which minimised the response of the sprung mass to the shock input shown in Fig 5.6. In this investigation the ranges for several parameters were studied. In particular, actuator forces were carefully determined after experimenting with a number of possible actuator ranges, the upper and lower bounds of the control forces were decided in such away to make the forces values comparable to the values obtained using the analytical LQR method. Another important parameter studied was force reversals. Initially, the actuator was allowed to generate as many values as the number of integration steps, this was equivalent to the number of variables in the control force plan. Firstly, it was assumed that allowing the maximum number of variables would enable the GA to iterate and find the most effective number of variables so that the control strategy becomes optimum. It was expected that the GA

would eliminate "unnecessary" variables (forces) by reducing their magnitudes to zero. After a lengthy investigation and many experiments, it was found that the GA was unable to reach such a number, to decide on which number is better, different numbers were tested to constitute the control force plan. The procedure followed was to find the control force plan which would result in the best sprung mass response to the shock input. As the Root Mean Square (RMS) of the system response would give better judgement on how good the response is, it was considered to be the measure to decide the number of reversal to be used in the GA optimisation process. To give more accurate results the Mean Value of the RMS (MVRMS) of 10 different tests of each force reversal number is given in Fig 5.2 and the accurate values are given in Table 5.3. One can clearly see that if the force reversals equal to four, the control force plan would result in the best response of the system. Consequently, only four forces are needed to be imposed by the GA scheme to constitute a chromosome.

The population size, which enables the GA to search for the range and density of sampling points at which fitness was assessed, was initially chosen to be equal to the number of the integration steps. Also, during the early stage of experimentation, the total number of generations was initially chosen to be equal to the number of the integration steps. Although there is no direct association between the number of generations, the population size and the number of genes in population, it was accepted that they were related and more genes in chromosome, and bigger population size would slow down the convergence. After many tests with different numbers of chromosomes and generations, it was found that a good convergence could be achieved by using the numbers presented in Table 5.4. The number of generations and the population size were chosen in such a way to ensure that the convergence will occur within the selected range; Fig 5.3 and Fig 5.4 shows two randomly selected tests, in which the GA was able to reach convergence in (52) and (32) generations respectively which are within the chosen range. While through out the whole tests the slowest convergence happened after (60) generations as shown in Fig 5.5, this verify that both the number of generation and population size chosen for the GA optimisation have adequate margin which guarantee that convergence will happen within these ranges, the chosen numbers also reduced the total time amount spent during the GA iterations.

Table 5.2 The upper and lower bounds of the control forces.

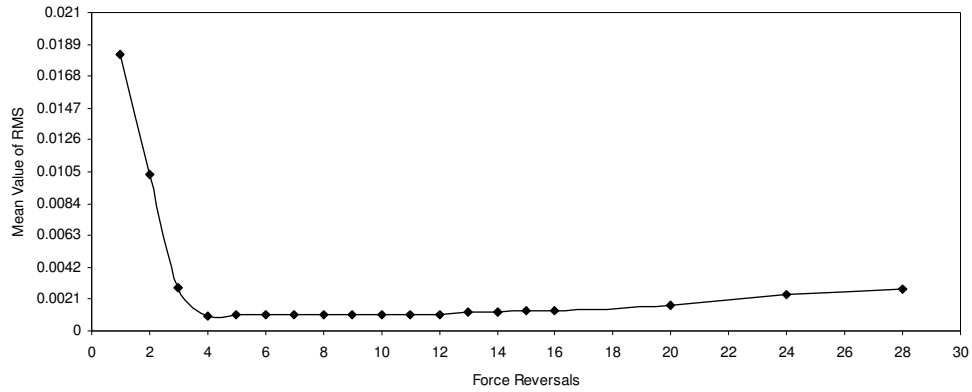| U_i	Value	Unit
The upper bound	+10000	N
The lower bound	-10000	N

Fig 5.2 The mean value of the RMS of the system response

Table 5.3 The Mean Value of the RMS (MVRMS) of the system response.

NO of Forces	MVRMS		NO of Forces	MVRMS
1	0.018203		15	0.001336
2	0.010335		16	0.001363
3	0.002803		20	0.001668
4	0.000984		24	0.002412
5	0.001074		28	0.002735
6	0.001085			
7	0.001024			
8	0.001102			
9	0.001038			
10	0.001028			
11	0.001084			
12	0.001111			
13	0.001233			
14	0.001255			
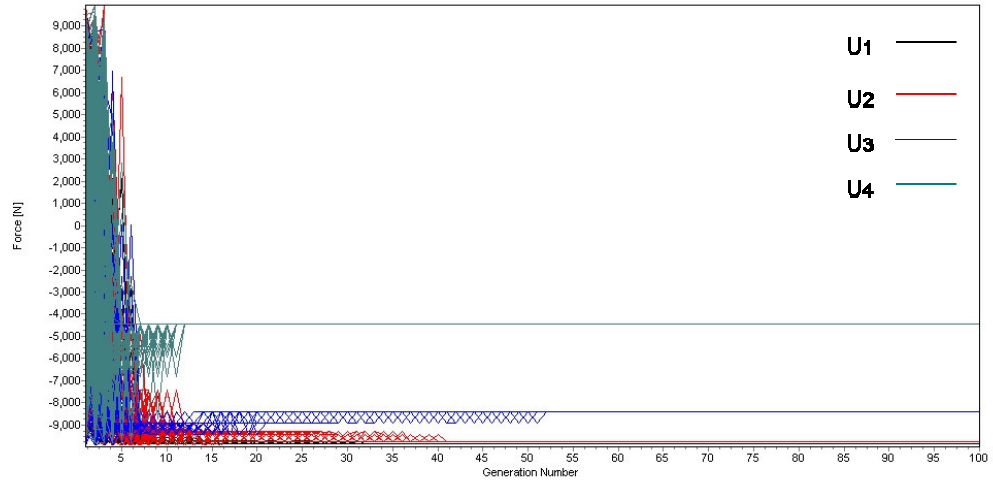
Fig 5.3 Genetic Algorithm Convergence test1.
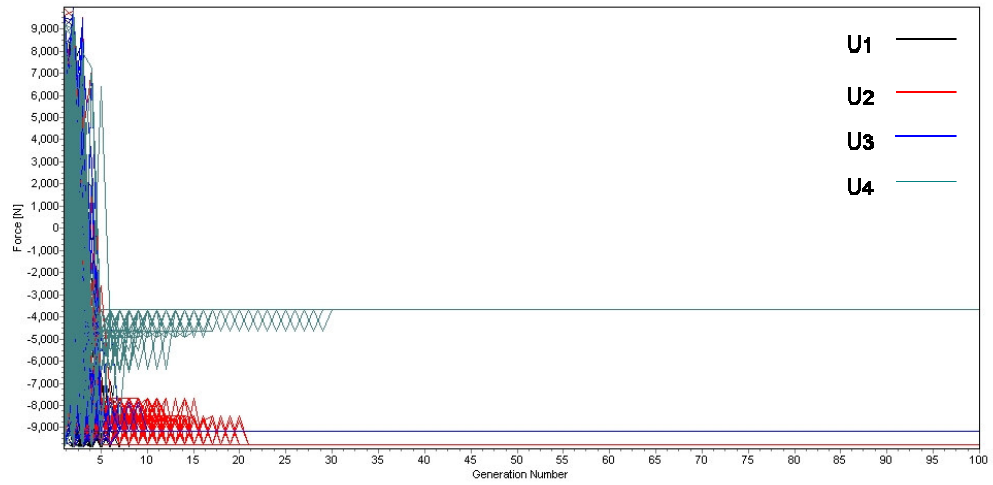
Fig 5.4 Genetic Algorithm Convergence test2.
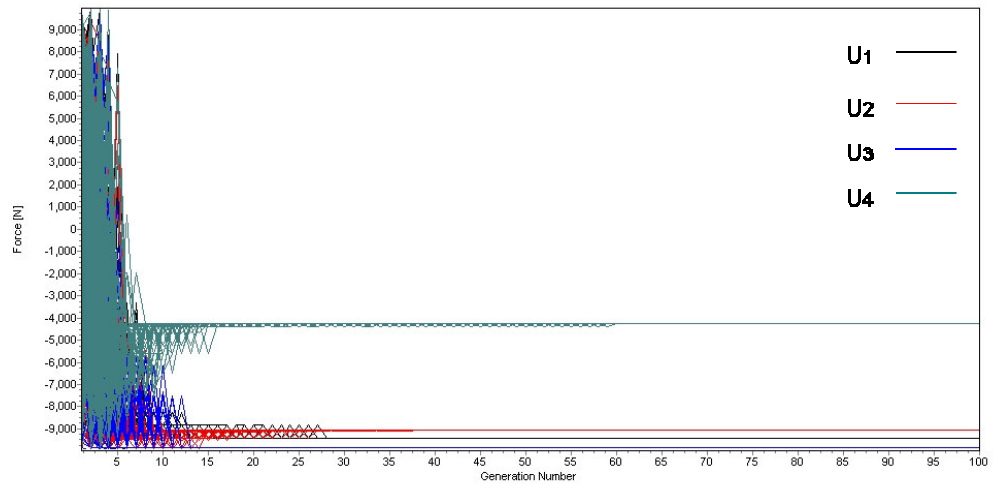
Fig 5.5 Genetic Algorithm slowest Convergence

Table 5.4 The parameters value required to implement the optimisation process.

Parameter	Value
No Of Variables (Control Forces)	4
Population Size	300
No Of Generations	100

To perform numerical tests, a computer program was developed using Visual Basic 6. The integration, which uses the Runge Kutta numerical integration method, was carried out for $t = 4$ sec with the time interval of $\Delta t = 0.02$ sec.

Based on the Genetic Algorithm set up explained above, a consistent family of solutions (i.e. control force plans) was obtained. In other words, the obtained solution is not a unique one, but it is part of a set of solutions that could result in a good response of the sprung mass to the shock input. Nevertheless, the GA optimised control force plan against shock excitation considered in the current work is shown in Fig 5.7 and the force values are tabulated in Table 5.5.

The controlled displacement response of the sprung mass (vehicle body) to the shock excitation is shown in Fig 5.8 while Fig 5.9 to Fig 5.11 show the controlled acceleration, suspension deflection and tyre deflection responses to the shock excitation respectively.
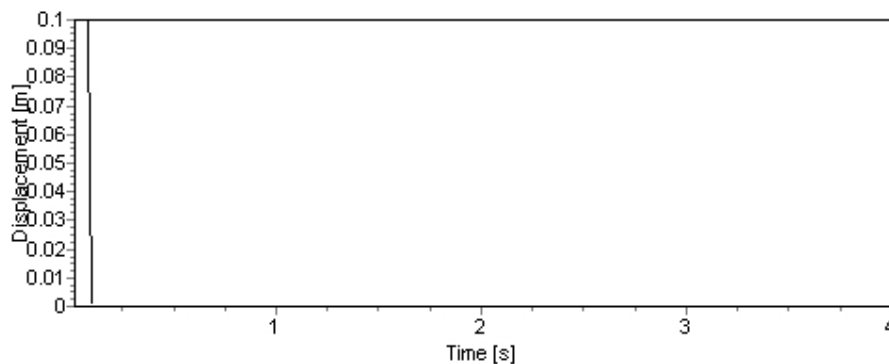
Fig 5.6 The Shock input
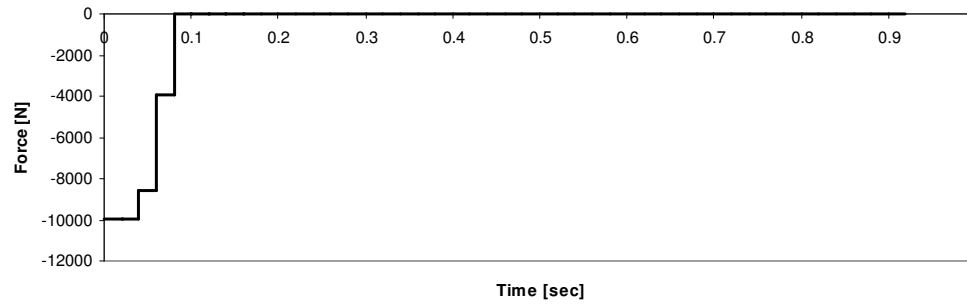
Fig 5.7 The GA obtained control force strategy against shock input.

Table 5.5 Control Force values obtained using Genetic algorithm against impulse input.

Force	U1	U2	U3	U4
Value (N)	-9977.45	-9950.16	-8581.16	-3959.39
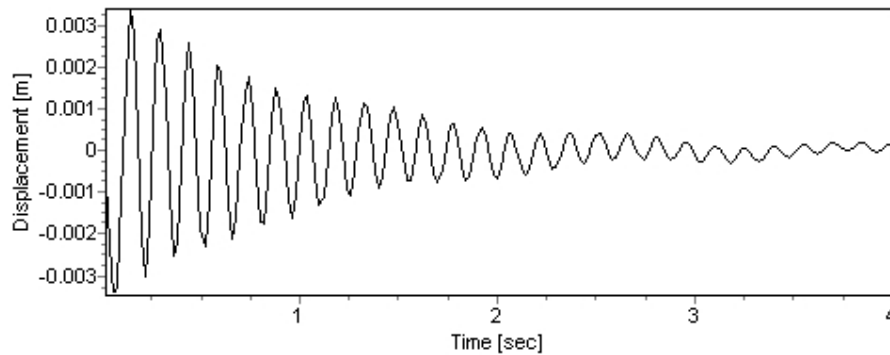
Fig 5.8 The controlled displacement response of m_s to the shock input
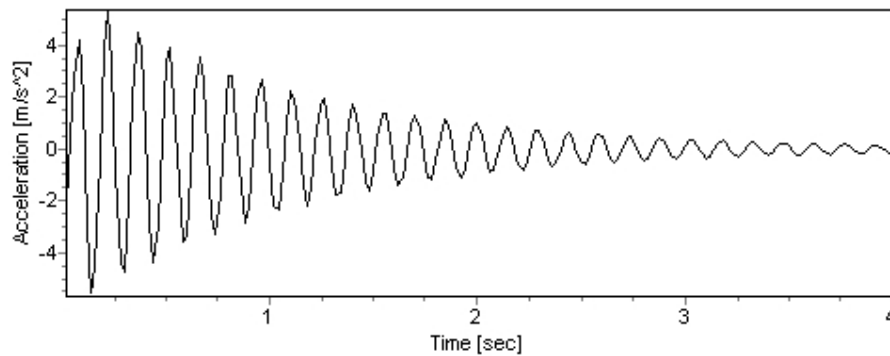
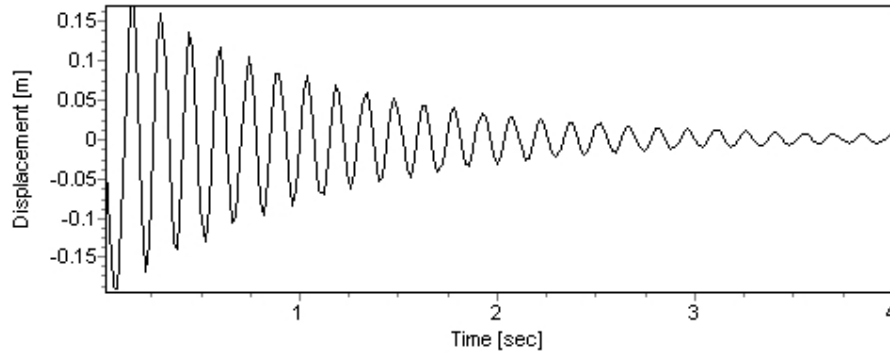Fig 5.9 The controlled acceleration response of m_s to the shock input.
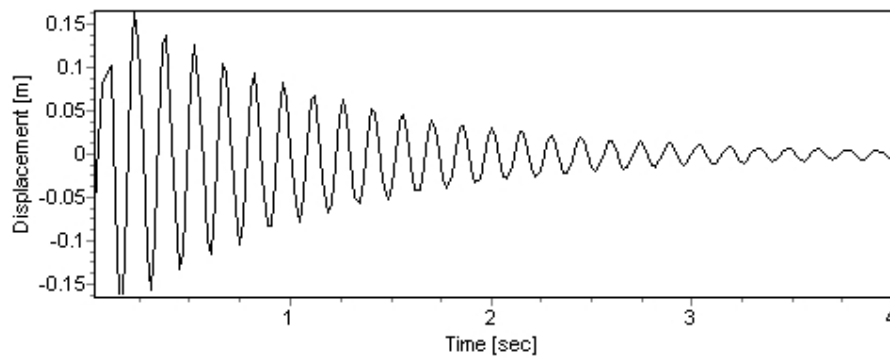
Fig 5.10 The controlled suspension deflection response

Fig 5.11 The controlled tyre deflection response

The obtained results of applying the CCFS method to control the quarter-vehicle response to a shock excitation were compared to the response of the passive suspension system under the same shock excitation. Fig 5.12 compares the passive and controlled sprung mass displacement response while the comparison between passive and active acceleration, suspension deflection and tyre deflection responses are shown if Fig 5.13 to Fig 5.15 respectively.
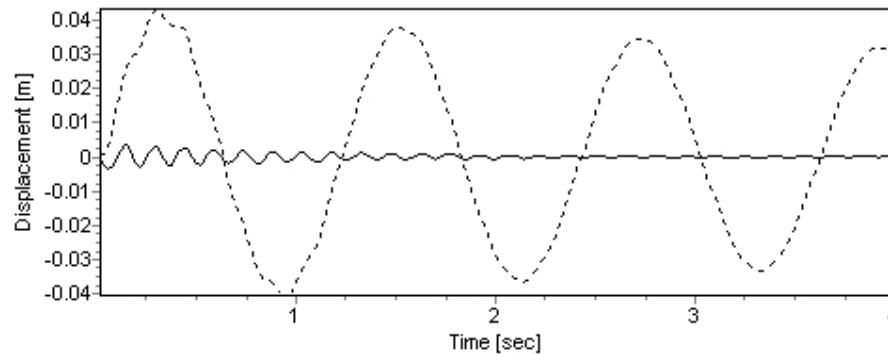
Fig 5.12 m_s displacement response to the shock excitation.

Passive ($\cdots\cdots$), CCFS (———).

71
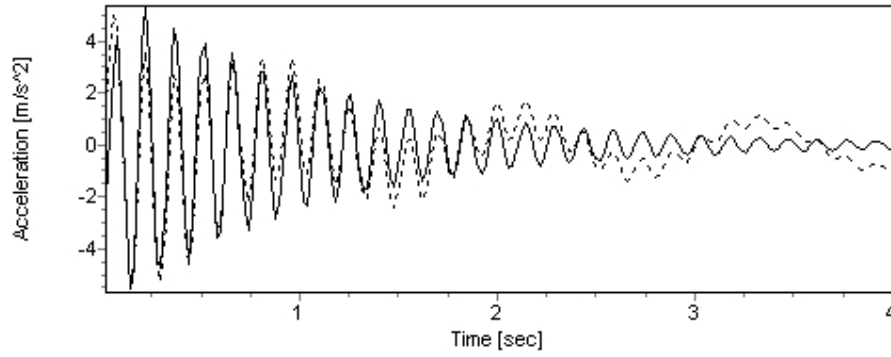
Fig 5.13 m_s acceleration response to the shock excitation.
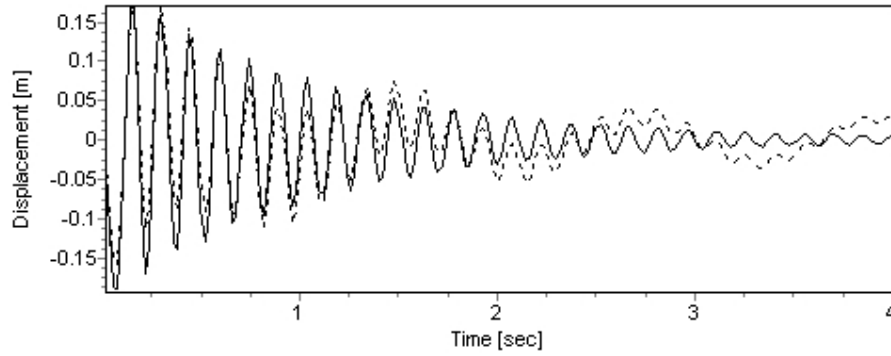
Passive (·········), CCFS (————).

Fig 5.14 Suspension deflection response to the shock input.

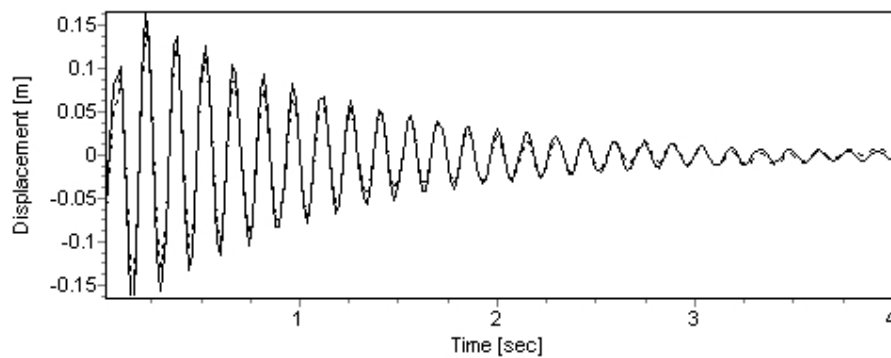Passive (·········), CCFS (————).

Fig 5.15 Tyre deflection response to the shock input.

Passive (·········), CCFS (————)

5.1.3. Quarter-vehicle response to an arbitrary external excitation

As presented, the aim was to control the sprung mass response to an arbitrary excitation using the control force strategy established through the CCFS method. To do this, first the control force plan obtained by the GA was saved. Then the generated arbitrary excitation as shown in Fig 5.16 was divided into impulses. Next the ratio λ was calculated for each of these impulses using Eq. (4.9) pp. 60. The saved control strategy was shifted and scaled by λ for each impulse of the arbitrary excitation, and by summation the general control force strategy which would produce controlled actuating forces is obtained as shown in Fig 5.17. The controlled displacement response of the quarter-vehicle model to the mentioned arbitrary excitation is shown in Fig 5.18 and is compared to the response of the passive system in Fig 5.19. The controlled acceleration response is shown in Fig 5.20 and it is compared to the passive response in Fig 5.21. Similarly, the actively controlled suspension deflection and tyre deflection responses are shown in Fig 5.22 and Fig 5.24, and they are compared to the passive responses in Fig 5.23 and Fig 5.25 respectively.
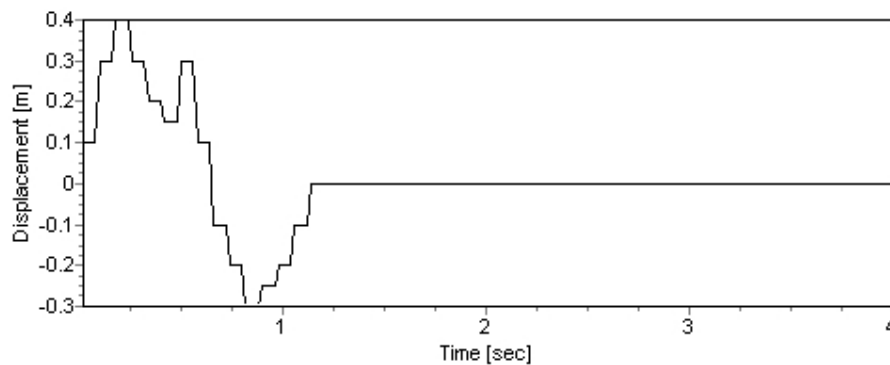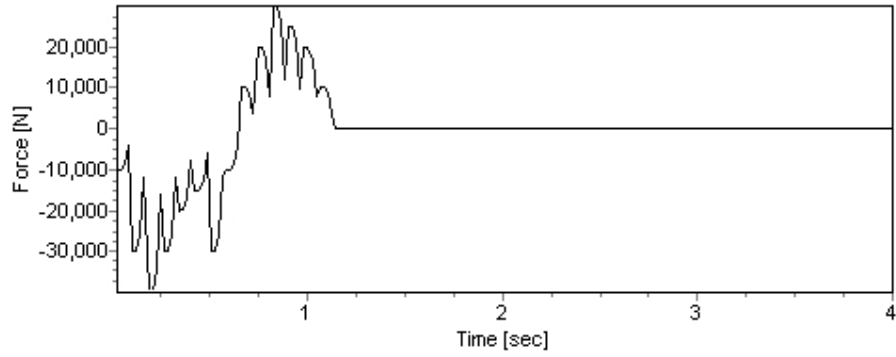

Fig 5.16 Arbitrary Input

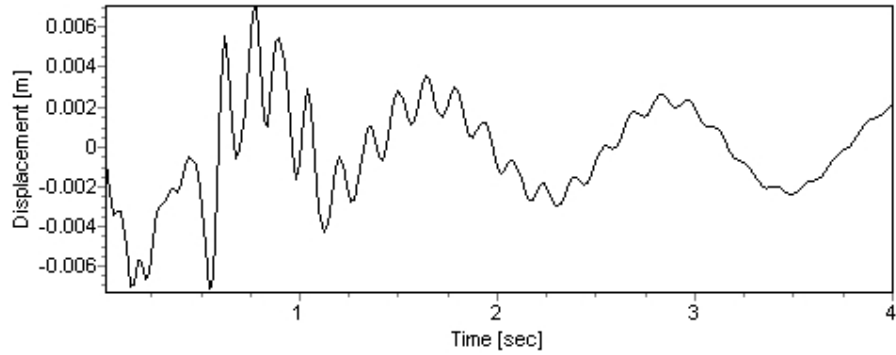Fig 5.17 The generated control force strategy against arbitrary input.

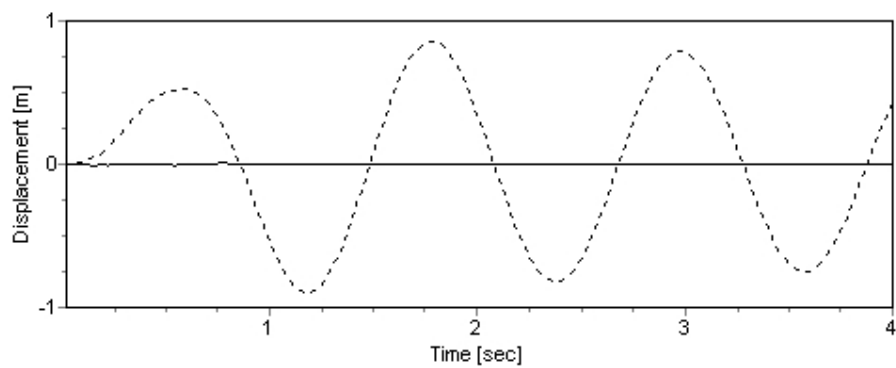Fig 5.18 The controlled m_s displacement response to the arbitrary excitation.

Fig 5.19 m_s displacement response to the arbitrary excitation.

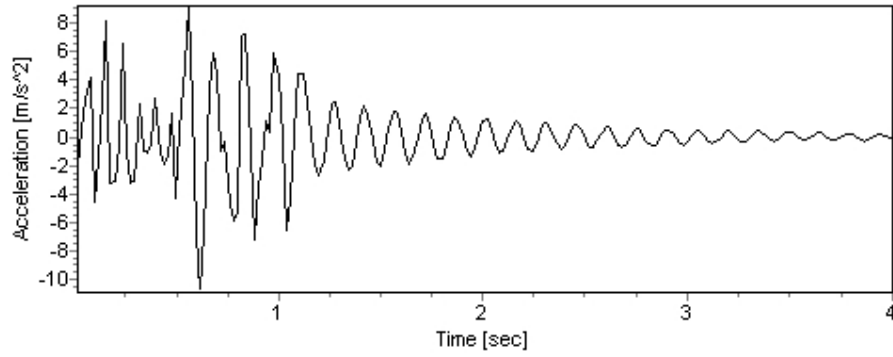Passive (- - - - - - - -), CCFS (———).

Fig 5.20 The controlled m_s acceleration response to the arbitrary excitation.
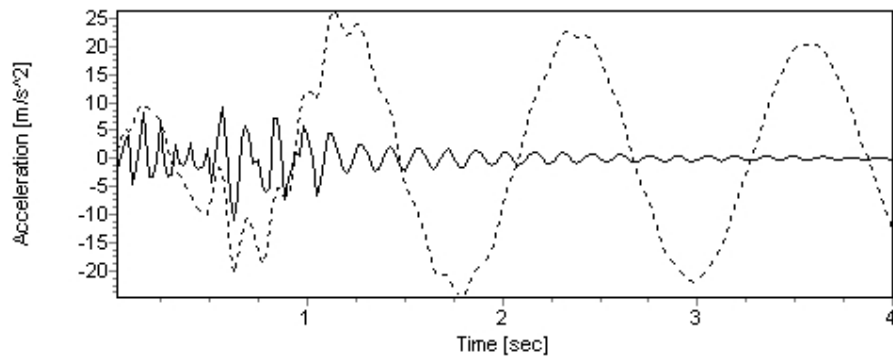

Fig 5.21 m_s acceleration response to the arbitrary excitation.
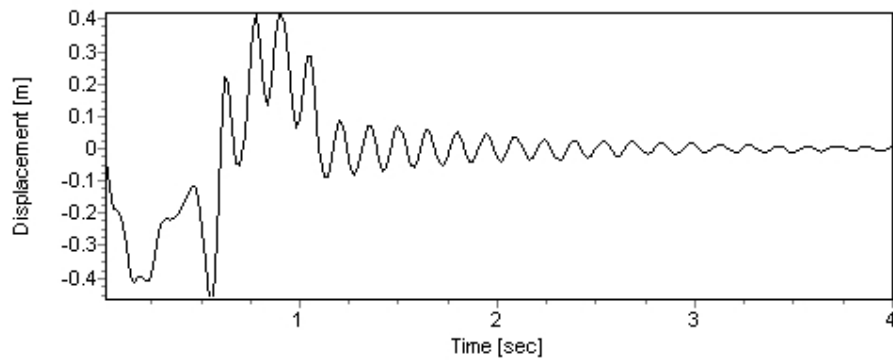
Passive (--------), CCFS (———).

Fig 5.22 The controlled Suspension deflection response to the arbitrary input.
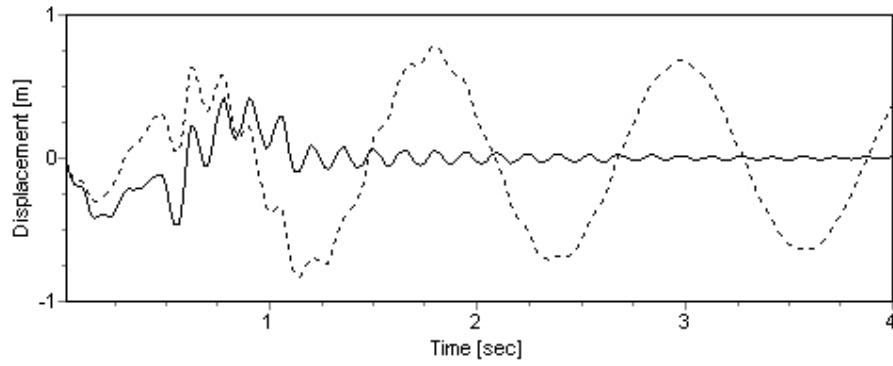
Fig 5.23 Suspension deflection response to the arbitrary input.
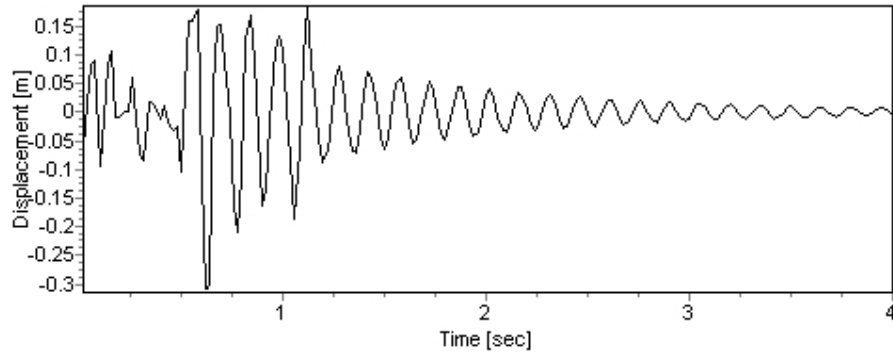
Passive (·········), CCFS (————).

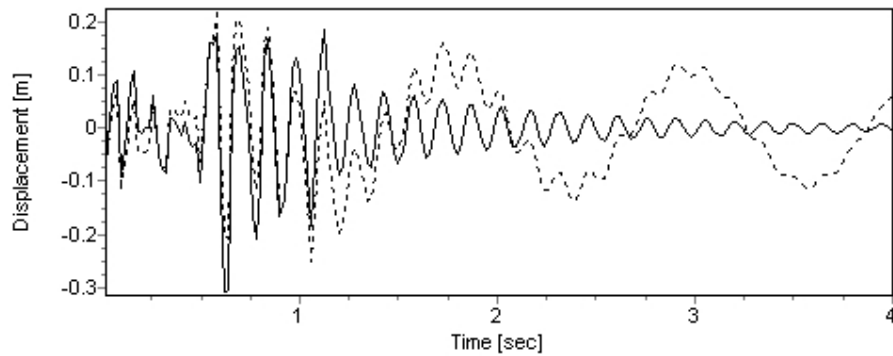Fig 5.24 The controlled tyre deflection response to the arbitrary input.

Fig 5.25 Tyre deflection response to the arbitrary input.

Passive (·········), CCFS (————).

5.1.4. The optimal control strategy using Linear Quadratic Regulator (LQR)

Solving the matrix Riccati equation is required to determine the gain matrix **D** given in Eq. (4.12) pp. 62, which is necessary to find the optimal control as a function of the state variables of the system. To achieve the same aim as that of the proposed method, minimising the sprung mass response to an arbitrary excitation, the quadratic performance index needs to be determined as follows,

$$J = \int_{0}^{T} \left(\mathbf{x}' \mathbf{R} \mathbf{x} + \mathbf{u}' \mathbf{Q} \mathbf{u} \right) dt , \tag{5.9}$$

where, $\mathbf{x} = [0 \ x_s \ 0 \ 0]'$, x_s is the sprung mass displacement.

As explained before choosing the matrices **R** and **Q** to minimise the performance index *J* is not based on a rigorous scientific method so they were chosen experimentally. After many numerical tests it was observed that as **Q** tends to zero, the control power demand increases. The control weighting matrix **Q** was therefore chosen to make the control power demand comparable to the one required by the CCFS method.

$$\mathbf{R} = \begin{bmatrix} 0 & 0 & 0 & 0 \\ 0 & 1 & 0 & 0 \\ 0 & 0 & 0 & 0 \\ 0 & 0 & 0 & 0 \end{bmatrix} \text{ is the state weighting matrix.} \tag{5.10}$$

$\mathbf{Q} = [4.5 \times 10^{-13}]$ is the control weighting matrix. \hfill (5.11)

And the performance index will be:

$$J = \int_{0}^{T} \left(x_s^2 + \left[4.5 \times 10^{-13} \right] u^2 \right) dt \tag{5.12}$$

The system matrices are:

$$\mathbf{B} = \begin{bmatrix} 0 & 0 & 1 & 0 \\ 0 & 0 & 0 & 1 \\ -\dfrac{k_{us}+k_s}{m_{us}} & \dfrac{k_s}{m_{us}} & -\dfrac{c_s+c_{us}}{m_{us}} & \dfrac{c_s}{m_{us}} \\ \dfrac{k_s}{m_s} & -\dfrac{k_s}{m_s} & \dfrac{c_s}{m_s} & -\dfrac{c_s}{m_s} \end{bmatrix} \quad (5.13), \qquad \mathbf{C} = \begin{bmatrix} 0 \\ 0 \\ -\dfrac{1}{m_{us}} \\ \dfrac{1}{m_s} \end{bmatrix} \qquad (5.14)$$

To find the (4×4) **K** matrix, the Riccati equation Eq. (4.13) pp. 62 should be solved, but for numerical integration of the differential equations it is more suitable to start with initial values, so the time is reversed as follow:

$$\tau = T - t \tag{5.15}$$

And Eq. (4.10) will take the form:

$$\frac{dK}{d\tau} = \mathbf{R} + \mathbf{B}'\mathbf{K} + \mathbf{K}\mathbf{B} - \mathbf{K}\mathbf{C}\mathbf{Q}^{-1}\mathbf{C}'\mathbf{K} \tag{5.16}$$

With null initial values [108].

The Runge-Kutta numerical integration algorithm was used to solve Eq. (5.16). The convergence of the elements of **K** matrix was almost completed after $T= 1.0$ sec, and the **K** matrix is found to be:

$$\mathbf{K} = \begin{bmatrix} 0.00008723468070 & 0.00065297820393 & 0.00000014905327 & 0.00000876347192 \\ 0.00065297820393 & 0.06042025294314 & 0.00002964812207 & 0.00182109008197 \\ 0.00000014905327 & 0.00002964812207 & 0.00000008722491 & 0.00000230420118 \\ 0.00000876347192 & 0.00182109008197 & 0.00000230420118 & 0.00011865145798 \end{bmatrix} \tag{5.17}$$

To find the optimal control gain matrix **D**, the matrices **Q**, **C**, **K** are substituted into the Eq. (4.12) pp. 62:

$$\mathbf{D} = \begin{bmatrix} d_1 & d_2 & d_3 & d_4 \end{bmatrix} \tag{5.18}$$

where:

$d_1 = - 6754.66066500$

$d_2 = -1412857.00293167$

$d_3 = -1442.45028500$

$d_4 = -89466.56556556$

As a result the optimal control forces that minimise the sprung mass response to any excitation as a function of the system state variables can be found by substituting **D** into Eq. (4.11) pp. 62:

$$u = -\begin{bmatrix} d_1 & d_2 & d_3 & d_4 \end{bmatrix} \begin{bmatrix} x_1 \\ x_2 \\ x_3 \\ x_4 \end{bmatrix} = -d_1 x_1 - d_2 x_2 - d_3 x_3 - d_4 x_4 \qquad (5.19)$$

Where, $x_1 = x_{us}$, $x_2 = x_s$, $x_3 = \dot{x}_1$ and $x_4 = \dot{x}_2$

In the following the results obtained using the LQR optimal control method will be illustrated and compared with the results of applying the CCFS method "convolution based control force strategy" to control the response of the quarter-vehicle model when it is subjected to the shock and the arbitrary excitation shown above.

Fig 5.26 shows the optimal control forces generated by LQR to control the quarter-vehicle response to a shock excitation, while in Fig 5.27 these forces are compared to the control strategy optimised by the Genetic Algorithm against the same shock excitation. Likewise the optimal control forces generated by LQR to control the quarter-vehicle response to the arbitrary excitation are shown in Fig 5.28 and compared to the generated control strategy by the proposed method in Fig 5.29.
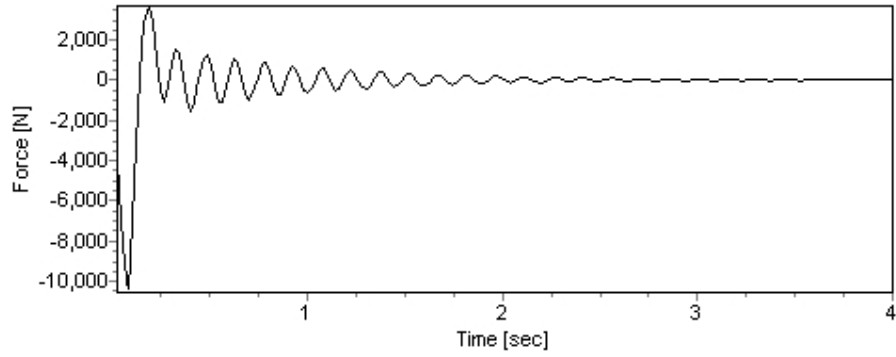
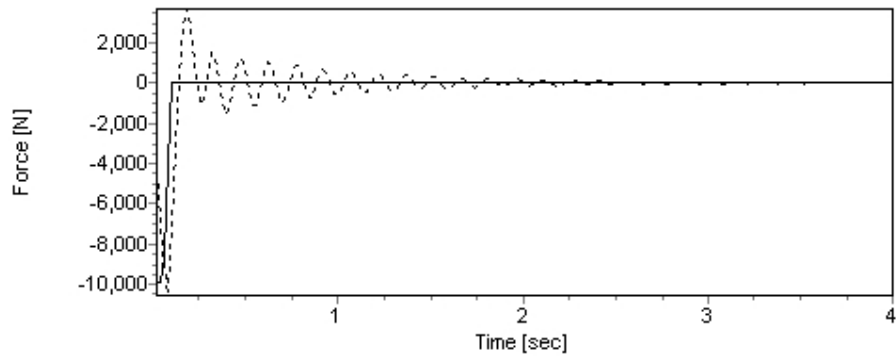Fig 5.26 The LQR generated control force strategy against shock input.

Fig 5.27 The generated control force strategy against shock input.
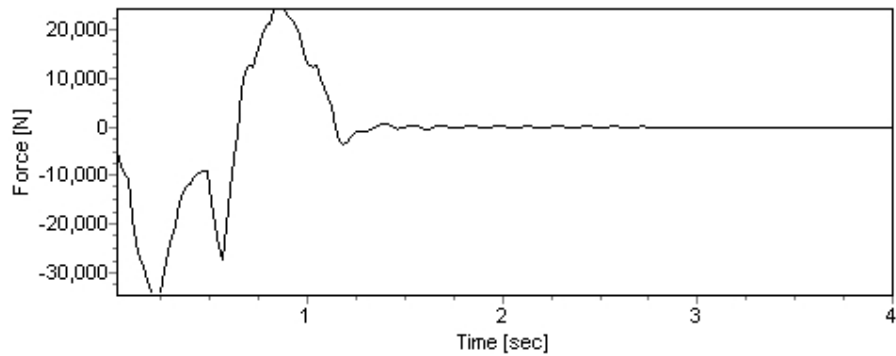
LQR (--------), GA(———).

Fig 5.28 The LQR generated control force strategy against arbitrary input.
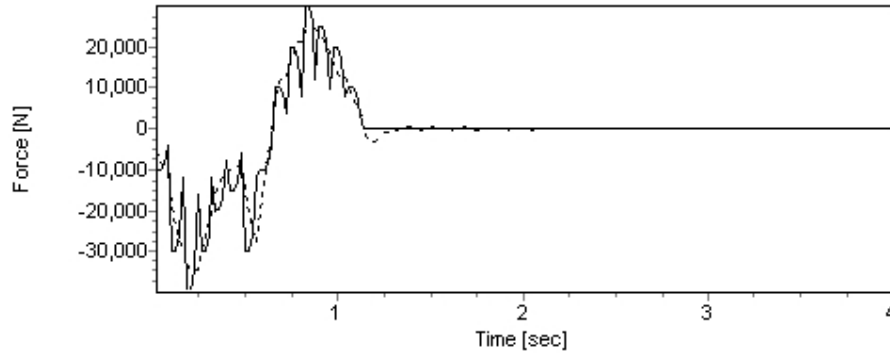
Fig 5.29 The generated control force strategy against arbitrary input.

LQR (·········), CCFS (———).

The sprung mass controlled displacement response by means of LQR against shock excitation is shown in Fig 5.30 and is compared to the controlled displacement response using the proposed method in Fig 5.31. Fig 5.32 shows the actively controlled displacement response to the arbitrary excitation using LQR method, and in Fig 5.33 it is compared to the response using the proposed method. The actively controlled sprung mass acceleration response using the LQR method to the shock excitation is shown in Fig 5.34 and the response to the arbitrary excitation is shown in Fig 5.36. Both are compared to the acceleration response obtained by applying the proposed method as shown in Fig 5.35 and Fig 5.37. The suspension deflection and tyre deflection responses with LQR are shown in Fig 5.38 and Fig 5.42 for shock excitation and in Fig 5.40 and Fig 5.44 for arbitrary excitation. These responses are compared to the ones obtained with the proposed method as shown in Fig 5.39 and Fig 5.43 for shock excitation and in Fig 5.41 and Fig 5.45 for arbitrary excitation respectively.
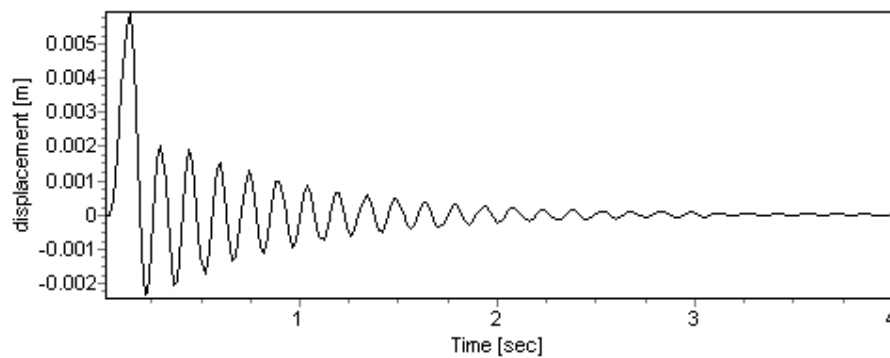

Fig 5.30 m_s displacement response to the shock excitation using LQR.
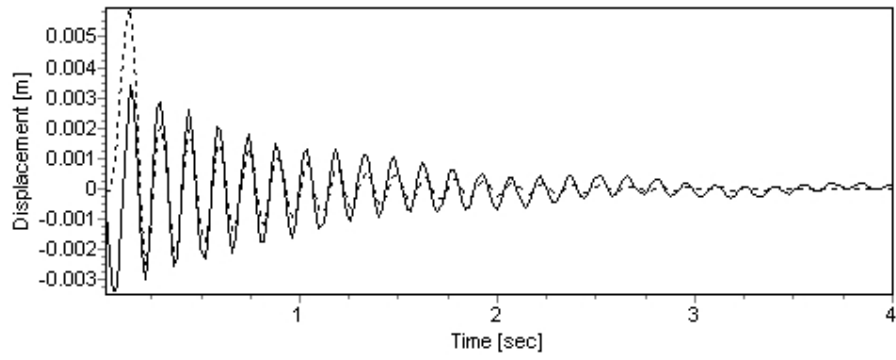
Fig 5.31 m_s displacement response to the shock excitation.
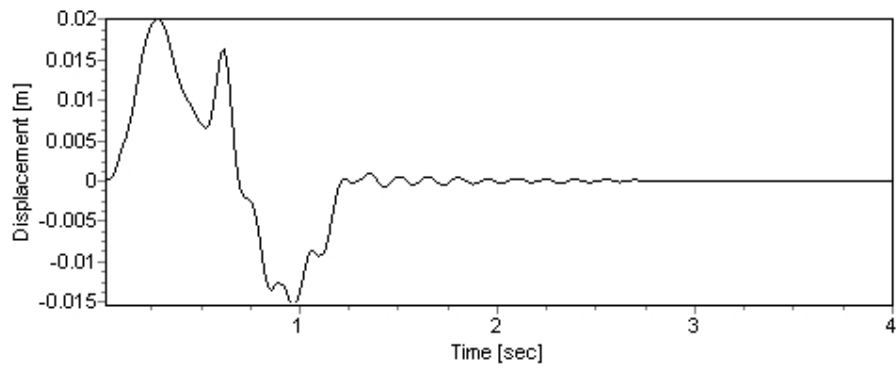
LQR (- - - - - - -), CCFS (———).

Fig 5.32 m_s displacement response to the arbitrary excitation using LQR.
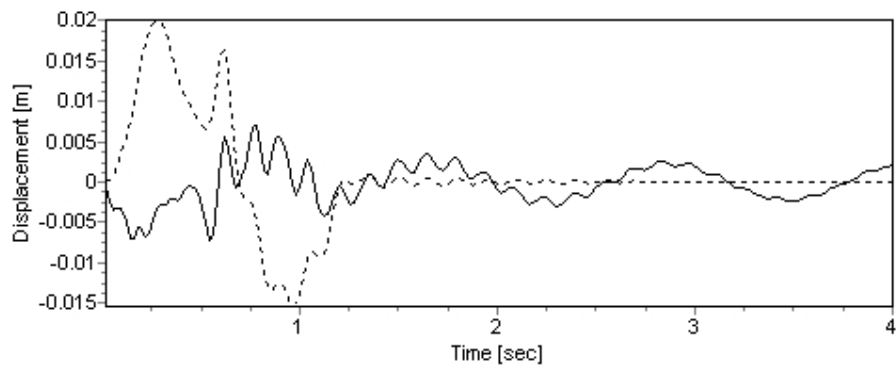
Fig 5.33 m_s displacement response to the arbitrary excitation.
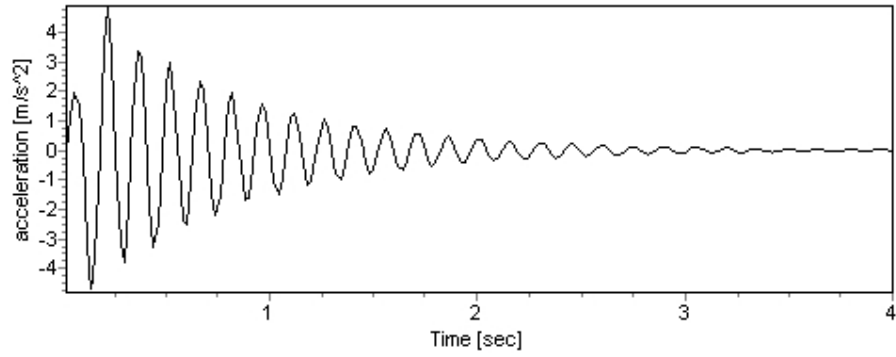
LQR (- - - - - - -), CCFS (———).

Fig 5.34 m_s acceleration response to the shock excitation using LQR.
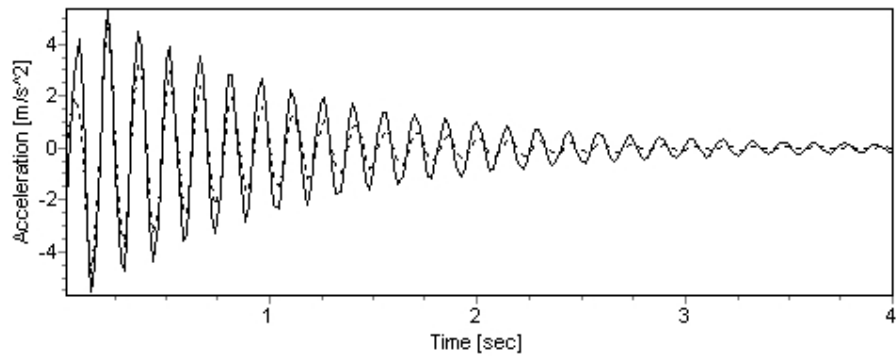
Fig 5.35 m_s acceleration response to the shock excitation.
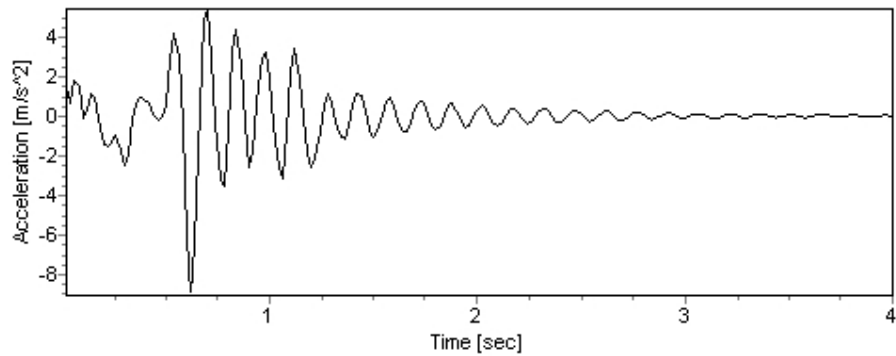
LQR (·········), CCFS (———).

Fig 5.36 m_s acceleration response to the arbitrary excitation using LQR.
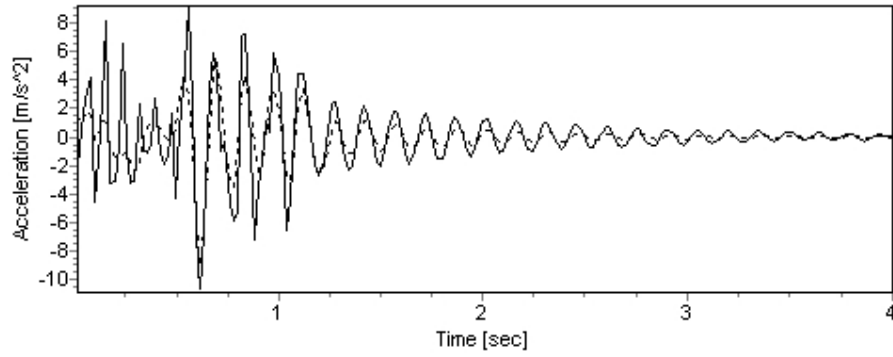
Fig 5.37 m_s acceleration response to the arbitrary excitation.
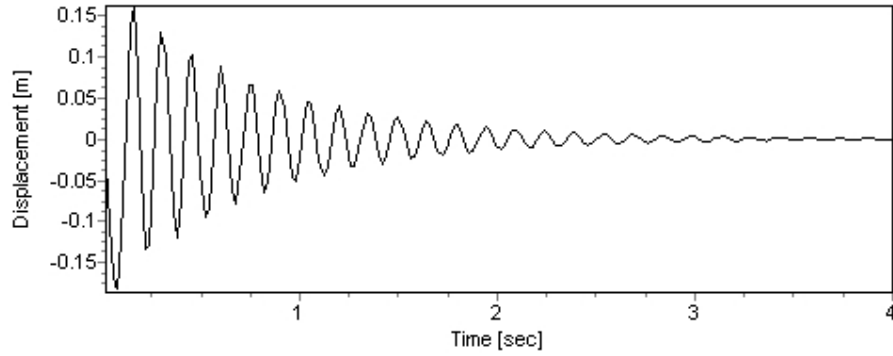
LQR (· · · · · · · · ·), CCFS (———).

Fig 5.38 Suspension deflection response to the shock input using LQR.
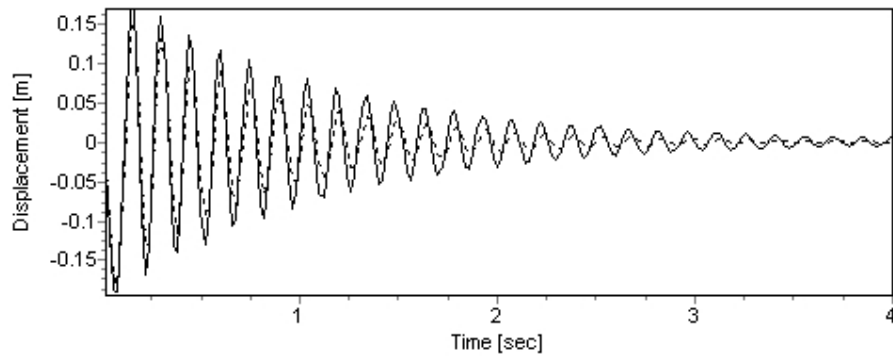
Fig 5.39 Suspension deflection response to the shock input,
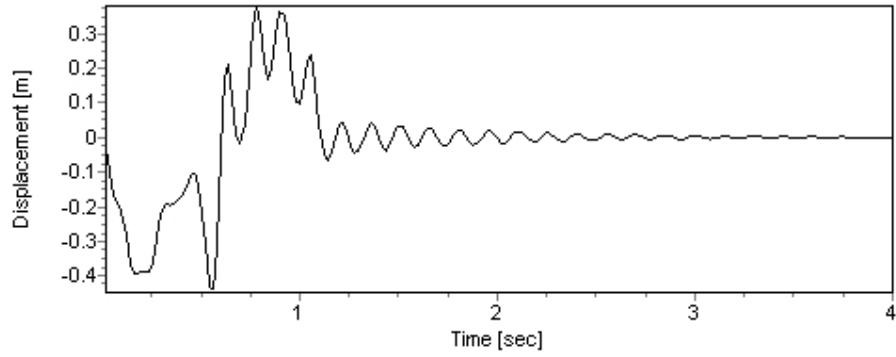
LQR (· · · · · · · · ·), CCFS (———).

Fig 5.40 Suspension deflection response to the arbitrary input using LQR.
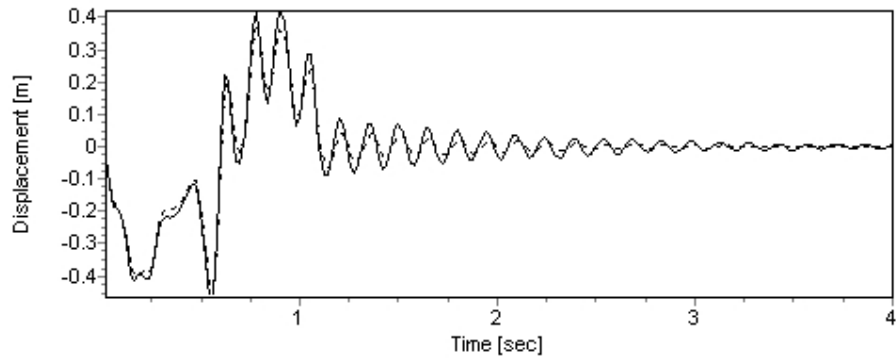
Fig 5.41 Suspension deflection response to the arbitrary input.
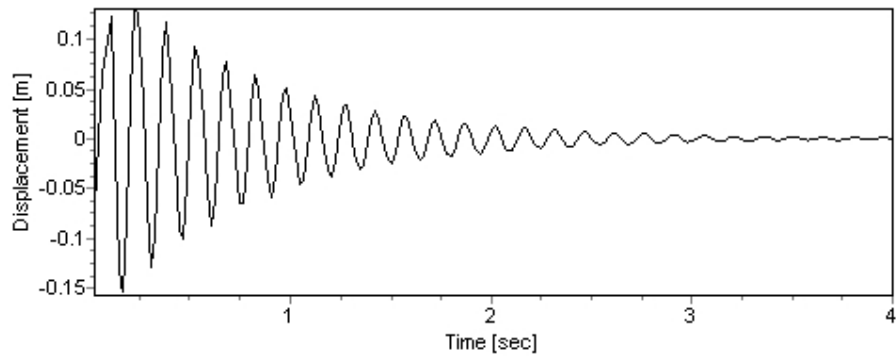
LQR (·········), CCFS (————).

Fig 5.42 Tyre deflection response to the shock input using LQR.
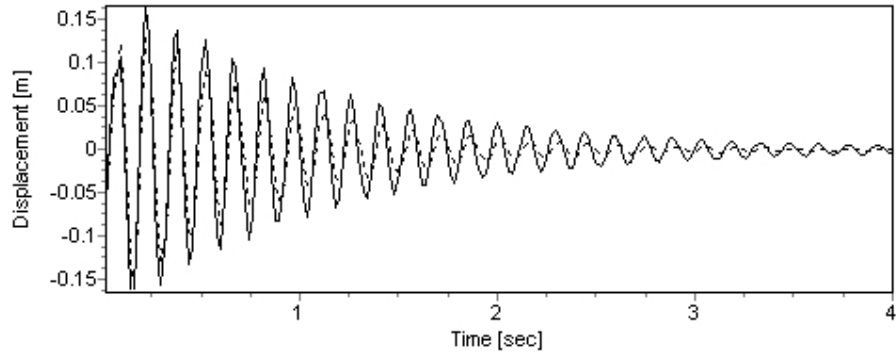
Fig 5.43 Tyre deflection response to the shock input.
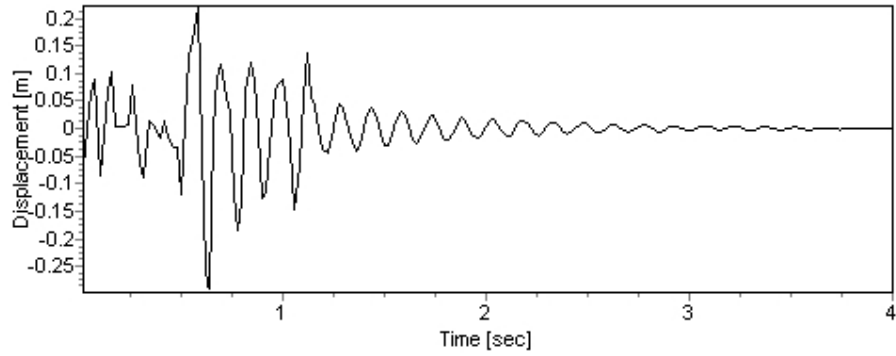
LQR (·········), CCFS (————).

Fig 5.44 Tyre deflection response to the arbitrary input using LQR.
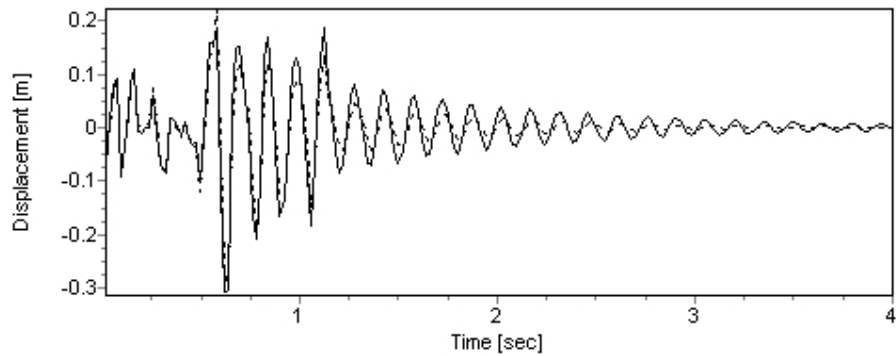
Fig 5.45 Tyre deflection response to the arbitrary input.

LQR (·········), CCFS (————).

5.2. Part II: Full-vehicle

5.2.1. Mathematical model

A 7-degree of freedom full-vehicle model subjected to road disturbances as shown in Fig 5.46 is considered in this part. It is assumed that the wheels have one degree of freedom in z (vertical) direction, so these are z_i which represent the unsprung masses vertical displacements where $i = 1$ *to* 4. The sprung mass (vehicle body) is described by Cartesian axes system centred at the centre of gravity (COG) of the body. The sprung mass has three degrees of freedom, one in z direction which is z_5 and two rotations, α_5 along *Ox* axis and β_5 along *Oy* axis. As the wheels can move just in the vertical direction, the mobility of the full vehicle model is given by Eq. (5.20).

$$\begin{bmatrix} z_1 & z_2 & z_3 & z_4 & z_5 & \alpha_5 & \beta_5 \end{bmatrix}^T \tag{5.20}$$

The wheels masses are given by m_i where $i = 1$ *to* 4, m_5 is the vehicle body mass, the inertias of the vehicle body are I_{5xx} and I_{5yy}.

k_i ($i = 1$ *to* 4) are the unsprung masses stiffness coefficients.

k_i ($i = 5$ *to* 8) are the sprung mass stiffness coefficients.

c_i ($i = 1$ *to* 4) are the damping coefficients of the unsprung masses.

c_i ($i = 5$ *to* 8) are the damping coefficients of the sprung mass.

u_i ($i = 1$ *to* 4) are actuators forces.
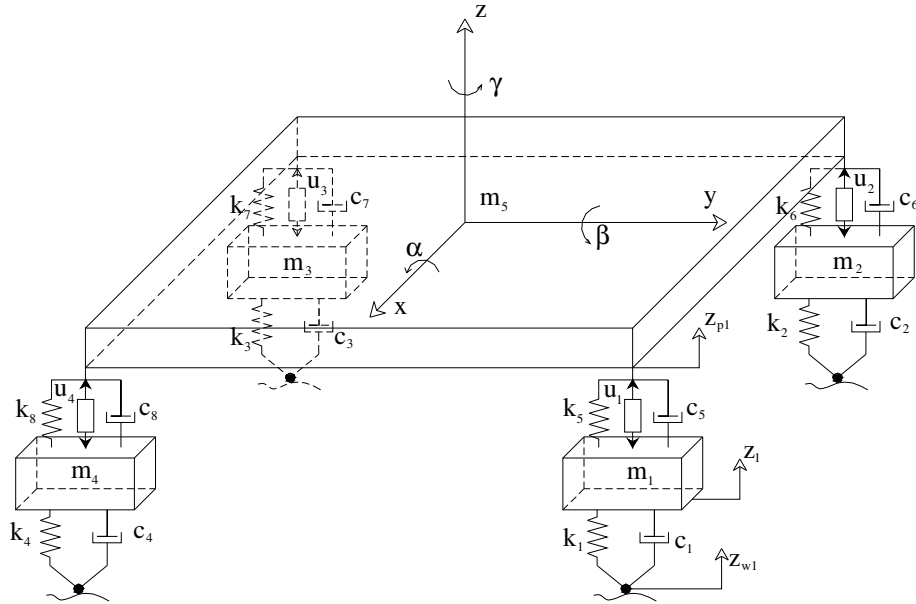
Fig 5.46 Full-Vehicle Model

The values of the model variables are given in Table 5.6.

The deflection at the points of suspension attachments z_{pi} need to be calculated based on x_{pi} and y_{pi} where $i = 1$ *to* 4, this is given in Eq. (5.21).

$$z_{pi} = \left(z_5 + \alpha\, y_{pi} - \beta\, x_{pi}\right) \tag{5.21}$$

The equations of motion are:

$$
\begin{bmatrix}
m_1 & 0 & 0 & 0 & 0 & 0 & 0 \\
0 & m_2 & 0 & 0 & 0 & 0 & 0 \\
0 & 0 & m_3 & 0 & 0 & 0 & 0 \\
0 & 0 & 0 & m_4 & 0 & 0 & 0 \\
0 & 0 & 0 & 0 & m_5 & 0 & 0 \\
0 & 0 & 0 & 0 & 0 & m_6 & 0 \\
0 & 0 & 0 & 0 & 0 & 0 & m_7
\end{bmatrix}
\begin{bmatrix}
\ddot{z}_1 \\ \ddot{z}_2 \\ \ddot{z}_3 \\ \ddot{z}_4 \\ \ddot{z}_5 \\ \ddot{\alpha}_5 \\ \ddot{\beta}_5
\end{bmatrix} =
$$

$$
\begin{bmatrix}
-(k_1+k_5) & 0 & 0 & 0 & k_5 & k_5 y_1 & -k_5 x_1 \\
0 & -(k_2+k_6) & 0 & 0 & k_6 & k_6 y_2 & -k_6 x_2 \\
0 & 0 & -(k_3+k_7) & 0 & k_7 & k_7 y_3 & -k_7 x_3 \\
0 & 0 & 0 & -(k_4+k_8) & k_8 & k_8 y_4 & -k_8 x_4 \\
k_5 & k_6 & k_7 & k_8 & -\sum\limits_{i=5}^{8}k_i & -\sum\limits_{i=1}^{4}k_{i+4}y_i & \sum\limits_{i=1}^{4}k_{i+4}x_i \\
k_5 y_1 & k_6 y_2 & k_7 y_3 & k_8 y_4 & -\sum\limits_{i=1}^{4}k_{i+4}y_i & -\sum\limits_{i=1}^{4}k_{i+4}y_i^2 & \sum\limits_{i=1}^{4}k_{i+4}y_i x_i \\
-k_5 x_1 & -k_6 x_2 & -k_7 x_3 & -k_8 x_4 & \sum\limits_{i=1}^{4}k_{i+4}x_i & \sum\limits_{i=1}^{4}k_{i+4}y_i x_i & -\sum\limits_{i=1}^{4}k_{i+4}x_i^2
\end{bmatrix}
\begin{bmatrix}
z_1 \\ z_2 \\ z_3 \\ z_4 \\ z_5 \\ \alpha_5 \\ \beta_5
\end{bmatrix} +
$$

$$
\begin{bmatrix}
-(c_1+c_5) & 0 & 0 & 0 & c_5 & c_5 y_1 & -c_5 x_1 \\
0 & -(c_2+c_6) & 0 & 0 & c_6 & c_6 y_2 & -c_6 x_2 \\
0 & 0 & -(c_3+c_7) & 0 & c_7 & c_7 y_3 & -c_7 x_3 \\
0 & 0 & 0 & -(c_4+c_8) & c_8 & c_8 y_4 & -c_8 x_4 \\
c_5 & c_6 & c_7 & c_8 & -\sum\limits_{i=5}^{8}c_i & -\sum\limits_{i=1}^{4}c_{i+4}y_i & \sum\limits_{i=1}^{4}c_{i+4}x_i \\
c_5 y_1 & c_6 y_2 & c_7 y_3 & c_8 y_4 & -\sum\limits_{i=1}^{4}c_{i+4}y_i & -\sum\limits_{i=1}^{4}c_{i+4}y_i^2 & \sum\limits_{i=1}^{4}c_{i+4}y_i x_i \\
-c_5 x_1 & -c_6 x_2 & -c_7 x_3 & -c_8 x_4 & \sum\limits_{i=1}^{4}c_{i+4}x_i & \sum\limits_{i=1}^{4}c_{i+4}y_i x_i & -\sum\limits_{i=1}^{4}c_{i+4}x_i^2
\end{bmatrix}
\begin{bmatrix}
\dot{z}_1 \\ \dot{z}_2 \\ \dot{z}_3 \\ \dot{z}_4 \\ \dot{z}_5 \\ \dot{\alpha}_5 \\ \dot{\beta}_5
\end{bmatrix} +
$$

$$
\begin{bmatrix}
k_1 & 0 & 0 & 0 \\
0 & k_2 & 0 & 0 \\
0 & 0 & k_3 & 0 \\
0 & 0 & 0 & k_4 \\
0 & 0 & 0 & 0 \\
0 & 0 & 0 & 0 \\
0 & 0 & 0 & 0
\end{bmatrix}
\begin{bmatrix}
z_{w1} \\ z_{w2} \\ z_{w3} \\ z_{w4}
\end{bmatrix} +
\begin{bmatrix}
c_1 & 0 & 0 & 0 \\
0 & c_2 & 0 & 0 \\
0 & 0 & c_3 & 0 \\
0 & 0 & 0 & c_4 \\
0 & 0 & 0 & 0 \\
0 & 0 & 0 & 0 \\
0 & 0 & 0 & 0
\end{bmatrix}
\begin{bmatrix}
\dot{z}_{w1} \\ \dot{z}_{w2} \\ \dot{z}_{w3} \\ \dot{z}_{w4}
\end{bmatrix} +
\begin{bmatrix}
-1 & 0 & 0 & 0 \\
0 & -1 & 0 & 0 \\
0 & 0 & -1 & 0 \\
0 & 0 & 0 & -1 \\
1 & 1 & 1 & 1 \\
y_1 & y_2 & y_3 & y_4 \\
-x_1 & -x_2 & -x_3 & -x_4
\end{bmatrix}
\begin{bmatrix}
U_1 \\ U_2 \\ U_3 \\ U_4
\end{bmatrix}
\tag{5.22}
$$

By converting the equations of motion to the state space form, they can be solved in time domain using the Runge Kutta numerical integration algorithm.

The application of the proposed CCFS method to find the control force strategy that minimises the full-vehicle model response when it is subjected to an external arbitrary excitation will follow a similar approach to that used to control the quarter-vehicle response to an arbitrary excitation explained in Part I. The only differences here are:

- The Objective Function (*Obj*), which is given in Eq. (5.23), and is defined as minimisation of the summation of the square of deflections at the four corners of the vehicle for the complete integration period [100].

$$Obj = \sum_{i=1}^{n}\sum_{j=1}^{v}\left(z_5 + \alpha\, y_i - \beta\, x_i\right)^2 \tag{5.23}$$

Where, *n*: is the total number of time steps, *v*: is the number of variables

- The ratio (λ_i) between the unit impulse and amplitudes of the arbitrary excitation impulses. This ratio equals to:

$$\lambda_i = \frac{z_{wi}}{z_w} \tag{5.24}$$

Where,

z_w: is the amplitude of the impulse used for GA optimisation.

z_{wi}: is the ith amplitude (treated as impulse in the short time interval) of the arbitrary excitation.

It is assumed that the vehicle speed is 72 km/h and the wheel will encounter a similarly uneven road, so the disturbance will affect the front and the rare wheels with a time lag equal to:

$$\Delta t = \frac{L}{V} \tag{5.25}$$

Where, L is the distance between front and rear wheels and *V* is the vehicle speed. The full- vehicle parameters values are shown in Table 5.6.

As each actuator will be responsible of controlling the vibration of a quarter of the full vehicle (i.e. at each corner), an extended approach of the one used in Part I, which was modified to adopt four different actuators, was used to obtain the control force plan for each of these actuators which will results in minimising the vibration of the full-vehicle model. The Genetic Algorithm parameters which achieved a good convergence are presented in Table 5.7. The same number of force reversal (4) was used; both the number of generations and the population size were decreased to minimise the time needed for optimisation process (because of the enormous calculations needed for full-vehicle model), but these numbers were chosen as explained in Part I in such away to enable GA to reach a good convergence within the allocated ranges. Once more a family of consistent solutions for each actuator was obtained; the control force plans used here represent one set of the possible solutions.

The optimised control forces values using the Genetic Algorithm that minimise the full-vehicle response to the shock excitation for each of the four actuators are presented in Table 5.8.

Table 5.6 The values of the full-vehicle model variables.

Model Variables	Values	Unit
m_5	10000	kg
m_1, m_2, m_3, m_4	320	kg
$k_1, k_2, k_3, k_4,$	500000	N m^{-1}
k_5, k_6, k_7, k_8	80000	N m^{-1}
c_1, c_2, c_3, c_4	20	N s m^{-1}
c_5, c_6, c_7, c_8	500	N s m^{-1}
I_{5xx}	37500	kg.m^2
I_{5yy}	15000	kg.m^2
x_{p1}	1.5	m
y_{p1}	3	m
The upper bound of (U_i)	+12500	N
The lower bound of (U_i)	-12500	N

Table 5.7 The parameters value required to implement the optimisation process by the GA.

Parameter	Value
v: No Of Variables (control Forces)	4
n: Population Size	150
No Of Generations	70

Table 5.8 Control Force values obtained using the Genetic algorithm for each actuator.

Forces [N]	Actuator No.1	Actuator No.2	Actuator No.3	Actuator No.4
U1	-6843.448	-10630.09	-11655.49	-11219.51
U2	-8045.136	-10556.86	-11884.69	-11540.42
U3	-6511.04	-11130.63	-11193.95	-10490.57
U4	-8956.903	-12403.83	-9546.905	-10979.13

In the following, the results of applying the CCFS method to control the response of the full-vehicle model to a shock excitation and arbitrary excitation will be illustrated particularly for the front right corner and vehicle body motion. These results will be compared to the results obtained with a passive (non-controlled) suspension system. Fig 5.47 shows the obtained control force plan for the front-right actuator against shock excitation, while Fig 5.48 shows the generated control strategy against the arbitrary excitation (Fig 5.16 pp. 73). The controlled displacement response at the front right corner of the vehicle to the shock input is shown in Fig 5.49 and is compared to the response of the passive system in Fig 5.50. In the case of arbitrary excitation the displacement response is shown in Fig 5.51 and is compared to the response with passive system in Fig 5.52. The controlled vehicle body displacement response to the shock excitation is compared to the displacement response with passive suspension in Fig 5.54. The controlled vehicle body displacement response to the arbitrary excitation is shown in Fig 5.53, and is compared to the displacement response of the passive system in Fig 5.55.
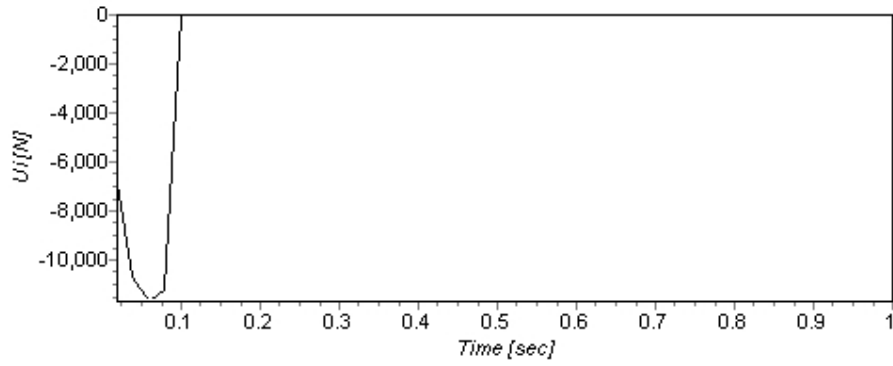
Fig 5.47 The GA-optimised control forces against shock excitation for actuator1.
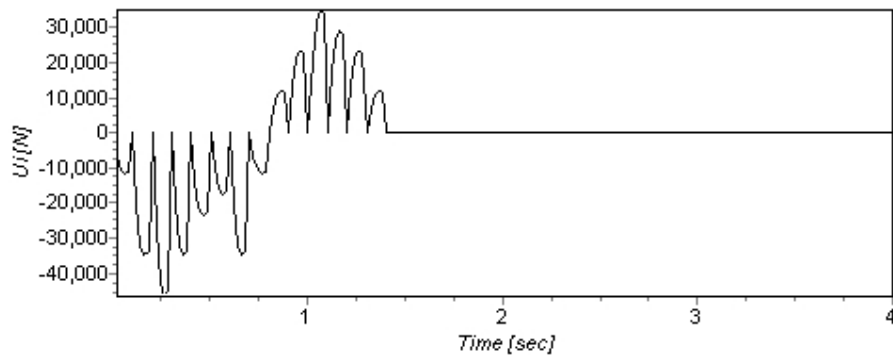
Fig 5.48 The generated control forces against arbitrary excitation for actuator1.
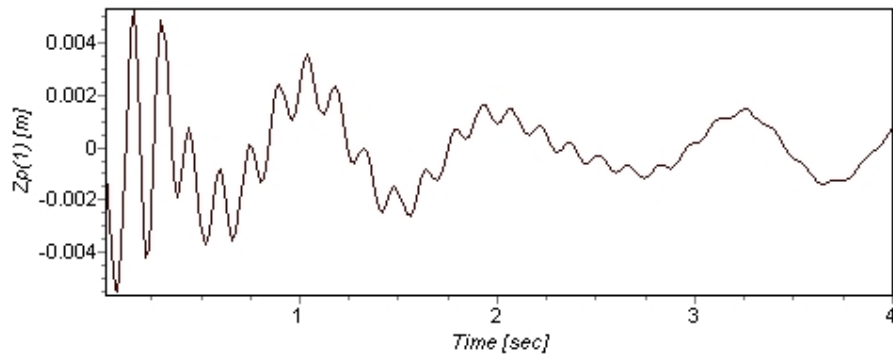
Fig 5.49 The controlled displacement response at front-right corner to the shock
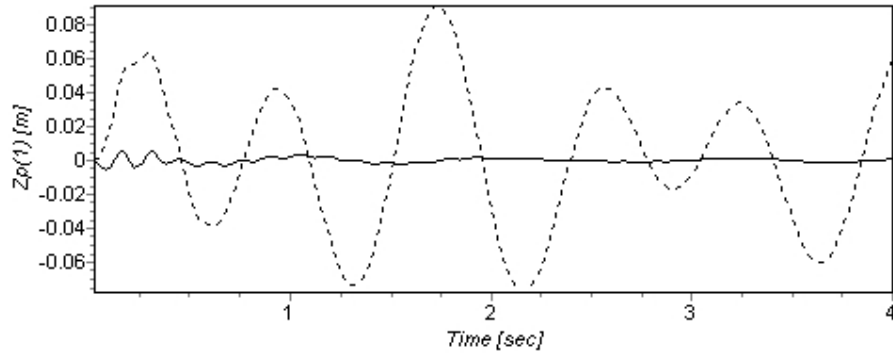
excitation.

Fig 5.50 The displacement response at front-right corner to shock excitation.
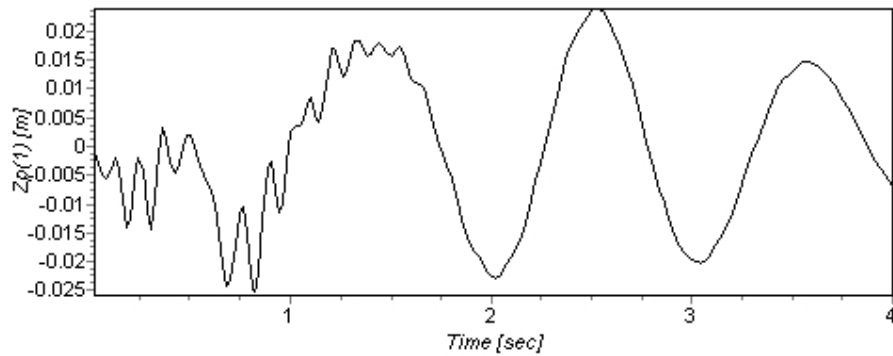
Passive (·-------·), CCFS (———).

Fig 5.51 The controlled displacement response at front-right corner to the arbitrary
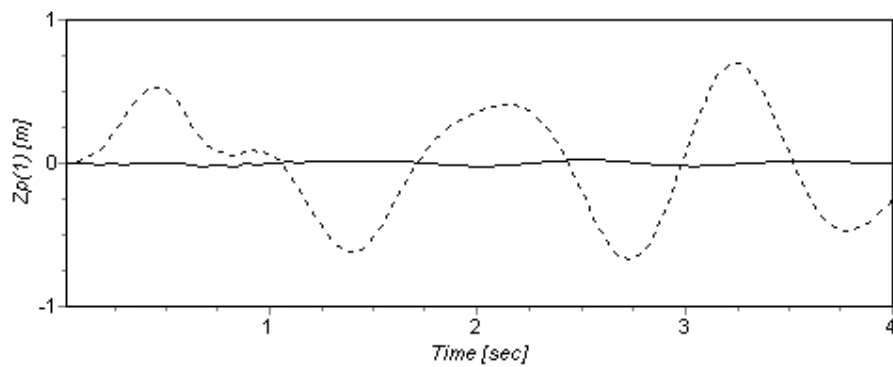
excitation.

Fig 5.52 The displacement response at front-right corner to the arbitrary excitation.
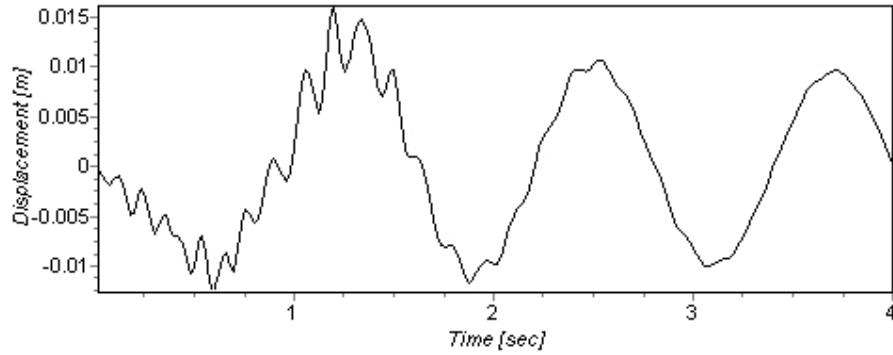
Passive (·-------·), CCFS (———).

Fig 5.53 The controlled vehicle body displacement response to arbitrary excitation.
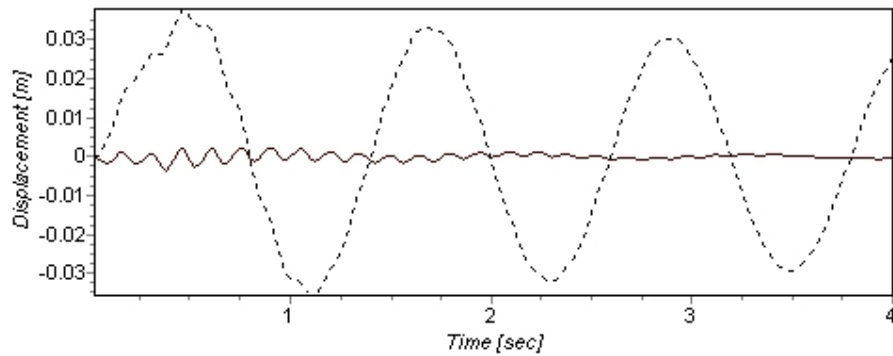
Fig 5.54 The vehicle body displacement response to the shock excitation.
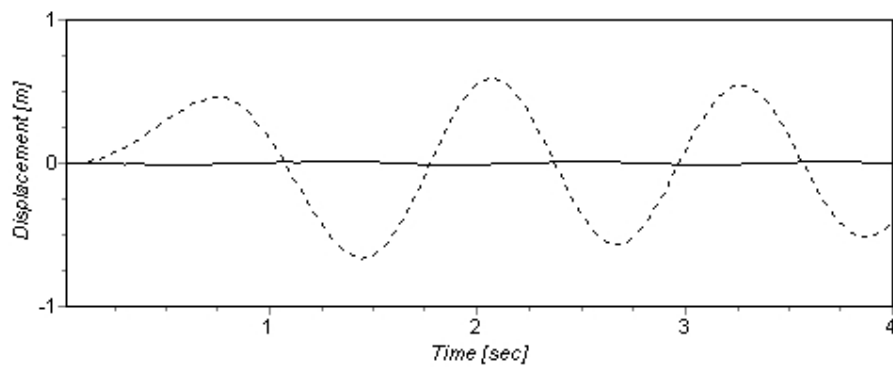
Passive (·········), CCFS (———).

Fig 5.55 The vehicle body displacement response to the arbitrary excitation.

Passive (·········), CCFS (———).

The controlled vehicle body acceleration response to the shock excitation is compared to the response with passive suspension in Fig 5.57. The controlled acceleration response of the vehicle body (sprung mass) to the arbitrary excitation is shown in Fig 5.56 and is compared to the passive response in Fig 5.58. The controlled vehicle body pitch acceleration response to shock excitation is compared to the response of the passive system in Fig 5.59, while the controlled pitch acceleration response of the vehicle body to arbitrary excitation is shown in Fig 5.60 and is compared to the response with passive suspension in Fig 5.61. The suspension deflection response is also shown in Fig 5.62 for the shock excitation and in Fig 5.64 for the arbitrary input. They are compared to the suspension deflection response of the passive system in Fig 5.63 and Fig 5.65 respectively.
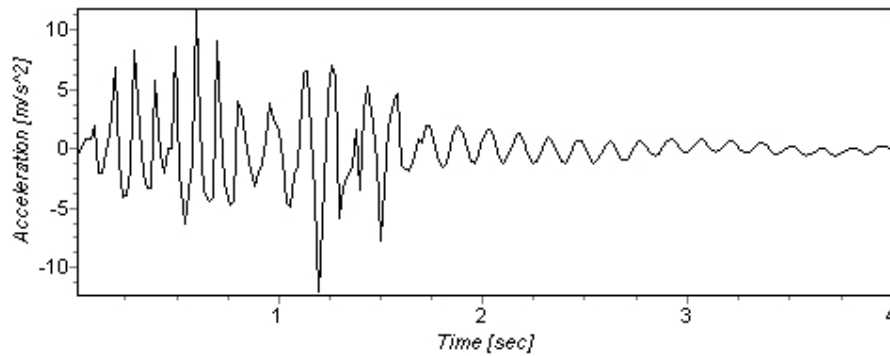
Fig 5.56 The controlled vehicle body acceleration response to the arbitrary excitation.
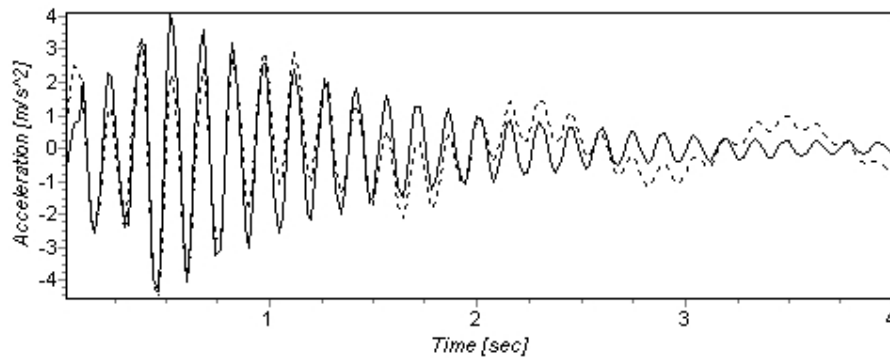
Fig 5.57 The vehicle body acceleration response to the shock excitation.
Passive (·········), CCFS (———).
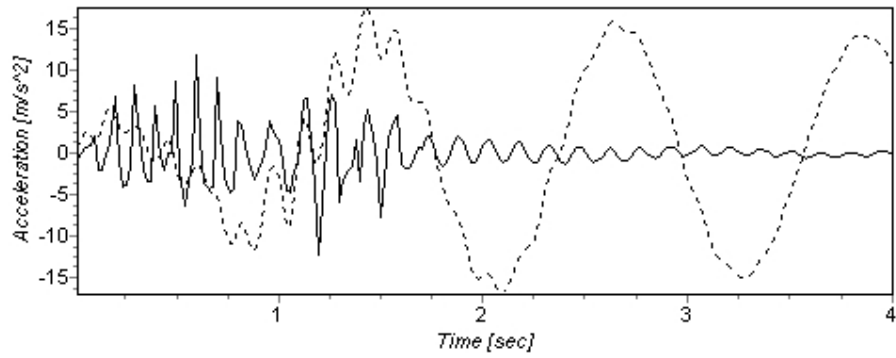
Fig 5.58 The vehicle body acceleration response to the arbitrary excitation.
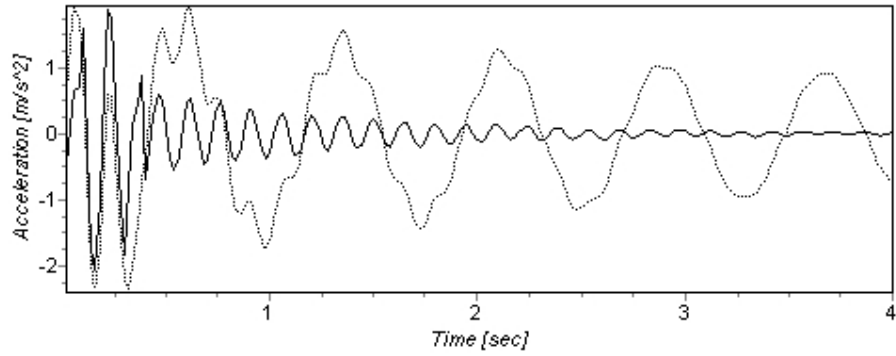
Passive (·--------), CCFS (————).

Fig 5.59 The pitch acceleration response to the shock excitation.
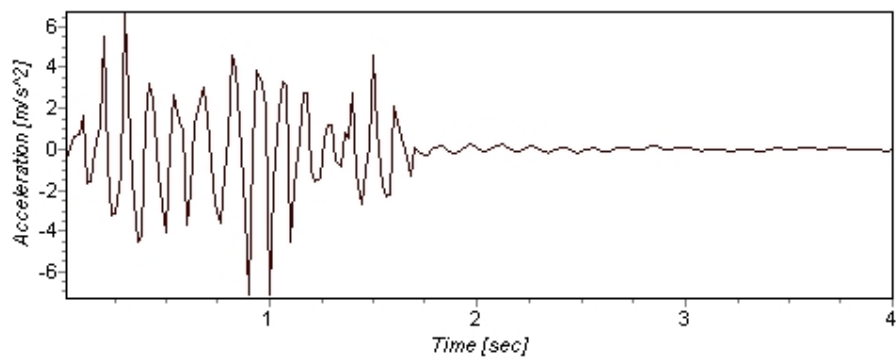
Passive (·················), CCFS (————).

Fig 5.60 The controlled pitch acceleration response to the arbitrary excitation.
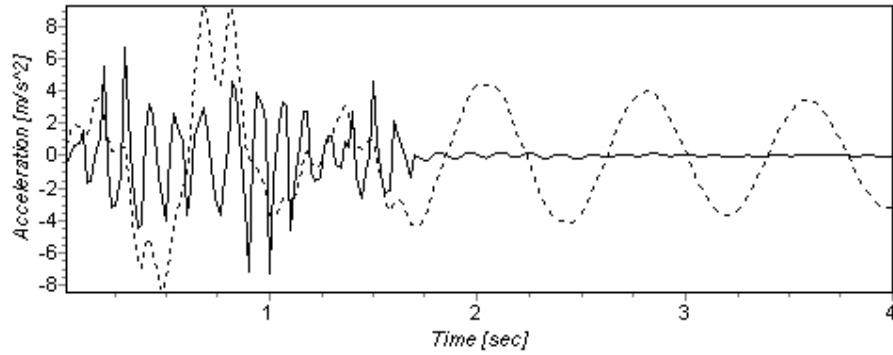
Fig 5.61 The pitch acceleration response to the arbitrary excitation.
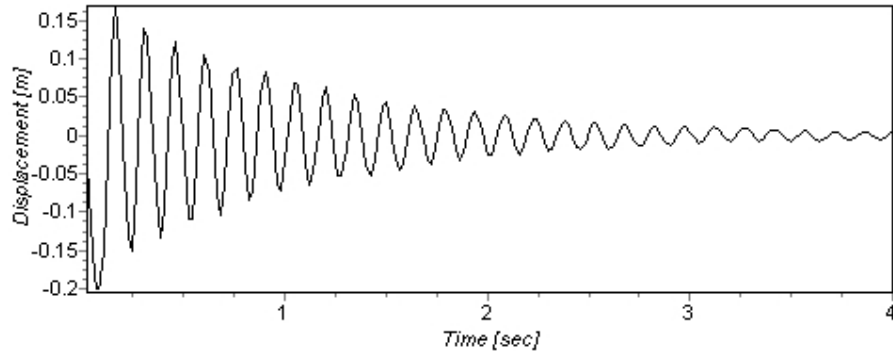
Passive (·········), CCFS (————).

Fig 5.62 The controlled suspension deflection response at the front right corner to the
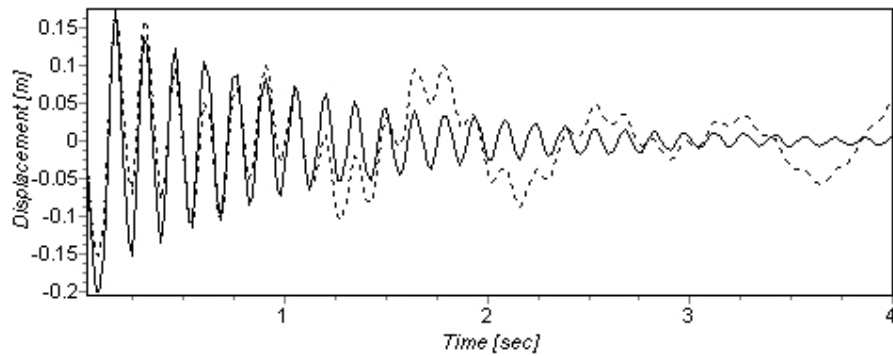
shock excitation.

Fig 5.63 The suspension deflection response at the front right corner to the shock

excitation. Passive (·········), CCFS (————).
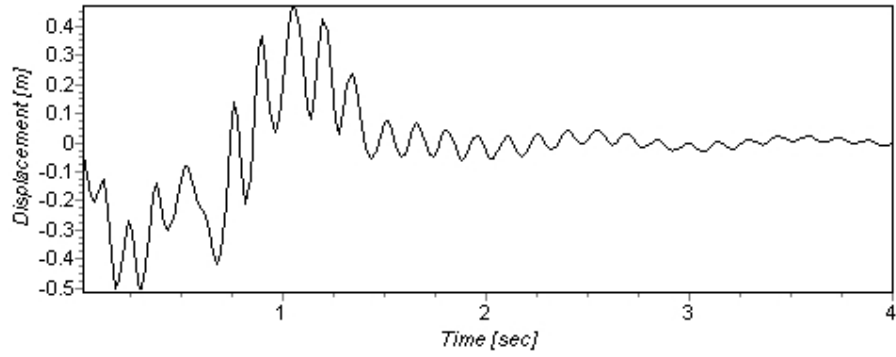
Fig 5.64 The controlled suspension deflection response at the front right corner to the arbitrary excitation.
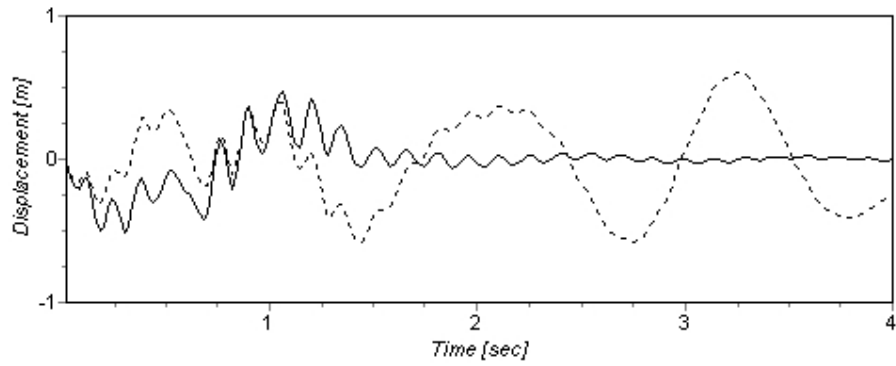
Fig 5.65 The suspension deflection response at the front right corner to the arbitrary excitation. Passive (--------), CCFS (———).

5.3. The effects of Time Delay

Time delay is an important issue for many engineering applications. For active suspension systems, time delay could result in poor performance or more likely to cause instability in the control system [66]. There are many sources of time delay in active suspension systems, such as the time taken by the digital controller to do the complex calculation and the time needed by the actuator to build up the control force [66]. A more practical model of the actuator can be obtained by the inclusion of time delays [66, 110]. Despite the fact that time delay could be small, it is capable of restraining the performance of the control system; therefore, the proposed methods are required to be robust regarding the time delay issue [66]. A small number of works published in the area of active suspension systems referred to the time delay and its effects on the system performance. One should note that the time delay does not refer to the apparent time lag between the front and rare wheels which was the case in the work done by Marzbanrad et al. [75]. Du and Zhang in [66] investigated the effects on including the actuator time delay on the performance of their proposed H_∞ control for active suspension system. It was shown that the method achieved good results with time delay value up to 40 ms. Whilst in [110] the proposed control method was tested with different actuator time delay values (5 and 25 ms) to illustrate the effects of the time delay along with the control parameters on the system performance.

In the present work the developed code for simulation was modified to accommodate different values of time delays, so it can allow the actuator to apply the control force strategy after receiving the control order by Δt sec [100]. This leads to the modification of Fig 3.7 pp. 42. to include the time delay values as shown in Fig 5.66-(a) and (b). The generated control force strategy, which uses the control force plan optimized by Genetic Algorithm against shock input, is applied to control the response of the system when it is subjected to a random input, but the control strategy is applied with a time delay Δt as shown in Fig 5.66-(b).
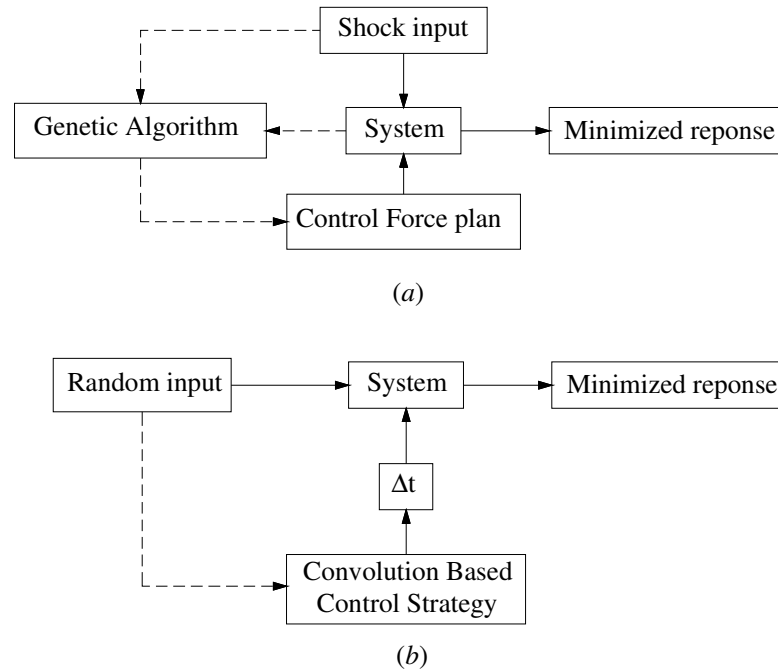
Fig 5.66 Schematic of the CCFS method with time delay.

For the full vehicle model, the obtained control force plane of each actuator (Table 5.8 pp. 92) was used to generate the control force strategy for each actuator using the CCFS method in order to control the full vehicle response when it was subjected to the random excitation shown in Fig 5.16 pp. 73, but the control strategy was applied with time delay; two different values: $\Delta t = 0.02$ sec and $\Delta t = 0.04$ sec.

The controlled displacement responses of the vehicle body at the front right corner when it was subjected to an arbitrary external excitation with different time-delay values are shown in Fig 5.67 and Fig 5.68.
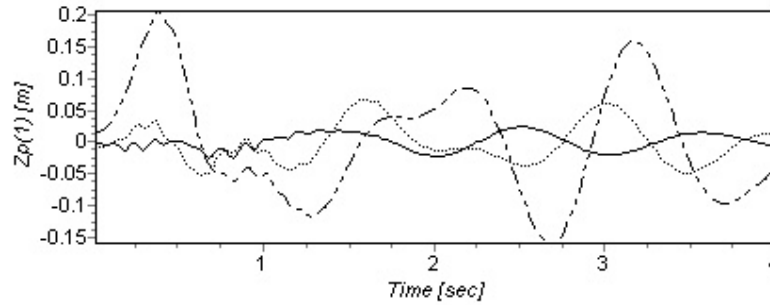
Fig 5.67 The front right corner displacement response with time delay. $\Delta t = 0$
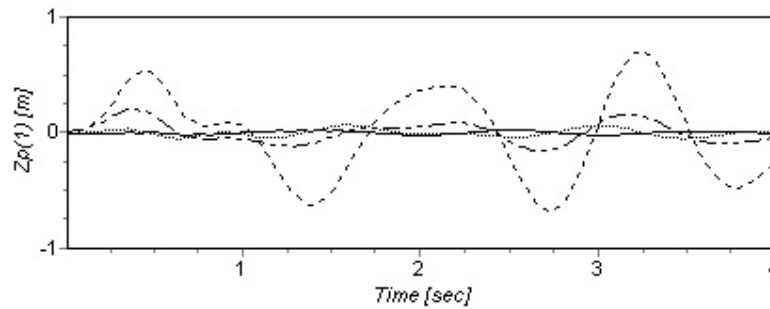
(———), $\Delta t = 0.02$ sec (⸱⸱⸱⸱⸱⸱⸱⸱⸱⸱⸱⸱), $\Delta t = 0.04$ sec (–⋅⋅–⋅⋅-).

Fig 5.68 The front right corner displacement response with time delay.

$\Delta t = 0$ (———), $\Delta t = 0.02$ sec (⸱⸱⸱⸱⸱⸱⸱⸱⸱⸱⸱), $\Delta t = 0.04$ sec (–⋅⋅–⋅⋅-), passive (⸱-⸱-⸱-⸱-⸱-).

On can clearly see that the CCFS method managed to achieve a good performance, even with the inclusion of up to 40 ms time delay in comparison to the non-controlled performance.

This demonstrates that CCFS is robust in dealing with substantial time delays (in this case 40ms) in the control system.

Chapter 6

6. Experimentation and Experimental Results

6.1. Introduction

In order to investigate the applicability of the proposed method in real time applications, a quarter-vehicle test rig was designed and a series of experiments were carried out to show that the proposed method can be easily implemented and can improve the system response when it is subjected to different kinds of external disturbances.

The quarter-vehicle model has been used in many research works for suspension systems investigation and design. Although the model is simple, many essential characteristics of the actual vehicle performance can be obtained [111]. A two mass system representing a quarter-vehicle model was designed to capture the responses of the model when it is subjected to different road inputs. The mentioned model can give an insight of the main criteria of interest such as ride comfort, suspension working space (suspension deflection) and road holding (tyre deflection).

The key issues of designing the test rig can be addressed as follows:

- **Experimental objective**

The primary objectives of the experimental test are:

- To show the ability of the proposed method to be implemented in real life applications.
- To verify that the proposed method is capable of controlling the suspension system and improving the system performance.

The proposed method intended to control the active suspension system in such a way to minimise the response of the sprung mass (vehicle body) when the system was subjected to an external excitation. The characteristics which will be captured from the designed quarter-vehicle test rig will also be used for evaluation and analysis of the "Convolution based Control Force Strategy" method.

- **Experimental requirements and the available laboratory resources**

The main requirements to design a quarter-vehicle test rig can be summarized as follow:

- Two masses representing sprung mass (vehicle body) and unsprung mass (tyre); these masses can slide along two shafts using Oilite bearings as only the vertical motion is of interest.

- Springs with different stiffness representing passive suspension and tyre rigidity.

- Vibrating source to simulate the road input.

- Actuation system to generate the control forces needed for the active suspension system.

- A set of linear displacement sensors and accelerometers for measurements and control.

- Data acquisition system (hardware and software).

Brunel University Vibration laboratory has a number of the required facilities such as the *VB85* shaker which is a medium thrust, high performance, electromagnetic vibration generator. This vibrator was designed to transmit sinusoidal or random vibrations which cover a wide range of frequencies and displacements; also it can generate different kinds of shocks including half sine, square, saw tooth, and triangular shock. The shaker can be used in compliance with all international and British environmental specifications [112]. In addition, there is a Froude Consine Omega amplifier designed to be used with vibration systems. It consists of a cabinet containing power modules, a control module, an optional degauss module and a user interface fitted in the front door. This amplifier can be used to drive the shaker through the user interface or it can receive the signal from external computer connected through a BNC cable. Additionally, there are different power supplies with both fixed and adjustable outputs, Endevco Model 4416B Battery powered Isotron conditioners, a PC-CARD-DAS16/16AO for data acquisition, and pneumatic equipment, which can be used in the test rig design.

6.2. Quarter-vehicle Test Rig setup

Taking into account the design issues and considering all the available resources, the test rig for quarter-vehicle active suspension system using pneumatic actuator was designed. The test rig is shown in Fig 6.1 and comprises the main system, the pneumatic system and the data acquisition system.

6.2.1. The main system

- Steel masses: m_1 and m_2 represent the tyre and the vehicle body masses respectively whilst m_0 is rigidly connected to the top plate of the shaker to simulate the road input. These masses will slide along two shafts using Oilite bearings.

- Steel springs: two springs have k_1 and k_2 stiffness values and represent the tyre rigidity and the passive suspension respectively. The spring with k_0 stiffness is used to support the weight of the top part of the test rig to protect the shaker as it is designed to endure a specific static weight.

- VB85 shaker with the Omega amplifier, the shaker signal input will be generated using *SignalCalc 350 Vibration Controller* software.

- Three Linear Displacement Sensors (LDS) shown in Fig 6.3(a). The first sensor is connected between the base and m_0, which measures the road input vertical displacement x_0. The second sensor is connected between the base and m_1, which measures the vertical displacement x_1. The third sensor is connected between m_1 and m_2, measures the relative displacement $x_2 - x_1$.

- Two accelerometers shown in Fig 6.3(b): A/120/VTN is needed to control the shaker whilst the other accelerometer A/120/VT is used to measure the vehicle-body acceleration $\ddot{x}_2$. The accelerometers are connected to the signal conditioners as they need constant current (4mA) to work.

The test rig components weight and values are tabulated in Table 6.1.

Table 6.1 The Test Rig parts weights and their values.

Part	Weight *kg*	Value *N/m*
Sprung mass m_2	12.147	-
Unsprung mass m_1	3.077	-
Two Spring k_2	0.165 each	1600
Two Spring k_1	0.120 each	12500
Pneumatic actuator	0.802	-
Fixing brackets	0.378	-

Fig 6.1 instrumentation of the active suspension test rig.

a) Froude Consine Omega amplifier. b) VB85 Electromagnetic Vibration Generator.

c) Air cooling system of the shaker. d) Two mass system main parts.

e) Pneumatic System.   f) Data Processing System.

6.2.2. Pneumatic system

A pneumatic system was assembled and fitted to the quarter-vehicle test rig to generate the required control forces. The main parts of the pneumatic system are:

- Lateral load resisting low Friction Cylinder *MQML D 25 TF H 100 D* from SMC, which will be used to generate the control forces.
- Electro-Pneumatic Regulator: *ITV 3050 31 2BS Q X88* from SMC to work as a Proportional Control Valve, shown in Fig 6.2(a).
- *SY3340R-SLOZ-01-Q* body ported solenoid valve from SMC shown in Fig 6.2(c).
- *AFD30-F02D* Micro-Mist separator from SMC shown in Fig 6.2(b).
- Air Compressor.
- Tubes and fittings from SMC.
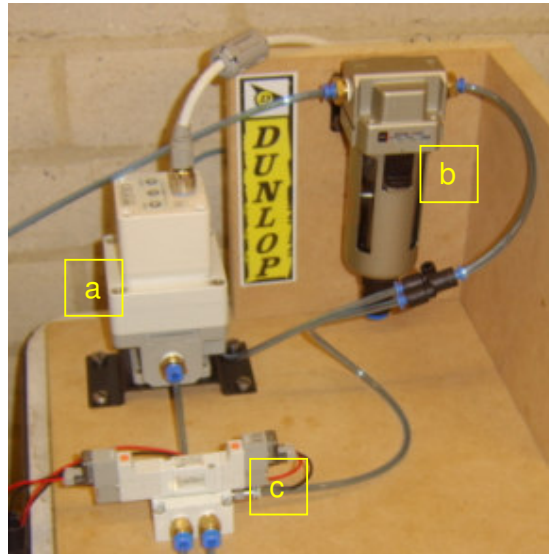
Fig 6.2 Pneumatic Control System:

- a) Electro-Pneumatic Regulator
- b) Micro-Mist Separator
- c) Solenoid Valve
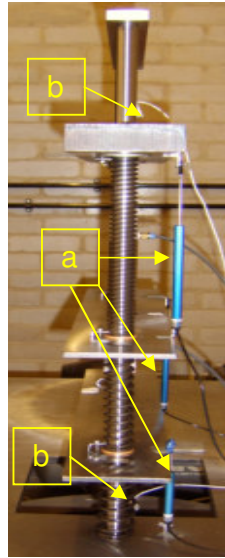
Fig 6.3 side view of the rig:

    a) Linear Displacement Sensors
    b) Accelerometers

6.2.3. Data Acquisition System

6.2.3.1. Hardware

- The PC-CARD-DAS16/16AO (200 kS/s) card was used for data acquisition as the linear displacement sensors and accelerometers are connected to its analogue input channels; also the card analogue output channels will be used to control the solenoid valve.

- USB-1208FS card is a USB-based DAQ module with 8 analogue input channels, up to 12-bit resolution, 50 kS/s, two D/A outputs and 16 DIO bits. The analogue output of this card will be used to control the Electro-Pneumatic Regulator.

6.2.3.2. Software

A Visual Studio.Net 2005 software program was developed using the cards universal library; this program enabled the user to collect the data and to receive/send signals from/to the test rig using both cards analogue channels. The user friendly interface is shown in Fig 6.4.
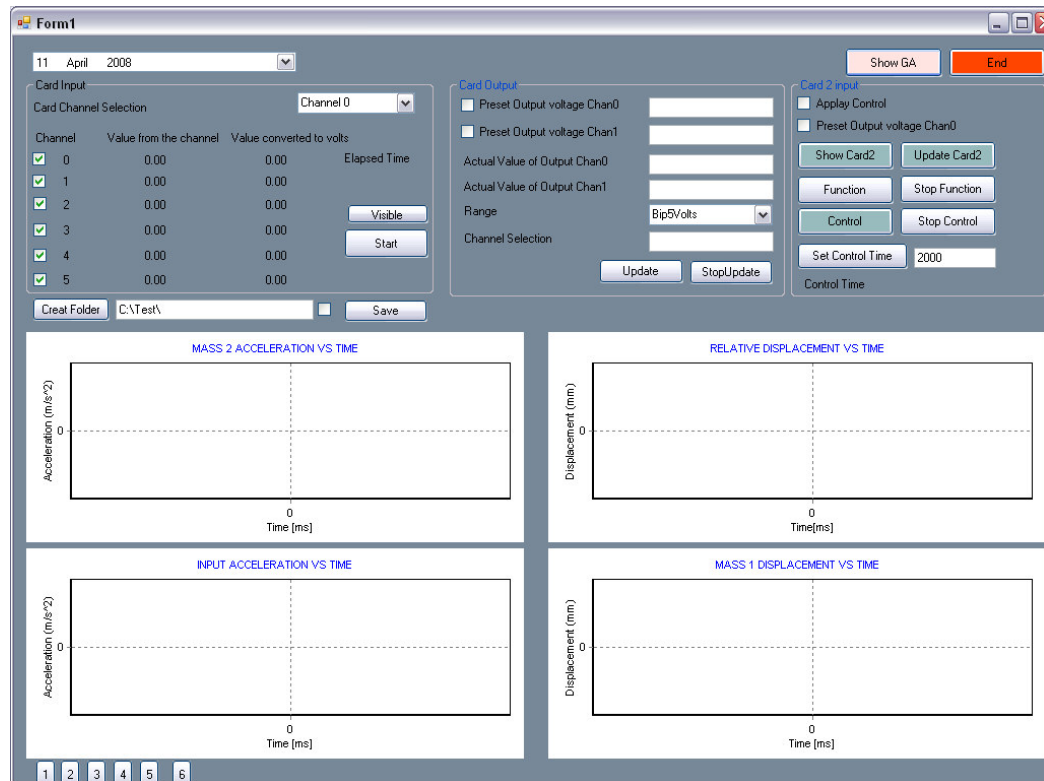
Fig 6.4 The developed user friendly interface for data acquisition and control software.

6.3. Test Procedure

The test was divided into two parts:

- The first part focused on finding the appropriate control force strategy against shock disturbance based on the quarter-vehicle mathematical model.

- The second part concentrated on actively controlling the suspension system when it is subjected to random disturbance using the CCFS method.

Throughout the experiment the following outputs were expected to be measurable or easily calculated based on the measurable data:

- The vertical displacements of the vehicle body, i.e. of the sprung mass (m_2).

- The vertical acceleration of the vehicle body.

- The relative vertical displacement between the sprung and unsprung mass.

- The relative vertical displacement between road input and the wheel.

These outputs are important to evaluate the criteria of ride-comfort, suspension rattle space and road holding, which are essential to assess the improvements achieved by applying the CCFS method.

6.3.1. Model based control force plan against shock input

In general, obtaining the impulse response of mechanical systems is a complex task as these systems have different structures which make it difficult to apply an impulsive force input and record the system response. Moreover, in the current designed test the shaker limits add more difficulty as it is not capable of generating a force with high amplitude for a short period of time. To overcome this problem, the mathematical model (quarter- vehicle model) which represents the test rig was used to find the control forces against a shock input numerically. The developed Genetic Algorithm optimisation software shown in Fig 6.5 was used to find the control force plan against a shock input using the same procedure described in chapter 5, section 5.1.
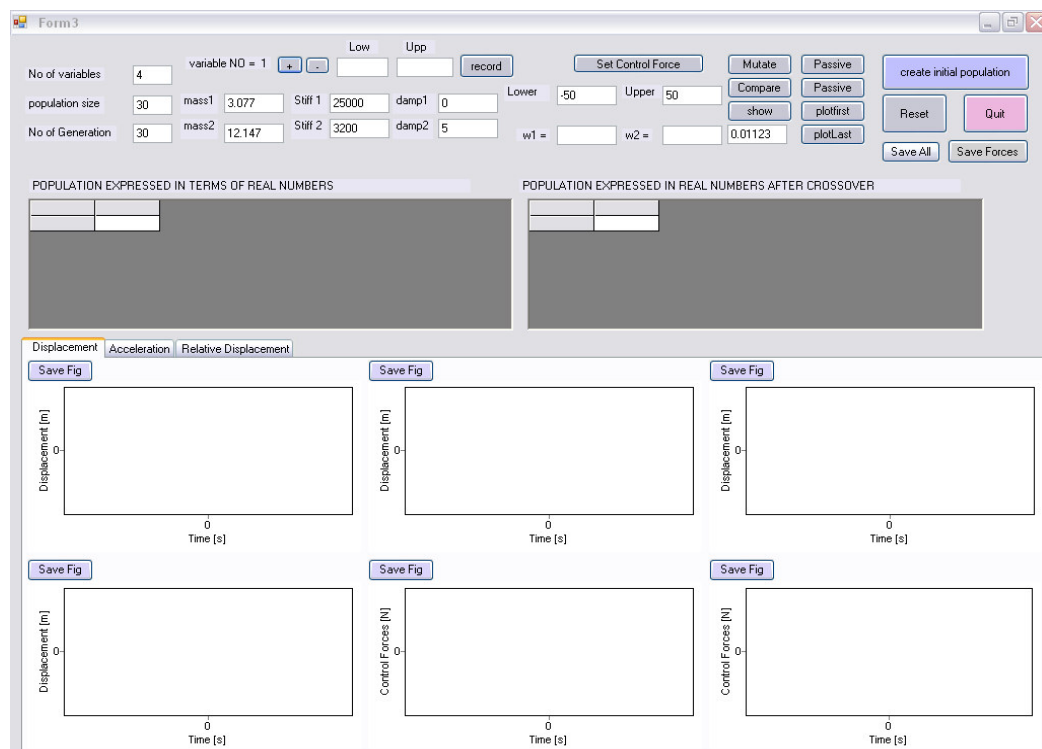
Fig 6.5 User friendly interface of the GA based optimisation software.

The GA was used to find the control force plan that minimises the sprung mass response when the system is subjected to the shock input shown in Fig 6.6. A consistent family of possible solutions was obtained. The GA-optimised control force plan considered here is shown in Fig 6.7 and the force values are tabulated in Table 6.2.
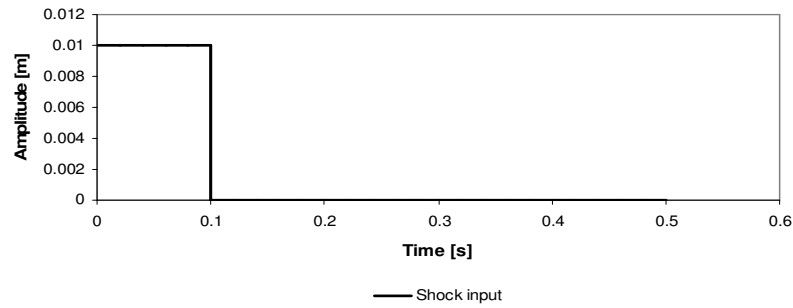
Fig 6.6 The shock input.
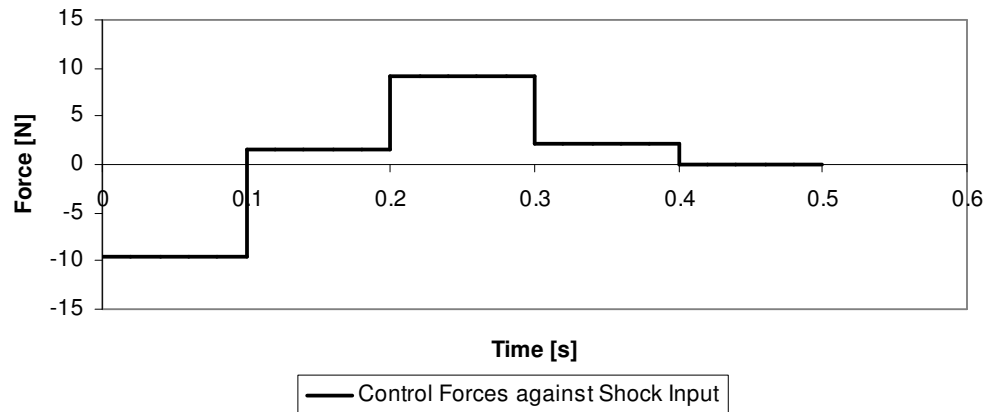
Fig 6.7 The optimised control forces by the GA against the shock input.

Table 6.2 The GA-optimised control force values.

Force	F_1	F_2	F_3	F_4
Value [N]	-9.632515	1.593025	9.085726	2.197852

111

The controlled response of the sprung mass in terms of displacement and acceleration is shown in Fig 6.8 and Fig 6.9 respectively. The relative displacement is shown in Fig 6.10. These figures show the improvement achieved by comparing the actively controlled response to the passive one.
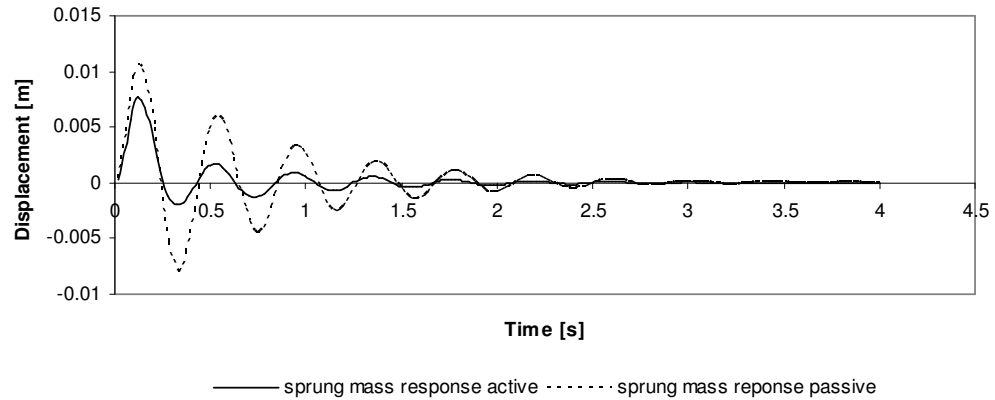
Fig 6.8 Displacement response of the sprung mass.
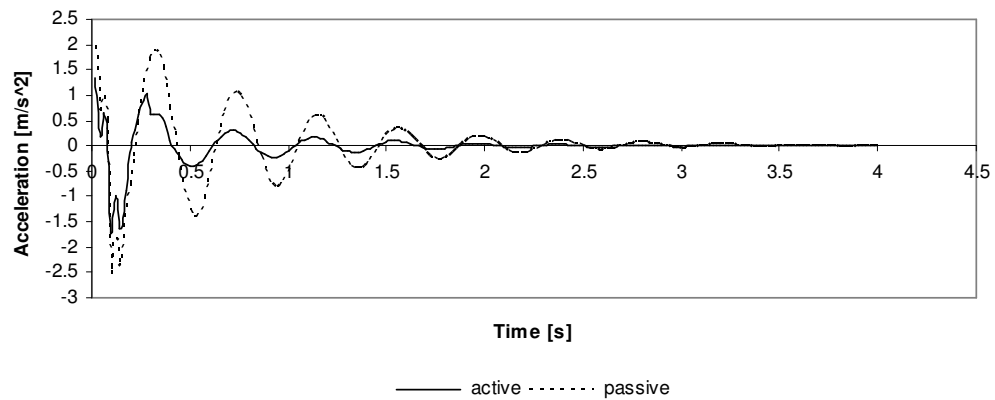
Fig 6.9 Acceleration response of the sprung mass.
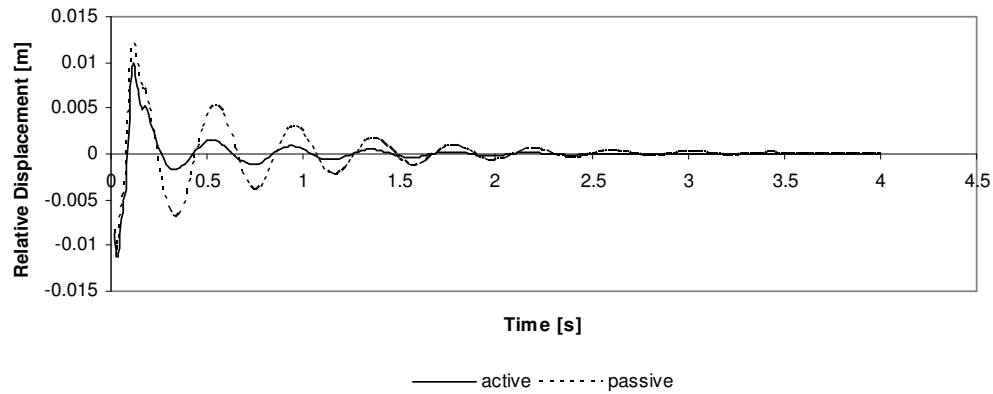
Fig 6.10 Relative Displacement (suspension deflection) response.

The optimised forces were saved to be used as the base for creating the control force strategy against the arbitrary excitation. To do so, the obtained control forces should now be converted into a voltage signal to be sent to the E-P Regulator as these forces will be generated by controlling the E-P Regulator pressure output and consequently the pneumatic actuator forces. The task now is to establish the relationship between the E-P Regulator input voltage and the force output of the pneumatic actuator, which can be found as follows:

1. Find the relationship between the Pneumatic actuator forces and the pressure supply.
2. Find the relationship between the Electro-Pneumatic pressure output and the voltage signal input.
3. As a result of combining step1 and 2 a new Force-Volt relationship emerged.

Fig 6.11 shows the relationship between the Pneumatic actuator forces and the pressure supply [113]. Fig 6.12 shows the relationship between the E-P Regulator Pressure output and the voltage input signal (in the range of interest). This graph was obtained experimentally by applying different voltage input signal and reading the output pressure of the E-P Regulator. Fig 6.13 shows the obtained relationship between the voltage input signal of the E-P Regulator and the output Forces of the Pneumatic actuator.

Pneumatic Actuator Force Vs Pressure
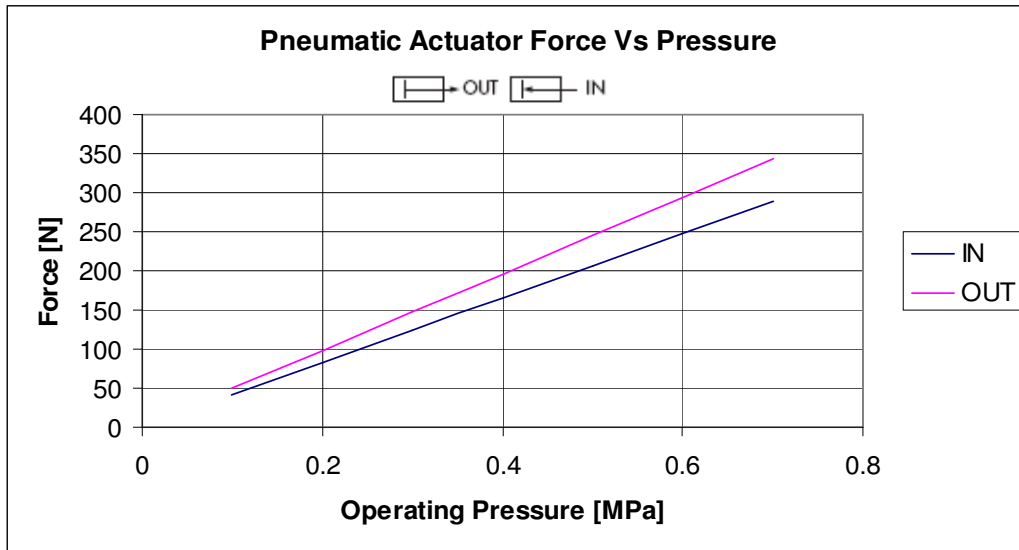
Fig 6.11 Pneumatic Actuator Forces Vs pressure supply.

E-P Regaulator Pressue Output Vs Volt
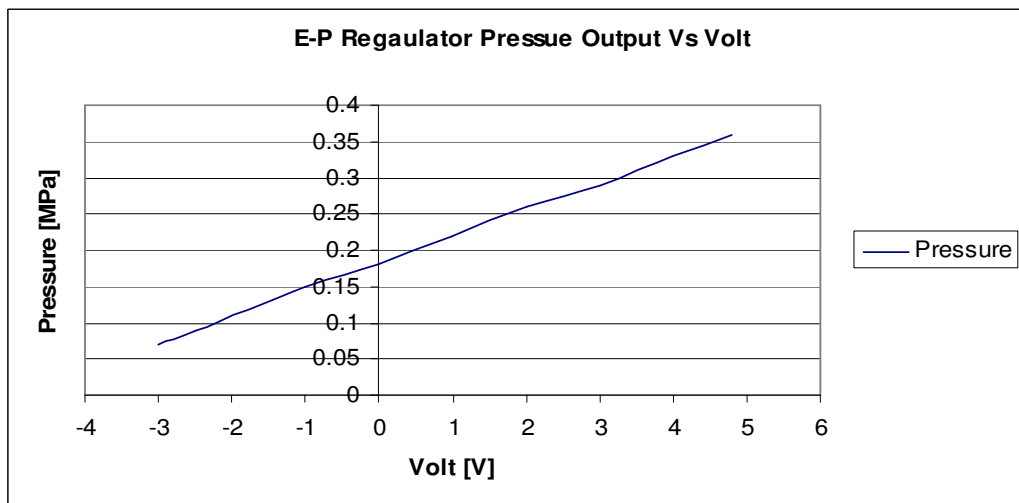
Fig 6.12 Electro-Pneumatic Regulator Pressure Vs Volt Input Signal.
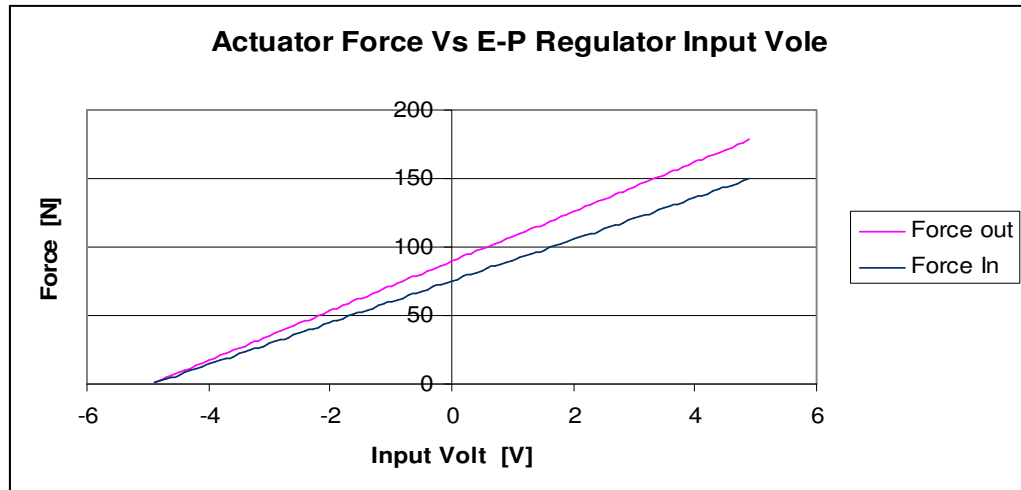
Fig 6.13 Actuator Force Vs Electro-Pneumatic Regulator Input Voltage.

As the Genetic algorithm optimisation program is connected to the main program of data processing and control, the values of the forces obtained by the GA will be imported and converted directly based on the relation in Fig. 6.13 to be used in controlling the system response against the arbitrary excitation input.

6.3.2. Control Strategy against arbitrary excitation

The obtained control force plan against shock input will now be used as the main base to generate a general control force strategy against arbitrary excitation in a real time application. Two kinds of excitation signals; random and sweep sine waves were chosen as an input to the system. The selected signal levels were chosen taking into account the shaker limits such as the low frequency and the maximum displacement that can be generated by the specified shaker. Fig 6.14 and Table 6.3 show the schematic drawing of the whole active suspension test rig and its parts.
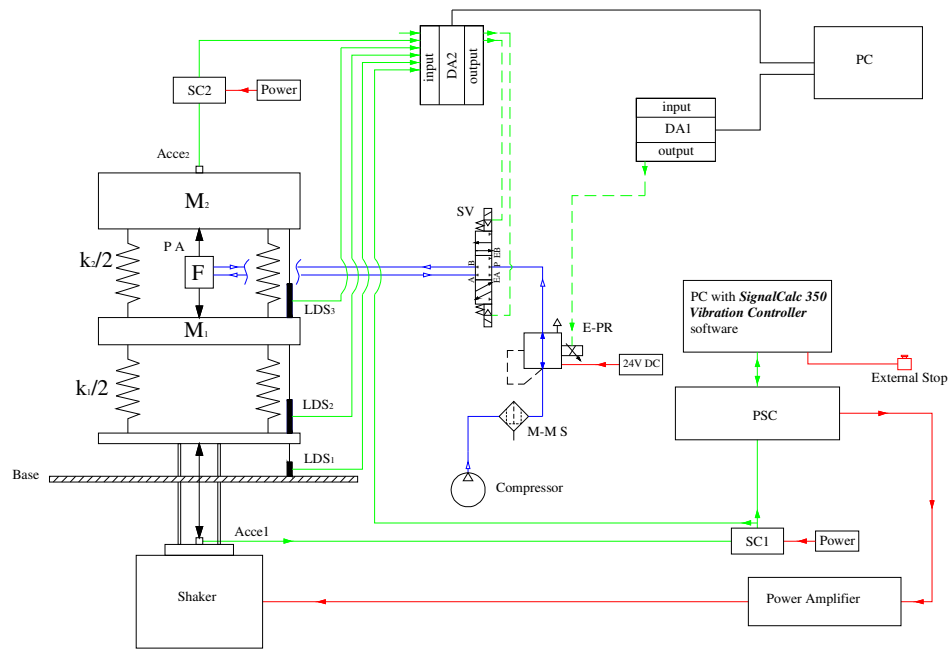
Fig 6.14 Schematic of the active suspension system.

Table 6.3 The main parts names of Fig 6.11.

Part	Specifications
PC	Personal Computer
PSC	Programmable Sine Controller
E-PR	Electro-Pneumatic Regulator
M-M S	Micro-Mist Separator
SV	Solenoid Valve
DA_i	Data Acquisition Card
SC_i	Signal Conditioner
$Acce_i$	Accelerometer
PA	Pneumatic Actuator
LDS_i	Linear Displacement Sensor

6.3.2.1. Test procedure

The test was carried out as follows: After checking that all the equipment was correctly connected and powered with the accurate input values, the generated signal by *SignalCalc 350* software was sent to the shaker through the Omega amplifier. As the shaker started vibrating the active control system was ready to deliver the right control forces by checking the LDS1 output (x_0 amplitude) and instantaneously calculating the right value of the force to be applied using an algorithm for calculating the scaling factor (λ_i) as explained in Eq.(6.1).

$$\lambda_i = \frac{the\,measured\,x_0\,Amplitude}{the\,Shock\,Amplitude\,used\,\,for\,GA\,optimization} \qquad (6.1)$$

The forces obtained by the GA were first scaled by λ_i and then applied according to their specified time which resulted in accumulating the forces to be applied by the pneumatic actuator at the right time to act in response to the arbitrary input excitation.

Force values were sent as a voltage input to the E-Pressure Regulator to control the pressure supply of the pneumatic actuator which consecutively provided the right forces that corresponded to these voltage input signals using the obtained relationship shown in Fig 6.13. The forces direction was achieved by controlling the solenoid valve which determined the direction of the pneumatic actuator pressure supply. The acceleration of the sprung mass, the relative displacement, the wheel displacement, and the road input displacement were measured, while the sprung mass displacement and tyre deflection were calculated based on the measured data. All these parameters were recorded and saved to be used for performance evaluation.

6.4. Experimental Results

This section presents the experimental results obtained by applying the CCFS method to control the response of a quarter-vehicle active suspension to an external arbitrary excitation. The experimental results of actively controlling the response of system when it is subjected to a random and sweep sine wave input are given below.

6.4.1. The results of applying the CCFS method against random input

The random signal generated by the *VB85* Shaker is shown in Fig 6.15. Using the procedure explained in section 6.3.2 to control the response of the system due to random input, the controlled sprung mass displacement response is compared to the passive response in Fig 6.16, while the acceleration response is compared to the passive one in Fig 6.17. The controlled suspension deflection and tyre deflection responses are compared to the passive ones in Fig 6.18 and Fig 6.19 respectively.
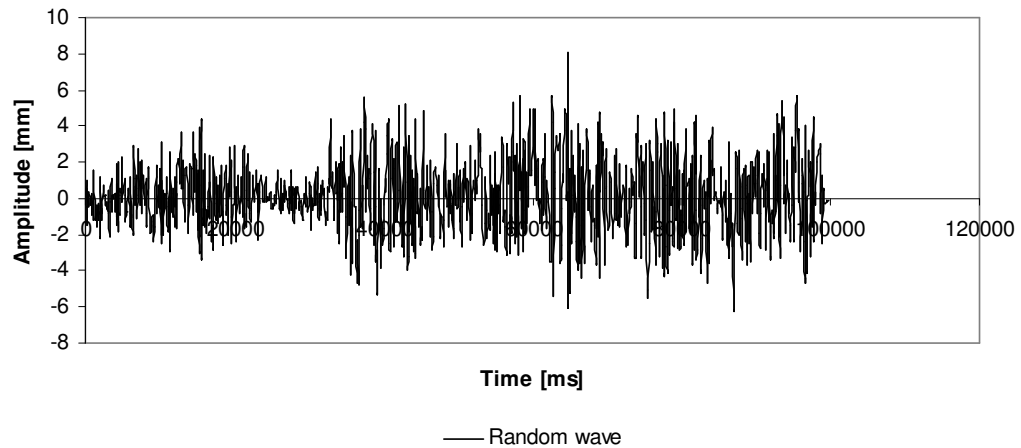
Fig 6.15 Random wave input.
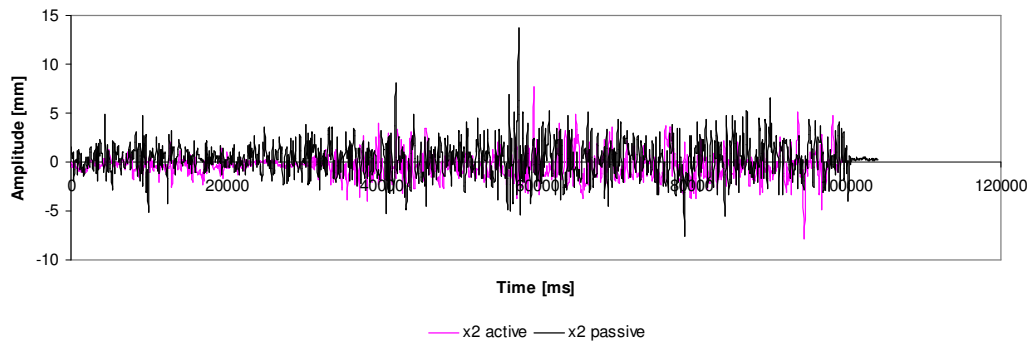
Fig 6.16 Displacement response of the sprung mass.
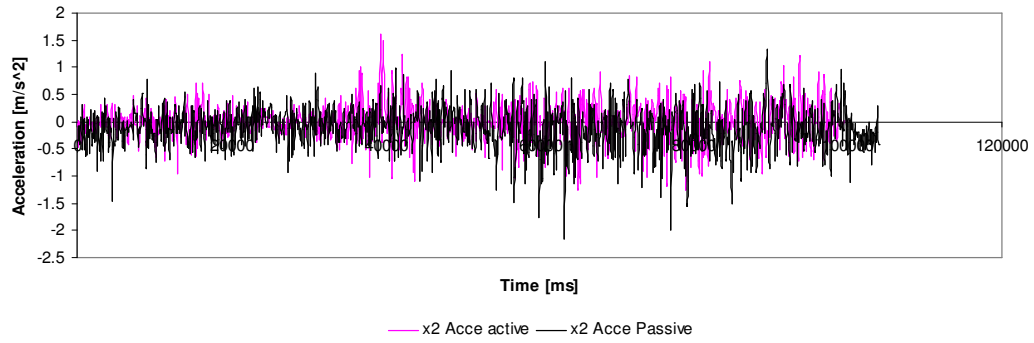
Fig 6.17 Acceleration response of the sprung mass.
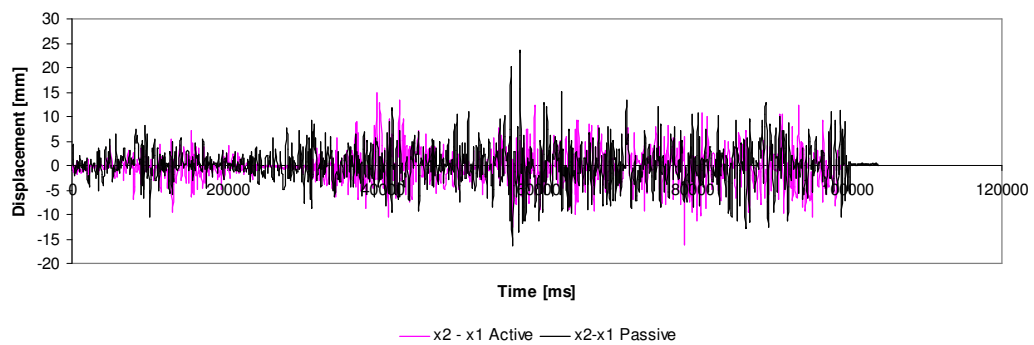
Fig 6.18 Relative Displacement (suspension deflection) response.
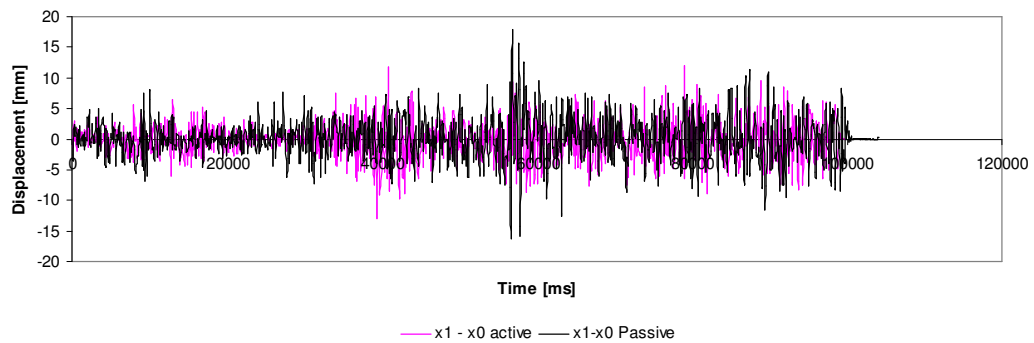
Fig 6.19 Tyre deflection response.

To verify the improvement achieved by applying the CCFS method to control the system response when it was subjected to the random input, the RMS values of the above responses were calculated and tabulated in Table 6.4.

119

Table 6.4 RMS values of the system response criteria (Random I).

		Passive	**CCFS**	**Improvement %**
RMS x_2	[mm]	1.805564	1.328456	26.42
RMS $\ddot{x}_2$	[m/s^2]	0.396666	0.345072	13.01
RMS $x_2 - x_1$ [mm]		3.966833	3.467429	12.59
RMS $x_1 - x_0$ [mm]		3.337446	3.084799	7.57

6.4.2. The results of applying the proposed method against a Sweep Sine input

A similar approach was used to control the system response to a sweep sine input with the objective of minimising the sprung mass response. The GA-optimised control force plan against the shock input is shown in Fig 6.20 and the forces values are tabulated in Table 6.5. The Sweep sine wave between 7-50 Hz generated by the *VB85* shaker is shown in Fig 6.21. The controlled displacement and acceleration responses of the sprung mass against the passive responses are shown in Fig 6.22 and Fig 6.23 respectively. Fig 6.24 shows the controlled suspension deflection response compared to the passive one, while the tyre deflection is shown in Fig 6.25.
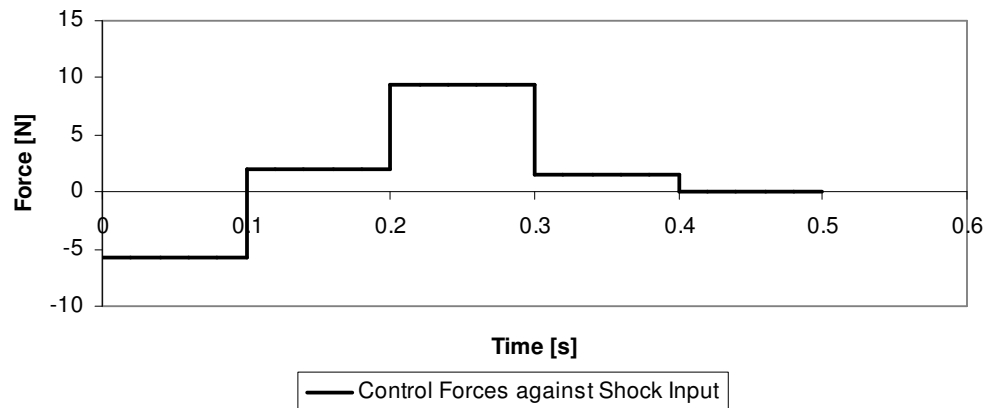
Fig 6.20 The GA-optimised control forces against shock input.

Table 6.5 The GA-optimised control forces values.

Force	F_1	F_2	F_3	F_4
Value [N]	-5.69649	2.075207	9.487933	1.520243
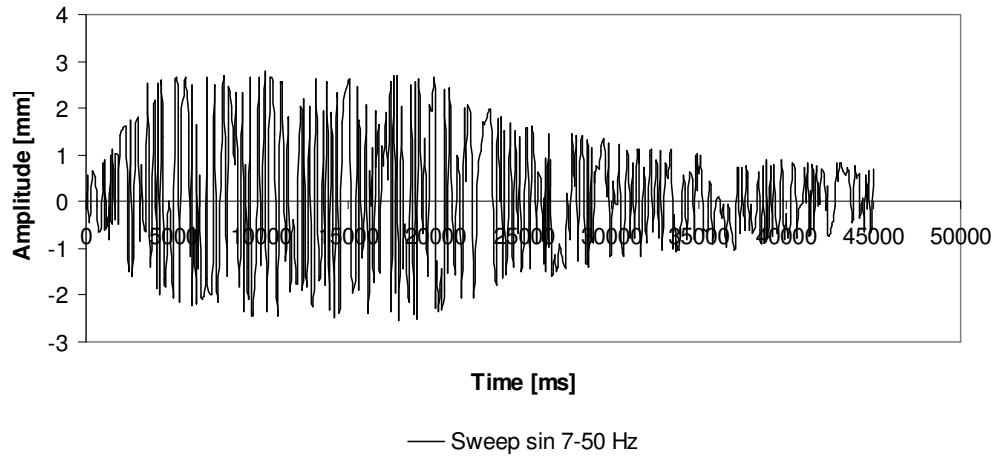
Fig 6.21 Sweep sine wave input.
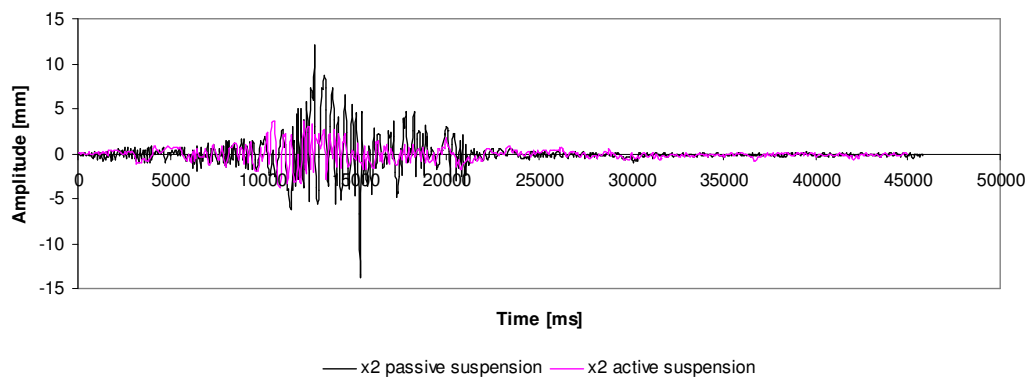
Fig 6.22 Displacement response of the sprung mass.
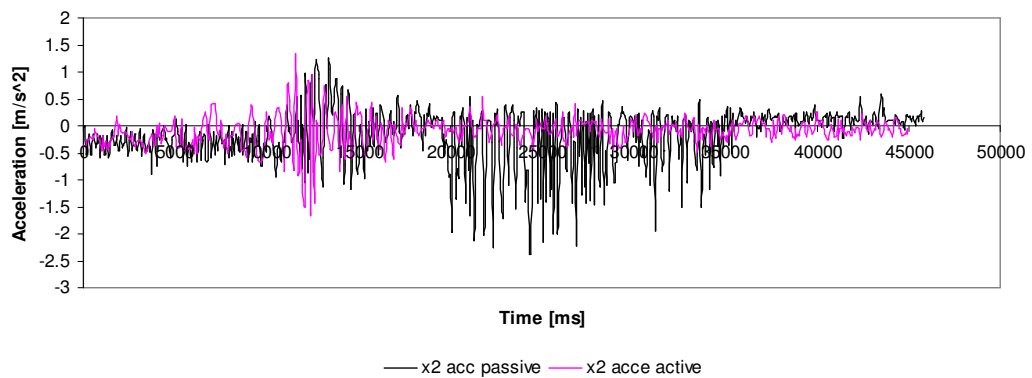
Fig 6.23 Acceleration response of the sprung mass.

121
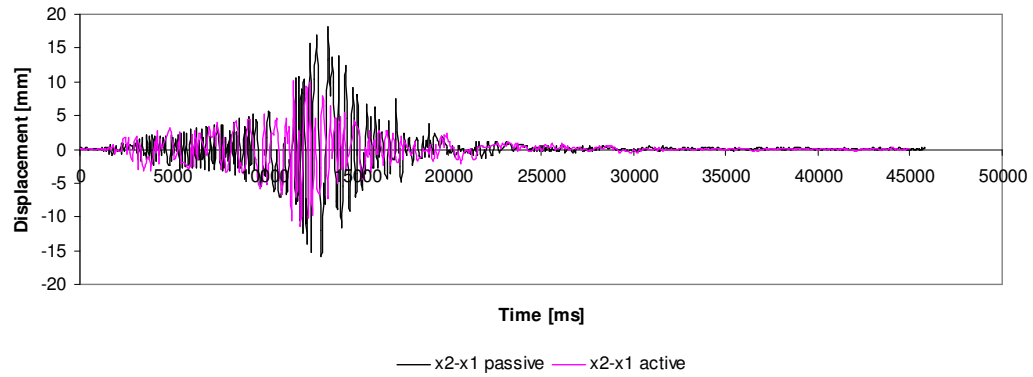
Fig 6.24 Relative displacement (suspension deflection) response.
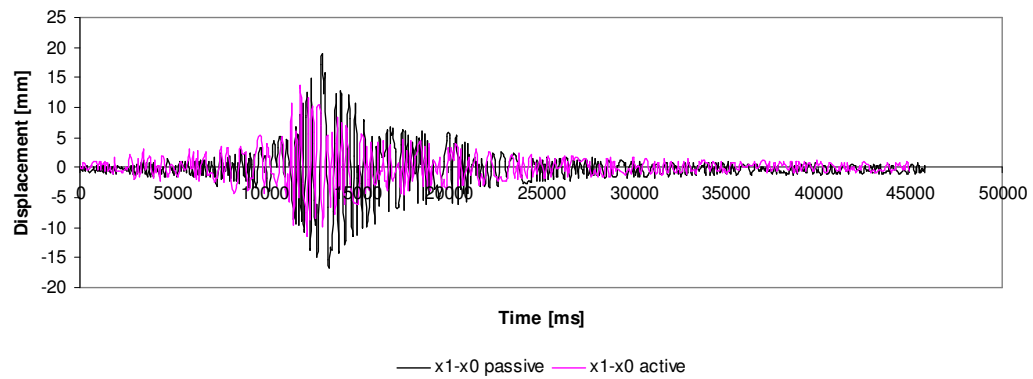
Fig 6.25 Tyre deflection response.

As it could be difficult to draw a conclusion out of the above graphs; therefore, the RMS values of the system responses were calculated and they are shown in Table 6.6.

Table 6.6 RMS values of the system responses (Sweep sine).

			Passive	**CCFS**	**Improvement %**
RMS	x_2	[mm]	1.729477	0.882546	48.97
RMS	$\ddot{x}_2$	[m/s²]	0.544824	0.294449	45.96
RMS	$x_2 - x_1$ [mm]		3.221245	2.188105	32.07
RMS	$x_1 - x_0$ [mm]		3.522901	2.736518	22.32

To demonstrate that the control forces obtained by GA to minimise the system response due to a shock input can be used as the base to generate a control force strategy against any arbitrary excitation input, <u>the same</u> forces shown in Fig 6.20 which was used to generate a control force strategy against Sweep Sine input were also used to generate a control force strategy against the random input. Fig 6.26 shows the controlled sprung mass displacement response against the passive one. The RMS values of the other criteria are shown in Table 6.7.
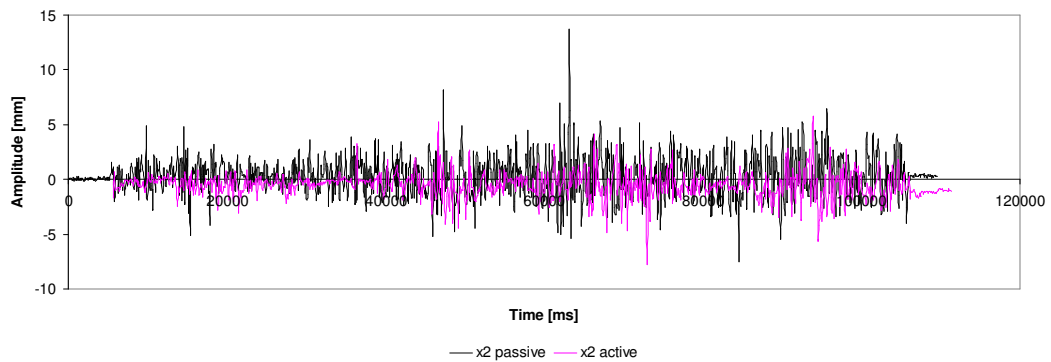
Fig 6.26 Displacement response of the sprung mass.

Table 6.7 RMS values of the system response criteria (Random II).

	Passive	**CCFS**	**Improvement %**
RMS x_2 [mm]	1.751325	1.250706	28.59
RMS $\ddot{x}_2$ [m/s^2]	0.397865	0.364758	8.32
RMS $x_2 - x_1$ [mm]	3.846004	3.606432	6.23
RMS $x_1 - x_0$ [mm]	3.236902	2.984413	7.8

6.5. Programmable Logic Controller (PLC)

To further investigate the capability of the proposed CCFS method to be implemented using different controller. A Programmable Logic Controller (PLC) was used to apply the proposed control algorithm, a Phoenix PLC (INLINE controller ILC 150 ETH) as shown in Fig 6.27 was used to control the quarter-vehicle active suspension system. The programming part was done using the PC WorX automation software as shown in Fig 6.28. The proposed "Convolution based control force strategy (CCFS)" approach was followed. The aim was to minimise the system response to a sweep sine (5-50 Hz) external excitation. Fig 6.29 shows the schematic diagram of the test setup including the PLC. The main parts of the system are presented in Table 6.8.

The same force values presented in Table 6.5 were used to generate the overall control force strategy following the same test procedure explained in section 6.3.2. Fig 6.27 shows the PLC used to control the quarter-vehicle test rig using the proposed method. The initial results obtained were quite promising, Fig 6.30 shows the sprung mass displacement response controlled using the CCFS method and compared to the passive (non-controlled) response. The suspension deflection response (controlled using CCFS and the passive one) is shown in Fig 6.31 and the sprung mass acceleration response is shown in Fig 6.32.

It can be clearly seen form the obtained results that the using the PLC to implement the CCFS method resulted in an improved response of the system. However, the application requires further investigations especially the timing issues of both the PLC and the control equipment
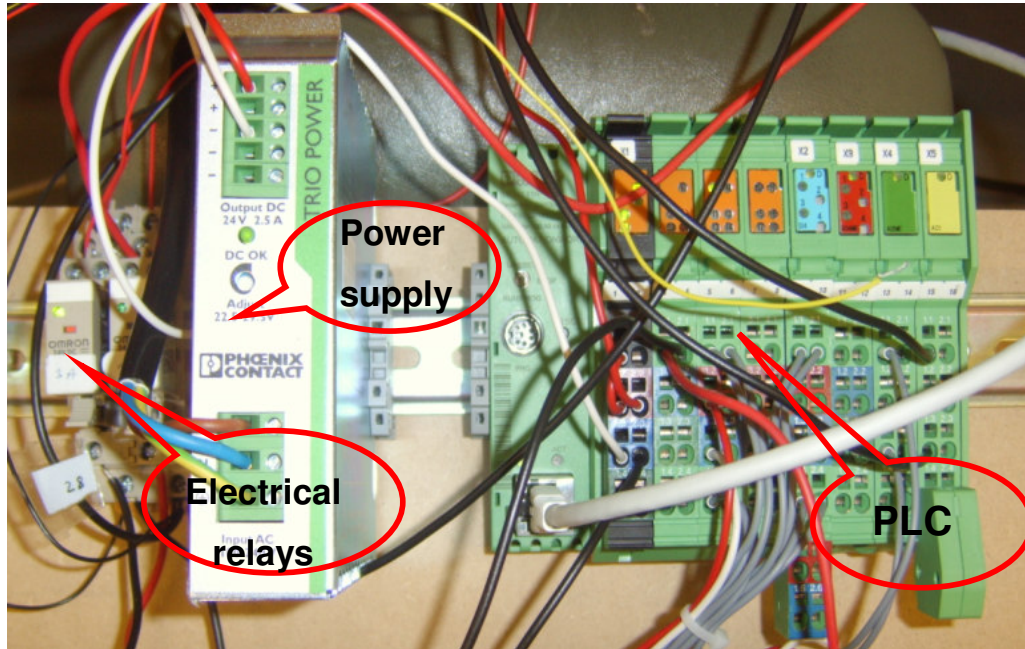
Fig 6.27 The Phoenix PLC connected to the relays and power supply.
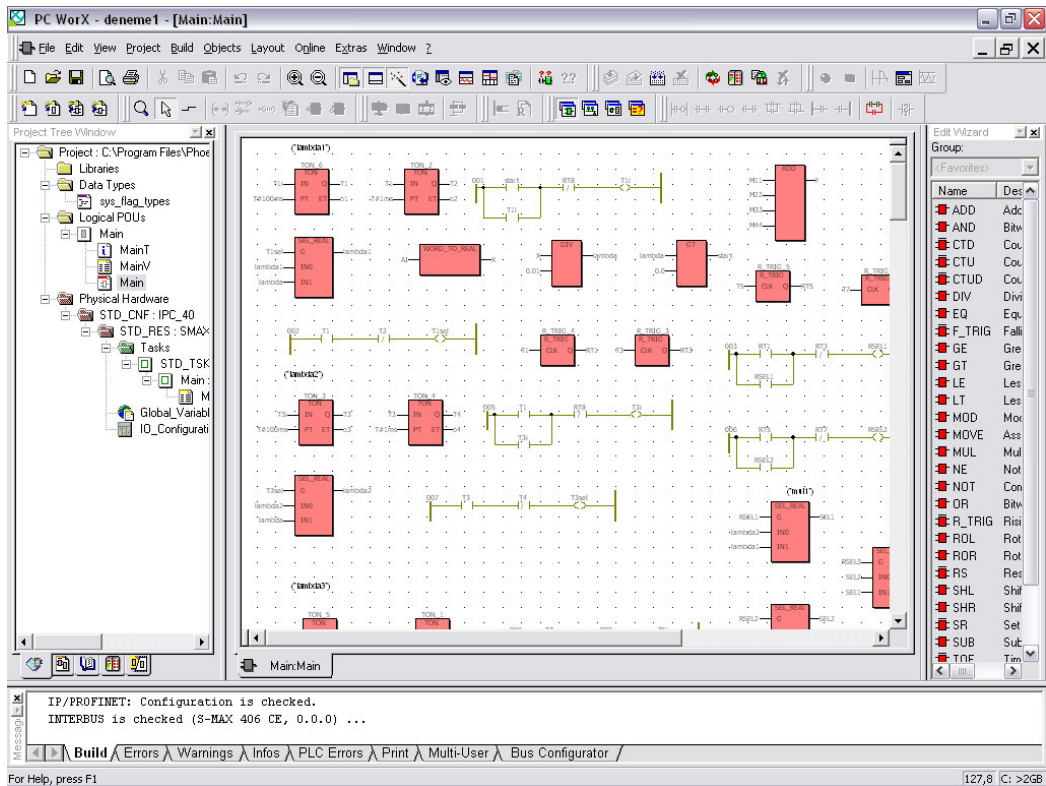
Fig 6.28 The user friendly interface of the PC WorX software.
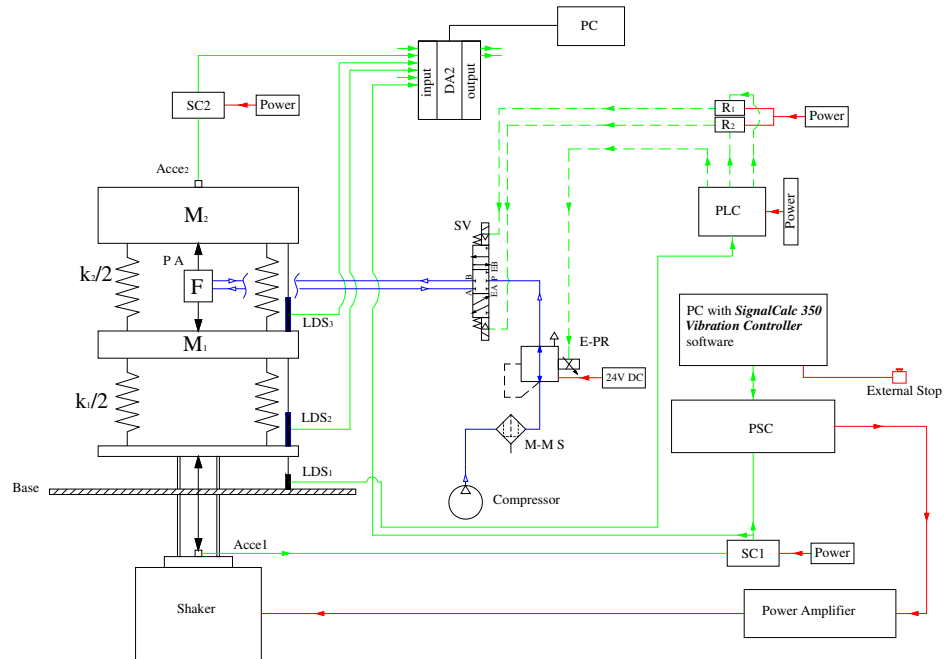
Fig 6.29 Schematic of the active suspension system with PLC.

Table 6.8 The main parts names of Fig 6.29.

Part	Specifications
PC	Personal Computer
PSC	Programmable Sine Controller
E-PR	Electro-Pneumatic Regulator
M-M S	Micro-Mist Separator
SV	Solenoid Valve
DA_i	Data Acquisition Card
SC_i	Signal Conditioner
$Acce_i$	Accelerometer
PA	Pneumatic Actuator
LDS_i	Linear Displacement Sensor
PLC	Programmable Logic Controller
R_i	Relay
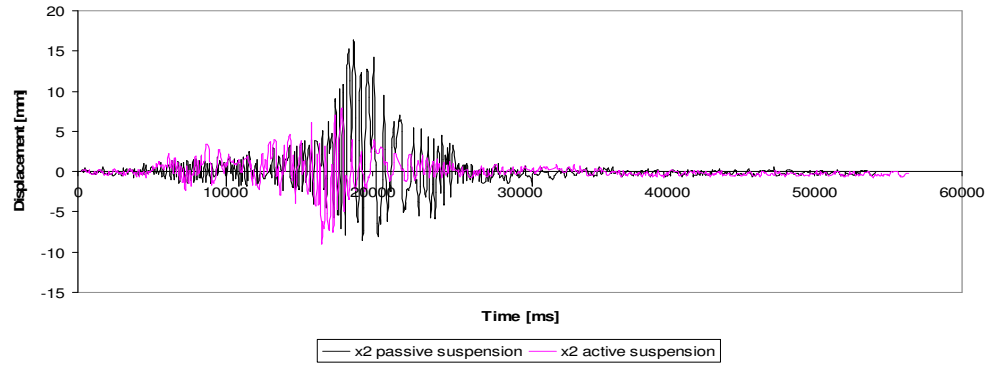
Fig 6.30 The sprung mass displacement response to sweep sine excitation.
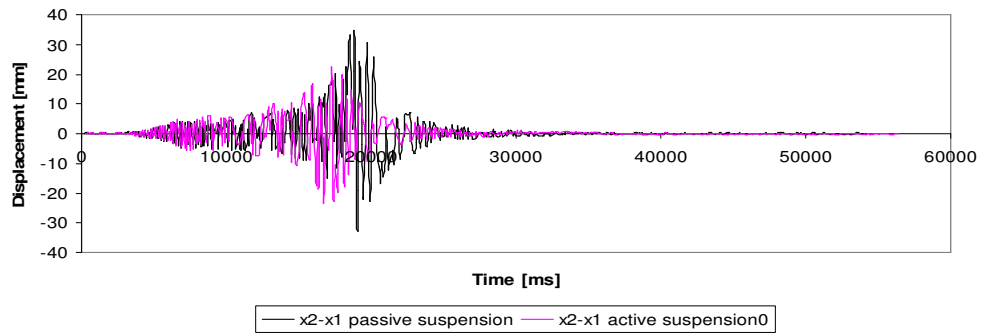
Fig 6.31 Relative displacement (suspension deflection) response.
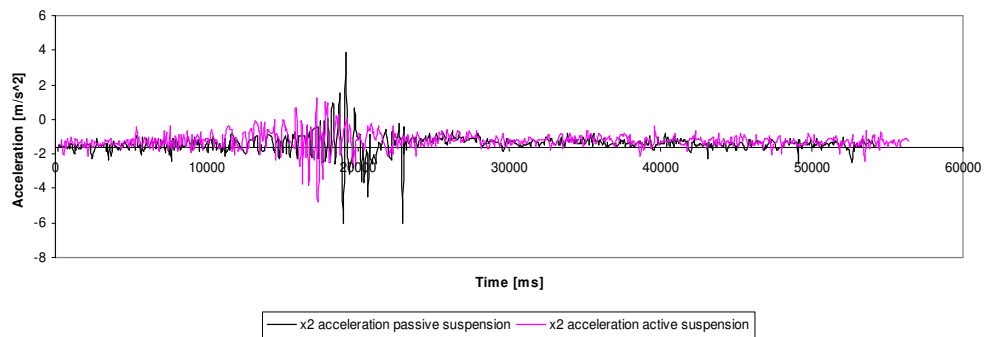
Fig 6.32 Sprung mass acceleration response.

Chapter 7

7. Discussion

In this chapter the improvements achieved by applying the proposed method "convolution of the control force strategy" to control the vibration of the quarter- and full- vehicle model will be discussed. In addition, the level of improvements accomplished from the experiments will be emphasised taking into consideration the objectives of the work; what was expected and what has been achieved.

Starting with the quarter-vehicle model, and based on the numerical results Fig 5.12 pp. 71 and Fig 5.19 pp. 74 and the Root Mean Square (RMS) values in Table 7.1 below, one can easily observe the superiority of the proposed method in reducing the quarter-vehicle displacement response for both shock and arbitrary excitations over the passive suspension response. The controlled displacement response of the vehicle body to the shock excitation using the proposed method was almost the same as the displacement response using the LQR method but with reduction of the peak value, as shown in Fig 5.31 pp. 82 and Table 7.1. The achievement was the improvement in the sprung mass displacement response to the arbitrary excitation using proposed method when compared to the response with LQR method as shown in Fig 5.33 pp. 82. This improvement was found to be a 59.68% reduction in the RMS value of the displacement response achieved using the proposed method as presented in Table 7.1. As expected there was a slight increase in the sprung mass acceleration response due to the shock excitation and a marginally higher acceleration response in the case of the arbitrary excitation using the CCFS method when compared to the responses using the LQR method as shown in Fig 5.35 pp.83 and Fig 5.37 pp. 84. The increase of the RMS value of the sprung mass acceleration response was expected due to the fact that the Genetic Algorithm attempted to obtain the control strategy that minimised the displacement response of the system, clearly stated in the objective function formula. While the sprung mass acceleration response using the proposed method is much better than the response with passive system; this is clear from the results shown in Fig 5.21 pp. 75 and RMS values in Table 7.1.

To see the effect of the proposed method on the other suspension criteria, the suspension deflection and tyre deflection responses were also checked. The controlled suspension deflection response to the arbitrary excitation using the proposed method was almost identical to that achieved using the LQR method as shown in Fig 5.41 pp. 85 and provided a significant improvement over that generated by the passive suspension as shown in Fig 5.23 pp. 76. The tyre deflection response to the arbitrary excitation was very similar to that obtained with the LQR method as shown in Fig 5.45 pp. 86, and was much improved in comparison to the tyre deflection of the passive system which can be seen in Fig 5.25 pp. 76. Therefore, it can be concluded that in comparison to the performance of the LQR method, the proposed method could significantly improve the displacement response of the vehicle body with a slight expected increase in the acceleration response. There was also no degradation in the suspension deflection or the tyre deflection for both shock and arbitrary excitation, and superior performance for all the suspension criteria in comparison to the passive suspension performance.

Table 7.1 Root Mean Square (RMS) for the Quarter-vehicle responses

	Shock input			**Arbitrary input**		
	Passive	**LQR**	**CCFS**	**Passive**	**LQR**	**CCFS**
RMS x_s [m]	0.026	0.00093	0.00097	0.531	0.0062	0.0025
RMS $\ddot{x}_s$ [m/s^2]	1.6	1.147	1.588	14.535	1.499	2.42
RMS Forces [N]	-	1373.49	1199.73	-	10202.96	10493.31

For the full-vehicle model, applying the proposed method resulted in the best displacement response at each corner of the full-vehicle model when compared to the response with passive suspension; this can be clearly seen for the front-right corner response (Z_{p1}) to the shock excitation in Fig 5.50 and to the arbitrary excitation in Fig 5.52 pp. 94. Moreover, one can easily observe the improvements achieved as the RMS values were significantly reduced by using the proposed method to control the vehicle response for both shock and arbitrary excitation as presented in Table 7.2. Similarly, the vehicle body displacement response (Z_5) was considerably reduced in comparison to the passive response for both shock excitation Fig 5.54 pp. 95 and

arbitrary excitation Fig 5.55 pp. 95; this can also be observed from the enormous reduction in the RMS values of the vehicle body displacement response presented in Table 7.2. From Fig 5.58 pp. 97 the vehicle body acceleration response ($\ddot{Z}_5$) to the arbitrary excitation was by far better than the one achieved with passive suspension. The pitch acceleration ($\ddot{\alpha}$) was also greatly improved in comparison to the passive response which can be seen in Fig 5.61 pp. 98; accordingly, the RMS values for ($\ddot{Z}_5$) and ($\ddot{\alpha}$) were also drastically improved as presented in Table 7.2. Exploring the effects of applying the proposed method on suspension deflection revealed that the suspension deflection response to both shock and arbitrary excitation was improved as shown in Fig 5.63 pp. 98 and Fig 5.65 pp. 99, together with the RMS values of Z_{p1}-Z_1 presented in Table 7.2.

Table 7.2 Root Mean Square (RMS) for the Full-vehicle responses:

	Shock input		**Arbitrary input**	
	Passive	**CCFS**	**Passive**	**CCFS**
RMS Z_{p1} [m]	0.0425	0.00165	0.3781	0.0131
RMS Z_5 [m]	0.0226	0.00093	0.3859	0.0075
RMS $\ddot{Z}_5$ [m/s^2]	1.304	1.348	9.677	2.724
RMS $\ddot{\alpha}$ [rad/s^2]	0.958	0.396	3.32	1.713
RMS $Z_{p1} - Z_1$ [m]	0.0544	0.0503	0.315	0.159

From previous discussion, it is possible to realize that the application of the proposed method "convolution of the control force strategy" to control the full-vehicle model response when it is subjected to a shock or to a random road excitation has shown the superiority of the proposed method in improving the vehicle body displacement and acceleration responses. Moreover, it was not only able to maintain the suspension deflection but also improve it over the response of a system with passive suspension.

The time-delay effects on the performance of the proposed method have also been studied to show the robustness of the method with regards of the time delay issue. The chosen time-delay value accounts for all the delay that could occur in the system due to the inability of the actuator to be able to deliver the required control forces at

the right time. The results shown in Fig 5.67 and Fig 5.68 pp. 102 demonstrate that even when increasing the time-delay value up to 40 ms the proposed method was able to control the vehicle body response to the arbitrary excitation and the response provided a significant improvement over the passive system response.

Throughout the experimental tests, great care was taken to minimise the experimental inaccuracies, especially eliminating the signal noise caused by the high voltage and high magnetic field generated by the shaker and its air cooling system. An A/120/VTN accelerometer was used for the shaker, which was specially designed to minimise the effects of the magnetic field on the signal, in addition, signal conditioners with low noise operation were used to guarantee supply power to the accelerometers from a constant current source. Two separate power supply sources were used to provide a constant 24v and 5v Dc for the E-P Regulator and the solenoid valve respectively, reducing the fluctuation in power supply. Most of the wires and the BNC cables were isolated and kept as far away form the magnetic field as possible. All the instruments, input and output channels were calibrated before running the tests. The aforementioned issues were done to reduce the effects of the inaccuracies in the system and to ensure that reliable, feasible and conclusive results would be obtained.

The observations obtained from applying the CCFS method to control the response of the quarter-vehicle test rig (in real time), can be expressed as follows:
For the random road input, the CCFS method managed to significantly improve the sprung mass displacement response in comparison to the passive response which can be seen in Fig 6.16 pp. 118. It was found that a 26.42% improvement was achieved in the RMS value of the sprung mass displacement response over the passive system as presented in Table 6.4. There was also a 13.01% improvement in the RMS value of the sprung mass acceleration response, a 12.59% improvement in the RMS value of the suspension deflection response, and a 7.57% improvement in the RMS value of the tyre deflection over the responses with the passive suspension system as shown in Table 6.4.

Table 6.4 RMS values of the system response criteria. (Random I)

	Passive	**CCFS**	**Improvement %**
RMS x_2 [mm]	1.805564	1.328456	26.42
RMS $\ddot{x}_2$ [m/s^2]	0.396666	0.345072	13.01
RMS $x_2 - x_1$ [mm]	3.966833	3.467429	12.59
RMS $x_1 - x_0$ [mm]	3.337446	3.084799	7.57

For the sweep sine wave input, the superiority of the proposed method in controlling the quarter-vehicle test rig responses could be clearly seen in Fig 6.22 pp. 121 for the sprung mass displacement response and from the 48.97% improvement of the associated RMS value presented in Table 6.6. The sprung mass acceleration response was also improved as shown in Fig 6.23 pp. 121; the improvement in the RMS value of the sprung mass acceleration was found to equal 45.96% displayed in Table 6.6. The other suspension criteria were also recorded to demonstrate how they were affected by the application of the proposed method. The suspension and tyre deflection responses to the sweep sine excitation were improved in comparison to the responses of passive system as shown in Fig 6.24 and Fig 6.25 pp. 122. A 32.07% improvement in the RMS value of suspension deflection and a 22.32% improvement in the RMS value of the tyre deflection as tabulated in Table 6.6 were observed.

Table 6.6 RMS values of the system responses (Sweep sine).

	Passive	**CCFS**	**Improvement %**
RMS x_2 [mm]	1.729477	0.882546	48.97
RMS $\ddot{x}_2$ [m/s^2]	0.544824	0.294449	45.96
RMS $x_2 - x_1$ [mm]	3.221245	2.188105	32.07
RMS $x_1 - x_0$ [mm]	3.522901	2.736518	22.32

As explained in Chapter 6 the control force strategy obtained by GA to minimise the system response to a shock input, which was used to generate the control force strategy against the sweep sine excitation, was also used as the base to generate a control force strategy against different arbitrary excitation. This was carried out to demonstrate that regardless of the excitation nature (random or otherwise) the

proposed method is capable of controlling the system response and this could be clearly seen in Fig 6.26 pp. 123 in which the sprung mass controlled response was compared to the passive one. A 28.59% improvement in the RMS value of the displacement response over the passive one was achieved. Moreover, all other suspension criteria were improved as can be observed from the RMS values in Table 6.7.

Table 6.7 RMS values of the system response criteria. (Random II).

	Passive	**CCFS**	**Improvement %**
$RMS \quad x_2 \qquad$ [mm]	1.751325	1.250706	28.59
$RMS \quad \ddot{x}_2 \qquad$ [m/s^2]	0.397865	0.364758	8.32
$RMS \quad x_2 - x_1$ [mm]	3.846004	3.606432	6.23
$RMS \quad x_1 - x_0$ [mm]	3.236902	2.984413	7.8

Consequently, the experimental results justify the obtained numerical results from the point that the proposed method could significantly improve some of the suspension criteria such as the displacement response and reasonably maintain or even improve the acceleration response, suspension deflection and tyre deflection.

The aforementioned results and discussion demonstrate that the proposed method can be used for real-time control applications. Once the control strategy for the shock disturbance is established, the results can then be used at each time step when online control is performed. Therefore, the system can be controlled in real time irrespective of the nature of the external excitation. The inclusion of the time delay made the approach more realistic as the majority of real time applications suffer from time-delay caused by many sources. The inclusion of different time delay values demonstrated that the proposed method was capable of achieving acceptable results.

One should also state that even though the control strategy was obtained by means of Genetic Algorithm, the method is applicable irrespective of the optimisation method. The simplicity of the proposed method would make implementation rather straight forward. One of the most significant advantages of the proposed method is the reduction in the number of sensors needed to construct the control strategy in

comparison to what currently exists in literature, resulting in less contaminated signals and reduced construction cost of the control system.

Chapter 8

8. Conclusion and Future works

8.1. Conclusion

A new method for obtaining a real-time control strategy to suppress the vibrations of oscillatory systems subjected to an arbitrary external excitation has been presented in this study. The proposed method "Convolution based Control Force Strategy (CCFS)" made use of the convolution concept to constitute a control force strategy which was able to achieve a real-time control of the system response caused by an external arbitrary disturbance. The only requirement to achieve this is to obtain a control strategy that minimises the system response to an impulse disturbance. In this study a Genetic Algorithm (GA) was used as the global optimisation tool to obtain the control strategy in preference to the methods from the classic optimal theory and it was shown to give promising results. Then by dividing the arbitrary excitation into impulses and simply following the convolution concept for each impulse, the GA-obtained control strategy would be scaled, shifted and by summation the overall control strategy against the arbitrary excitation was established. The proposed method was applied to control the response of a quarter-vehicle active suspension system subjected to an arbitrary external disturbance. The results showed significant improvements achieved especially for the vehicle body displacement response in comparison to results obtained using both the LQR method and a passive suspension system. The method was also applied to control the response of a simulated full-vehicle active suspension system, where the time lag between front and rare wheels was considered. The effect of a time-delay on the proposed approach performance was also studied and the numerical results showed that the proposed method was capable of achieving a good performance even when it was subjected to 40 ms time delay. To show the ability of the proposed method to be implemented and its applicability for real-time control, sets of experimental test were completed on a quarter-vehicle test rig with a pneumatic active suspension system. The experimental results demonstrated the performance enhancement achieved in terms of displacement, acceleration, suspension deflection and tyre deflection responses to different road inputs.

Finally, the CCFS method, which utilised the Convolution concept to construct a real-time control, is a generic robust control method which can be applied in many other fields. The simplicity of the method makes implementation straight forward, especially that less number of sensors are needed for measurements, as the disturbance amplitude is the only input to be measured. This indeed will give a good insight to the suspension system designers in the automotive field.

8.2. Future works

- The proposed method has been applied to a quarter-vehicle test-rig, but it would be more interesting to extend the method to facilitate field testing on a real vehicle. For real vehicle testing many modifications are required, including implementation of the proposed control algorithm using an embedded system, microprocessor or Programmable Logic Controller (PLC). More investigations are needed for the pneumatic system especially the response time of each equipment to ensure that the correct components can be chosen to fit the real vehicle test.

8.3. Published Papers

[1] I. I. Esat and M. Saud, "A novel approach to obtain a real time control force strategy by using genetic algorithm and convolution integral," in *Integrated Design and Process Technology,* San Diego, 2006.

[2] M. Saud and I. I. Esat, "A novel method for obtaining real time control strategy using GA for dynamical systems subjected to external arbitrary excitations," in *Second International Symposium on Leveraging Applications of Formal Methods, Verification and Validation,* Paphos, 2006, pp. 161 – 168.

[3] M. Saud and I. I. Esat, "GA-based control force strategy for full-vehicle active suspension system using convolution integral," in *Integrated Design and Process Technology,* Antalya, 2007.

[4] I. I. Esat, M. Saud and S. N. Engin, "A Novel Method for Obtaining a Real-Time Control Force Strategy using Genetic Algorithm for Dynamic Systems Subjected to External Arbitrary Excitations," submitted to *Journal of Sound and Vibration*.

References

[1] C. R. Fuller, S. J. Elliot and P. A. Nelson, *Active Control of Vibration.* London: Academic Press, 1997.

[2] J. T. Xing, Y. P. Xiong and W. G. Price, "Passive–active vibration isolation systems to produce zero or infinite dynamic modulus: theoretical and conceptual design strategies," *Journal of Sound and Vibration,* vol. 286, pp. 615-636, 2005.

[3] S. S. Rao, *Mechanical Vibrations.* , Forth Edition in SI Units, Prentice Hall Singapore, 2005.

[4] A. Alkhatib and M. F. Golnaraghi, "Active Structural Vibration Control: A Review," *The Shock and Vibration Digest*, vol. 35, pp. 367-383, 2003.

[5] J. P. Hunt, *Dynamic Vibration Absorbers.* London: Mechanical Engineering Publications, 1979.

[6] J. L. Almazán, J. C. De la Llera, J. A. Inaudi, D. López-García and L. E. Izquierdo, "A bidirectional and homogeneous tuned mass damper: A new device for passive control of vibrations," *Engineering Structures,* vol. 29, pp. 1548-1560, 2007.

[7] T. Pinkaew and Y. Fujino, "Effectiveness of semi-active tuned mass dampers under harmonic excitation," *Engineering Structures,* vol. 23, pp. 850-856, 2001.

[8] C. M. Harris, *Shock and Vibration Handbook.* ,4Rev edition .London: McGraw Hill Higher Education, 1995.

[9] Y. Liu, T. P. Waters and M. J. Brennan, "A comparison of semi-active damping control strategies for vibration isolation of harmonic disturbances," *Journal of Sound and Vibration,* vol. 280, pp. 21-39, 2005.

[10] J - H. Koo, M. Ahmadian, M. Setareh and T. M. Murray, "In search of suitable control methods for semi-active tuned vibration absorbers," *JVC/Journal of Vibration and Control,* vol. 10, pp. 163-174, 2004.

[11] T. M. Whalen, K. M. Bhatia and G. C. Archer, "Semi-active vibration control for the 3rd generation benchmark problem including spillover suppression," in *Proceedings of the 15th ASCE Engineering Mechanics Conference,* New York, 2002.

[12] C. Liangbin and C. Dayue, "A two-stage vibration isolation system featuring an electrorheological damper via the semi-active static output feedback variable structure control method," *JVC/Journal of Vibration and Control,* vol. 10, pp. 683-706, 2004.

[13] M. Unsal, C. Niezrecki and C. D. I. Crane, "A new semi-active piezoelectric-based friction damper," in *Proceedings of SPIE - the International Society for Optical Engineering,* 2003, pp. 413-420.

[14] C. H. Hansen and S. D. Snyder, *Active Control of Noise and Vibration.* London: Spon Press, 1997.

[15] M. Appleyard and P. E. Wellstead, "Active suspension: Some background," in *Control Theory and Applications, IEE Proceedings,* 1995, pp. 123-128.

[16] F. Oueslati and S. Sankar, "A Class of Semi-Active Suspension Schemes for Vehicle Vibration Control," *Journal of Sound and Vibration,* vol. 172, pp. 391-411, 1994.

[17] M. Gobbi and G. Mastinu, "Analytical description and optimization of the dynamic behaviour of passively suspended road vehicles," *Journal of Sound and Vibration,* vol. 245, pp. 457-481, 2001.

[18] A. F. Naudé and J. A. Snyman, "Optimisation of road vehicle passive suspension systems. Part 1. Optimisation algorithm and vehicle model," *Applied Mathematical Modelling,* vol. 27, pp. 249-261, 2003.

[19] A. F. Naudé and J. A. Snyman, "Optimisation of road vehicle passive suspension systems. Part 2. Qualification and case study," *Applied Mathematical Modelling,* vol. 27, pp. 263-274, 2003.

[20] J. A. Tamboli and S. G. Joshi, "Optimum design of a passive suspension system of a vehicle subjected to actual random road excitations," *Journal of Sound and Vibration,* vol. 219, pp. 193-205, 1999.

[21] I. Youn and A. Hac, "Semi-active suspensions with adaptive capability," *Journal of Sound and Vibration,* vol. 180, pp. 475-492, 1995.

[22] D. Fischer and R. Isermann, "Mechatronic semi-active and active vehicle suspensions," *Control Engineering Practice,* vol. 12, pp. 1353-1367, 2004.

[23] G. Z. Yao, F. F. Yap, G. Chen, W. H. Li and S. H. Yeo, "MR damper and its application for semi-active control of vehicle suspension system," *Mechatronics,* vol. 12, pp. 963-973, 2002.

[24] M. Nagai and T. Hasegawa, "Vibration isolation analysis and semi-active control of vehicles with connected front and rear suspension dampers," *JSAE Review,* vol. 18, pp. 45-50, 1997.

[25] J-H. Kim and C-W. Lee, "Semi-active damping control of suspension systems for specified operational response mode," *Journal of Sound and Vibration,* vol. 260, pp. 307-328, 2003.

[26] P. E. Uys, P. S. Els and M. Thoresson, "Suspension settings for optimal ride comfort of off-road vehicles travelling on roads with different roughness and speeds," *Journal of Terramechanics,* vol. 44, pp. 163-175, 2007.

[27] M. Yokoyama, J. K. Hedrick and S. Toyama, "A model following sliding mode controller for semi-active suspension systems with MR dampers," in *Proceedings of the American Control Conference*, Arlington, 2001, pp. 2652-2657.

[28] Y. Shen, M. F. Golnaraghi and G. R. Heppler, "Semi-active vibration control schemes for suspension systems using magnetorheological dampers," *JVC/Journal of Vibration and Control,* vol. 12, pp. 3-24, 2006.

[29] M. A. Karkoub and M. Zribi, "Active/semi-active suspension control using magnetorheological actuators," *International Journal of Systems Science,* vol. 37, pp. 35-44, 2006.

[30] C-W. Zhang, J-P. Ou and J-Q. Zhang, "Parameter optimization and analysis of a vehicle suspension system controlled by magnetorheological fluid dampers," *Structural Control and Health Monitoring,* vol. 13, pp. 885-896, 2006.

[31] S. Choi and W. Kim, "Vibration control of a semi-active suspension featuring electrorheological fluid dampers," *Journal of Sound and Vibration,* vol. 234, pp. 537-546, 2000.

[32] S. B. Choi, H. K. Lee and E. G. Chang, "Field test results of a semi-active ER suspension system associated with skyhook controller," *Mechatronics,* vol. 11, pp. 345-353, 2001.

[33] Y. M. Han, M. H. Nam, S. S. Han, H. G. Lee and S. B. Choi, "Vibration control evaluation of a commercial vehicle featuring MR seat damper," *Journal of Intelligent Material Systems and Structures,* vol. 13, pp. 575-579, 2002.

[34] M. B. Barron and W. F. Powers, "The role of electronic controls for future automotive mechatronic systems," *IEEE/ASME Transactions on Mechatronics,* vol. 1, pp. 80-88, 1996.

[35] D. Hrovat, "Survey of Advanced Suspension Developments and Related Optimal Control Applications," *Automatica,* vol. 33, pp. 1781-1817, 1997.

[36] R. A. Williams, "Automotive active suspensions Part 1: Basic principles," *Proceedings of the Institution of Mechanical Engineers, Part D: Journal of Automobile Engineering,* vol. 211, pp. 415-426, 1997.

[37] R. A. Williams, "Automotive active suspensions Part 2: Practical considerations," *Proceedings of the Institution of Mechanical Engineers, Part D: Journal of Automobile Engineering,* vol. 211, pp. 427-444, 1997.

[38] S. Türkay and H. Akçay, "Aspects of achievable performance for quarter-car active suspensions," *Journal of Sound and Vibration,* vol. 311, pp. 440-460, 2008.

[39] D. A. Mántaras and P. Luque, "Ride comfort performance of different active suspension systems," *International Journal of Vehicle Design,* vol. 40, pp. 106-125, 2006.

[40] H. Peng, R. Strathearn and A. G. Ulsoy, "Novel active suspension design technique - simulation and experimental results," in *Proceedings of the American Control Conference*, Albuquerque ,1997, pp. 709-713.

[41] I. Ballo, "Comparison of the properties of active and semiactive suspension," *Vehicle System Dynamics,* vol. 45, pp. 1065-1073, 2007.

[42] F. H. Besinger, D. Cebon and D. J. Cole, "Force control of a semi-active damper," *Vehicle System Dynamics,* vol. 24, pp. 695-723, 1995.

[43] S. Ikenaga, F. L. Lewis, J. Campos and L. Davis, "Active suspension control of ground vehicle based on a full-vehicle model," in *Proceedings of the American Control Conference*, Chicago, Illinois, 2000, pp. 4019-4024.

[44] M. S. Kumar and S. Vijayarangan, "Analytical and experimental studies on active suspension system of light passenger vehicle to improve ride comfort," *Mechanika,* vol. 65, pp. 34-41, 2007.

[45] A. Alleyne, R. Liu and H. Wright, "On the limitation of force tracking control for hydraulic active suspensions," *Proceedings of the American Control Conference,* Philadelphia, Pennsylvania, pp. 43-47, 1998.

[46] X. Shen and H. Peng, "Analysis of active suspension systems with hydraulic actuators," *Vehicle System Dynamics,* vol. 41, pp. 143-152, 2004.

[47] G. D. Buckner, K. T. Schuetze and J. H. Beno, "Active vehicle suspension control using intelligent feedback linearization," in *Proceedings of the 2000 American Control Conference*, Chicago, 2000, pp. 4014-4018.

[48] G. D. Buckner, K. T. Schuetze and J. H. Beno, "Intelligent feedback linearization for active vehicle suspension control," *Journal of Dynamic Systems, Measurement and Control, Transactions of the ASME,* vol. 123, pp. 727-733, 2001.

[49] S. S. Parthasarathy and Y. G. Srinivasa, "Design of an active suspension system for a quarter-car road vehicle model using model reference control," *Proceedings of the Institution of Mechanical Engineers. Part I: Journal of Systems and Control Engineering,* vol. 220, pp. 91-108, 2006.

[50] A. J. Barr and J. L. Ray, "Control of an active suspension using fuzzy logic," in *Proceedings of the Fifth IEEE International Conference on Fuzzy Systems*,1996, pp. 42-48.

[51] S. Y. Moon and W. H. Kwon, "Genetic-based fuzzy control for half-car active suspension systems," *International Journal of Systems Science,* vol. 29, pp. 699-710, 1998.

[52] T. Yoshimura, K. Nakaminami, M. Kurimoto and J. Hino, "Active suspension of passenger cars using linear and fuzzy-logic controls," *Control Engineering Practice,* vol. 7, pp. 41-47, 1999.

[53] J. Sun and Y. Sun, "A fuzzy method improving vehicle ride comfort and road holding capability," in *Second IEEE Conference on Industrial Electronics and Applications*, 2007, pp. 1361-1364.

[54] A. Giua, C. Seatzu and G. Usai, "Active axletree suspension for road vehicles with gain-switching," in *Proceedings of the 39th IEEE Conference on Decision and Control*, Sydney, 2000, pp. 438-443.

[55] A. Giua, C. Seatzu and G. Usai, "A mixed suspension system for a half-car vehicle model," *Dynamics and Control,* vol. 10, pp. 375-397, 2000.

[56] S. Chantranuwathana and H. Peng, "Adaptive robust control for active suspensions," in *Proceedings of the American Control Conference*, San Diego,California, 1999, pp. 1702-1706.

[57] S. Chantranuwathana and H. Peng, "Force tracking control for active suspensions - theory and experiments," in *Proceedings of the IEEE International Conference on Control Applications*, Hawai'i, 1999, pp. 442-447.

[58] S. Chantranuwathana and H. Peng, "Practical adaptive robust controllers for active suspensions," in *Proceedings of the 2000 ASME International Congress and Exposition (IMECE),* Orlando, 2000,

[59] S. Chantranuwathana and H. Peng, "Adaptive robust force control for vehicle active suspensions," *International Journal of Adaptive Control and Signal Processing,* vol. 18, pp. 83-102, 2004.

[60] I. Fialho and G. J. Balas, "Road adaptive active suspension design using linear parameter-varying gain-scheduling," *IEEE Transactions on Control Systems Technology,* vol. 10, pp. 43-54, 2002.

[61] Z. Liu and C. Luo, "Road Adaptive Active Suspension Control Design," *Multiconference on Computational Engineering in Systems Applications, IMACS,* pp. 1347-1350, 2006.

[62] H. -Y. Chen and S. -J. Huang, "Adaptive sliding controller for active suspension system," in *International Conference on Control and Automation*, 2005, pp. 282-287.

[63] S. -J. Huang and H. -Y. Chen, "Adaptive sliding controller with self-tuning fuzzy compensation for vehicle suspension control," *Mechatronics,* vol. 16, pp. 607-622, 2006.

[64] K. Hayakawa, K. Matsumoto, M. Yamashita, Y. Suzuki, K. Fujimori and H. Kimura, "Robust H∞-output feedback control of decoupled automobile active suspension systems," *IEEE Transactions on Automatic Control,* vol. 44, pp. 392-396, 1999.

[65] H. Chen, Z. -Y. Liu and P. -Y. Sun, "Application of constrained H_∞ control to active suspension systems on half-car models," *Journal of Dynamic Systems, Measurement and Control, Transactions of the ASME,* vol. 127, pp. 345-354, 2005.

[66] H. Du and N. Zhang, "H$_\infty$ control of active vehicle suspensions with actuator time delay," *Journal of Sound and Vibration,* vol. 301, pp. 236-252, 2007.

[67] T. Yoshimura, A. Kume, M. Kurimoto and J. Hino, "Construction of an active suspension system of a quarter car model using the concept of sliding mode control," *Journal of Sound and Vibration,* vol. 239, pp. 187-199, 2001.

[68] Y. M. Sam, J. H. S. Osman and M. R. A. Ghani, "Active suspension control: Performance comparison using proportional integral sliding mode and linear quadratic regulator methods," in *Proceedings of IEEE Conference on Control Applications*, 2003, pp. 274-278.

[69] Y. M. Sam, J. H. S. Osman and M. R. A. Ghani, "A class of proportional-integral sliding mode control with application to active suspension system," *Systems and Control Letters,* vol. 51, pp. 217-223, 2004.

[70] X. Ji, W. Wei and H. Su, "Comments on "A class of proportional-integral sliding mode control with application to active suspension system"," *Systems and Control Letters,* vol. 56, pp. 253-254, 2007.

[71] A. Chamseddine, H. Noura and T. Raharijaona, "Control of linear full vehicle active suspension system using sliding mode techniques," in *Proceedings of IEEE International Conference on Control Applications*, 2007, pp. 1306-1311.

[72] A. G. Thompson and C. E. M. Pearce, "Direct computation of the performance index for an optimally controlled active suspension with preview applied to a half-car model," *Vehicle System Dynamics,* vol. 35, pp. 121-137, 2001.

[73] H. -S. Roh and Y. Park, "Stochastic optimal preview control of an active vehicle suspension," *Journal of Sound and Vibration,* vol. 220, pp. 313-330, 1999.

[74] H. -J. Kim, H. Seok Yang and Y. -. Park, "Improving the vehicle performance with active suspension using road-sensing algorithm," *Computers and Structures,* vol. 80, pp. 1569-1577, 2002.

[75] J. Marzbanrad, G. Ahmardi, Y. Hojjat and H. Zohoor, "Optimal active control of vehicle suspension system including time delay and preview for rough roads," *JVC/Journal of Vibration and Control,* vol. 8, pp. 967-991, 2002.

[76] J. Marzbanrad, G. Ahmadi, H. Zohoor and Y. Hojjat, "Stochastic optimal preview control of a vehicle suspension," *Journal of Sound and Vibration,* vol. 275, pp. 973-990, 2004.

[77] A. G. Thompson and B. R. Davis, "Computation of the rms state variables and control forces in a half-car model with preview active suspension using spectral decomposition methods," *Journal of Sound and Vibration,* vol. 285, pp. 571-583, 2005.

[78] M. Jonasson and F. Roos, "Design and evaluation of an active electromechanical wheel suspension system," *Mechatronics,* vol. 18, pp. 218-230, 2008.

[79] T. Yoshimura and A. Takagi, "Pneumatic active suspension system for a one-wheel car model using fuzzy reasoning and a disturbance observer," *Journal of Zhejiang University: Science,* vol. 5, pp. 1060-1068, 2004.

[80] A. Kruczek and A. Stribrsky, "A full-car model for active suspension - some practical aspects," in *Proceedings of the IEEE International Conference on Mechatronics*, 2004, pp. 41-45.

[81] N. Yagiz and Y. Hacioglu, "Backstepping control of a vehicle with active suspensions," *Control Engineering Practice,* 2008.

[82] H. Gao, J. Lam and C. Wang, "Multi-objective control of vehicle active suspension systems via load-dependent controllers," *Journal of Sound and Vibration,* vol. 290, pp. 654-675, 2006.

[83] M. Gobbi, F. Levi and G. Mastinu, "Multi-objective stochastic optimisation of the suspension system of road vehicles," *Journal of Sound and Vibration,* vol. 298, pp. 1055-1072, 2006.

[84] E. M. Elbeheiry and D. C. Karnopp, "Optimal control of vehicle random vibration with constrained suspension deflection," *Journal of Sound and Vibration,* vol. 189, pp. 547-564, 1996.

[85] J. W. Choi, Y. B. Seo, W. S. Yoo and M. H. Lee, "LQR approach using eigenstructure assignment with an active suspension control application," in *Proceedings of the IEEE International Conference on Control Applications*, 1998, pp. 1235-1239.

[86] M. M. Elmadany and Z. S. Abduljabbar, "Linear quadratic Gaussian control of a quarter-car suspension," *Vehicle System Dynamics,* vol. 32, pp. 479-497, 1999.

[87] Y. M. Sam, M. R. H. A. Ghani and N. Ahmad, "LQR controller for active car suspension," in *Proceedings TENCON 2000*, 2000, pp. 441-444.

[88] P. Gaspar, I. Szaszi and J. Bokor, "Active suspension design using linear parameter varying control," *International Journal of Vehicle Autonomous Systems,* vol. 1, pp. 206-221, 2003.

[89] Y. J. Tsao and R. Chen, "The design of an active suspension force controller using genetic algorithms with maximum stroke constraints," *Proceedings of the Institution of Mechanical Engineers, Part D: Journal of Automobile Engineering,* vol. 215, pp. 317-327, 2001.

[90] C. -C. Sun, H. -Y. Chung and W. -J. Chang, "GA-based robust H2 controller design approach for active suspension systems," in *Proceedings of the IEEE International Conference on Robotics and Automation*, 2003, pp. 2330-2335.

[91] H. Du, J. Lam and K. Y. Sze, "Non-fragile output feedback H_∞ vehicle suspension control using genetic algorithm," *Engineering Applications of Artificial Intelligence,* vol. 16, pp. 667-680, 2003.

[92] Y. He and J. McPhee, "Multidisciplinary design optimization of mechatronic vehicles with active suspensions," *Journal of Sound and Vibration,* vol. 283, pp. 217-241, 2005.

[93] T. Chuanyin and Z. Tiaoxia, "The research on control algorithms of vehicle active suspension system," in *IEEE International Conference on Vehicular Electronics and Safety*, 2005, pp. 320-325.

[94] M. S. Kumar, "Genetic Algorithm-based proportional derivative controller for the development of active suspension system," *Information Technology And Control*, vol. 36, pp. 58-67, 2007.

[95] A. Shirahatt, P. S. S. Prasad, P. Panzade and M. M. Kulkarni, "Optimal design of passenger car suspension for ride and road holding," *Journal of the Brazilian Society of Mechanical Sciences and Engineering,* vol. 30, pp. 66-76, 2008.

[96] H. Du and N. Zhang, "Designing H∞/GH 2 static-output feedback controller for vehicle suspensions using linear matrix inequalities and genetic algorithms," *Vehicle System Dynamics,* vol. 46, pp. 385-412, 2008.

[97] B. P. Lathi, "*Linear Systems and Signals*," Second Edition, Oxford University Press, Inc, 2005.

[98] I. I. Esat and M. Saud, "A novel approach to obtain a real time control force strategy by using genetic algorithm and convolution integral," in *Integrated Design and Process Technology,* San Diego, 2006.

[99] M. Saud and I. I. Esat, "A novel method for obtaining real time control strategy using GA for dynamical systems subjected to external arbitrary excitations," in *Second International Symposium on Leveraging Applications of Formal Methods, Verification and Validation,* Paphos, 2006, pp. 161 – 168.

[100] M. Saud and I. I. Esat, "GA-based control force strategy for full-vehicle active suspension system using convolution integral," in *Integrated Design and Process Technology,* Antalya, 2007.

[101] S. Naidu, *Optimal Control Systems.* CRC Press Inc, 2002.

[102] G. V. Reklaitis, A. Ravindran and K. M. Ragsdell, *Engineering Optimization Methods and Applications.* Canada: John Wiley & Sons, 1983.

[103] M. Jamshidi, L. D. S. Coelho, R. A. Krohling and P. J. Fleming, *Robust Control Systems with Genetic Algorithms.* London: CRC press Inc, 2002.

[104] M. Mithchell, *An Introduction to Genetic Algorithms.* Massachusetts Institute of Technology, MIT Press, 1995.

[105] D. E. Goldberg, *Genetic Algorithms in Search, Optimization and Machine Learning.* Addison Wesley, 1989.

[106] http://www.nd.com/genetic/, NeuroDimension, "Genetic Server and Genetic Library," last date entered 06/07/2008.

[107] G. M. Siouris, *An Engineering Approach to Optimal Control and Estimation Theory.* WileyBlackwell, JOHN WILEY & SONS, 1996.

[108] A. R. M. NOTON, *Introduction to Variational Methods in Control Engineering* ,1st ed., Pergamon Press, 1965.

[109] http://www.engin.umich.edu/class/ctms/simulink/examples/susp/suspsim.htm, last date entered 06/07/2008.

[110] N. Jalili and E. Esmailzadeh, "Optimum active vehicle suspensions with actuator time delay," *Journal of Dynamic Systems, Measurement and Control, Transactions of the ASME,* vol. 123, pp. 54-61, 2001.

[111] C. Kim, P. I. Ro and H. Kim, "Effect of the suspension structure on equivalent suspension parameters," *Proceedings of the Institution of Mechanical Engineers, Part D: Journal of Automobile Engineering,* vol. 213, pp. 457-470, 1999.

[112] Froude Consine, Installation, Operation and Maintenance Procedures, Instruction Manual IM 1278/1, issue2, Omega Amplifier. Instruction manual IM 1280/1, issue1, VP85 Vibrator. Instruction manual IM 1268/1, issue1, programmable swept sine controller-type PSC, And TA 600 Amplifier, 1995.

[113] http://www.smcetech.com/CC_catalogs/smc/pdf/MQ_EU.pdf, SMC, Lateral load resisting low friction cylinder, Series MQM, pp.11.

Appendix

9. The signals generated using the *SignalCalc 350* software

Two kinds of excitation signals; random and sweep sine waves were chosen as an input to the system. Fig 9.1 shows the random signal generated using the *SignalCalc 350* software, with reference levels defined in terms of acceleration Power Spectra Density. Fig 9.2 shows the sweep sine wave to be generated by the shaker. The selected signal levels were chosen taking into account the shaker limits such as low frequency and the maximum displacement that can be generated by the *VB85* shaker.
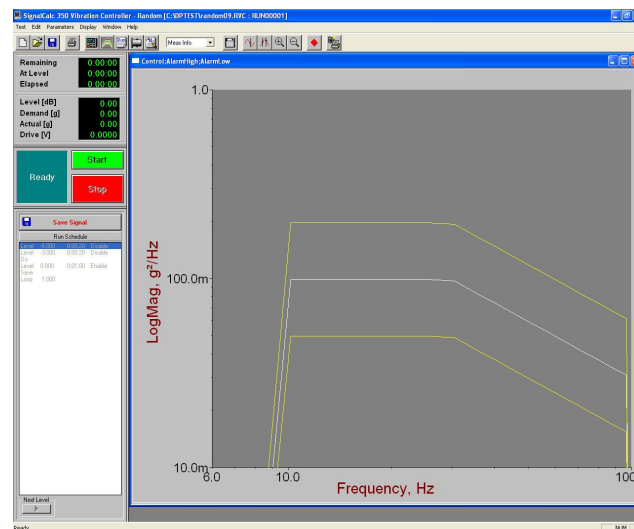

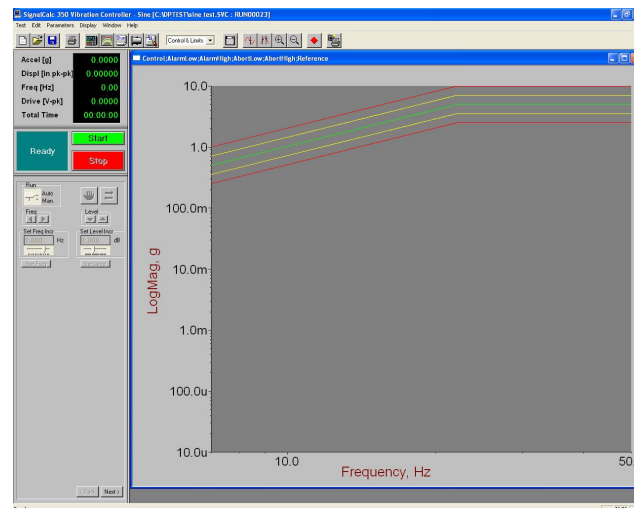Fig 9.1 The generated random signal using *SignalCalc 350* software.

Fig 9.2 The Sweep Sine wave generated using *SignalCalc 350* software.

149